2004

MULTISCALE MODELING AND ANALYSIS OF FAILURE AND STABILITY DURING SUPERPLASTIC DEFORMATION -- UNDER DIFFERENT LOADING CONDITIONS

Naveen Thuramalla
University of Kentucky, naveen@engr.uky.edu

ABSTRACT OF THESIS

MULTISCALE MODELING AND ANALYSIS OF FAILURE AND STABILITY DURING SUPERPLASTIC DEFORMATION – UNDER DIFFERENT LOADING CONDITIONS

Superplastic forming (SPF) is a valuable near net shape fabrication method, used to produce very complex, contoured and monolithic structures that are often lighter, stronger and safer than the assemblies they replace. However, the widespread industrial use of Superplastic (SP) alloys is hindered by a number of issues including low production rate and limited predictive capabilities of stability during deformation and failure. Failure during SPD may result from geometrical macroscopic instabilities and/or microstructural aspects. However, the available failure criteria are either based on geometrical instabilities or microstructural features and do not account for both failure modes. The present study presents a generalized multi-scale stability criterion for SP materials, accounting for both aspects of failure under various loading conditions. A combined model accounting for cavity nucleation and plasticity controlled cavity growth along with a grain growth model and a modified microstructure based constitutive equation for SP materials is incorporated into Hart's stability analysis to develop the proposed stability criterion for different loading conditions. Effects of initial grain size, initial levels of cavitation, nucleation strain, strain-rate sensitivity, and grain-growth exponent on the optimum forming curves of different SP alloys are investigated, for different loading conditions.

KEYWORDS: SPF, Multiscale Failure Criterion, Stability Analysis, Optimum Forming Paths, SP Alloys.

NAVEEN THURAMALLA

Date: May-26, 2004.

MULTISCALE MODELING AND ANALYSIS OF FAILURE AND STABILITY DURING SUPERPLASTIC DEFORMATION-UNDER DIFFERENT LOADING CONDITIONS

By

Naveen Thuramalla

Dr. Marwan Khraisheh

Director of Thesis

Dr. George Huang

Director of Graduate Studies

Date : May 26, 2004

RULES FOR THE USE OF THESES

Unpublished theses submitted for the Master's degree and deposited in the University of Kentucky Library are a rule open for inspection, but are to be used only with due regard to the rights of the authors. Bibliographical references may be noted, but quotations or summaries of parts may be published only with the permission of the author, and with the usual scholarly acknowledgements.

Extensive copying or publication of the theses in whole or in part also requires the consent of the Dean of the Graduate School of the University of Kentucky.

THESIS

Naveen Thuramalla

The Graduate School

University of Kentucky

2004

MULTISCALE MODELING AND ANALYSIS OF FAILURE AND STABILITY DURING SUPERPLASTIC DEFORMATION – UNDER DIFFERENT LOADING CONDITIONS

THESIS

A thesis submitted in partial fulfillment of the requirements for the degree of Master of Science in Mechanical Engineering from the College of Engineering at the University of Kentucky

By

Naveen Thuramalla

Lexington, Kentucky

Director: Dr. M.K. Khraisheh, Assistant Professor
Center for Manufacturing, Department of Mechanical Engineering
Lexington, Kentucky

2004

Dedicated to My Parents

ACKNOWLEDGEMENTS

I would like to sincerely acknowledge the mentorship and support that my advisor, Dr. Marwan Khraisheh, has extended throughout the course of my M.S. It would not be an overstatement to say without his enthusiasm for research, and encouragement towards success; I would not have successfully completed my thesis. It is his motivation that is responsible for all my awards and publications. I would like to express my sincere gratefulness to Dr. Rouch, who has been very encouraging and supportive all through my M.S. and also for his kindness in agreeing to be on my committee. I was fortunate to be his teaching assistant for three semesters and also a student in his course. I would then like to extend my thankfulness to Dr.Jawahir, for agreeing to be on my committee. He has been instrumental in motivating me towards manufacturing by giving me an insight into various techniques of forming/manufacturing. I would like to thank my D.G.S. Dr. Huang, for giving me an opportunity to pursue my MS at University of Kentucky and also for offering me teaching assistantship, all through my MS. I would also like to thank all the faculty members and staff of ME dept. for their continued cooperation. I also have to acknowledge each and every member of my research team and all my friends, whose support has made my life in US very comfortable and also helped me achieve my tasks with ease.

Above all, I would like to thank my parents and my sister for supporting and motivating me to pursue my master's. I am ever indebted for their motivation and encouragement, which made every hurdle surmountable and every task achievable. I dedicate each and every achievement to them and consider myself blessed to have such a family.

Naveen Thuramalla

Table of Contents

List of Figures

List of Files

NAVEEN.pdf …….. 644MB

Chapter 1 INTRODUCTION

1.1 Superplasticity

Superplasticity is the ability of polycrystalline solids to undergo extraordinarily large uniform neck-free tensile deformation prior to fracture, under appropriate conditions of temperature and strain rate [1]. Elongations in excess of 200% are usually indicative of superplasticity, although many superplastic (SP) alloys can attain stable elongations of several thousand percent. A maximum elongation of 8000% that was observed in commercial bronze alloy [2] stands a world record. These materials have exceptional stability during uniaxial tensile deformation, which leads to extreme elongation without fracture, whereas for conventional materials, equivalent values for fracture are usually <<100%.

Sherby and Wadsworth [3] postulated that ancient bronzes (Copper-Arsenic) date as far back as 2500 B.C. because of the fine and stable grain structure of the two-phase arsenic rich bronzes. They also speculated that the ultra high carbon Damascus steel, dating back to 300 B.C. exhibited SP behavior. However, Bochvar and Sviderskaya [4] coined the term “superplasticity” in 1945 by combining a Latin word “super” meaning “excess” and a Greek word “plastikos” meaning “to form”. Underwood and Backofen [5] showed that SP Zn-Al alloy could be formed into a hemispherical shape by blowing air on one side of a sheet blank into a die. This is considered as the first demonstratio of superplasticity as a practical forming operatio. This created a surge in commercial applications of superplasticity, which in turn attracted many investigators from both scientific and industrial communities.

There are two main types of superplastic behavior. First is the micrograin superplasticity or structural superplasticity when there is a characteristic microstructure that is stable during tensile deformation. Second is environmental superplasticity where special environmental conditions exist during superplastic deformation. The three basic requirements necessary to achieve superplasticity include [1,6]:

1. Fine and equiaxed grain size, usually less than 10 microns, that is stable during deformation;

2. Forming temperature greater than approximately half the absolute melting temperature of the subject materials; and

3. Controlled deformation rate.

Some of the typical SP alloys include [1]: Titanium alloys (Ti-6Al-4V, Ti-6Al-2Sn-4Zr-2Mo, Ti-6Al-4V-2Co); Aluminum alloys (AA5083, AA7475, Supral); Magnesium alloys (ZK60, AZ31); Copper alloys (CDA 638); Nickel alloys (IN-100, IN-738, MAR M-247); Eutectic alloys (Mg-33Al, Pb-62Sn, Bi-44Sn, Ag-28Cu) and also Ceramics (Y-TZP, ZrO_2-Al_2O_3); and Composites. Nickel based alloys are used to form turbine discs with integral blades, while titanium alloys are used to produce fan and compressor blades for aeroengines, some sports equipment like golf-club head and also in the fabrication of medical devices and dental implants. Aluminum alloys can be used in the fabrication of airframe control surfaces and small-scale structural elements where low weight and high stiffness are required. Non-aerospace applications of Al alloys include containers with complex surface profiles and decorative panels for internal and external cladding of buildings, window frames for trains and gate panels.

1.2 Superplastic Forming

Superplastic forming (SPF) is an advanced technique used in the metal forming industry on account of several advantages offered by superplastic materials. It is a valuable fabrication tool used to produce very complex, contoured and monolithic structures that are often lighter, stronger and safer than the assemblies they replace [7]. SPF produces complex metal components by applying gentle pressure to help the heated metal to creep into a mould over several hours rather than forging it instantaneously. In contrast to conventional metal forming methods, the high levels of uniform deformation that occur in superplastic forming metals can be used to form uniform, complex and intricate structures in a single forming process. Greater design flexibility, low forming pressure due to low flow stress, low die cost, higher structural integrity, elimination of fasteners and fixtures, reduction of subsequent machining steps and assembly operations,

reduced part count, reduction in the weight of the component, reduction in cost and minimization of material waste, ability to form complex shapes from hard materials and low forming pressure on account of low flow stress are some of the typical advantages of SPF. Due to these advantages, SP materials find extensive applications in the aircraft industry, automotive industry, sheet metal industry, and also in the field of medicine. However, the widespread industrial application of SPF is hindered due to certain limitations, which include:

a) Low production rate due to slow forming process;

b) Expensive pre-forming steps (preparation of the fine grain-structure & the high forming temperature) and

c) Limited predictive capabilities of deformation and failure due to lack of accurate constitutive models for superplastic deformation.

1.2.1 Forming Processes

Flow stresses of SP materials generally lie between 2-10MPa. Gas pressure is used to drive deformation rather than liquid hydraulic or mechanically applied loads. Superplastic sheet forming processes are therefore fundamentally different from the processes that are used in conventional metal forming, and have more in common with the techniques used for shaping thermoplastics. Different forming processes include [1]:

1.2.1.1 Simple Female Forming

The simplest form of Superplastic forming involves the free bulging of a sheet, which is clamped around its periphery, into a female mould, as shown in Figure 1-1. During the initial stages of deformation, when the sheet is not in contact with deformation, when the sheet is not in contact with the tool, deformation is concentrated at the pole of the dome and consequently this region shows the greatest strain. Once the pole comes in contact with the surface of the die, the material is locked against the tool by friction and the forming pressure, and this prevents further deformation within that region. The remaining free regions of the dome continue to deform

making the formed section more uniform. Since the corners of the die are usually the last regions to be filled, the greatest strain is developed at these points. The limiting factors in simple female forming are the aspect ratio of the die and the corner radii. Simple female forming is generally preferred over other forming techniques when the aspect ratio of the component is low or when the convex surface of the finished component has to be a specific shape, regardless of thickness.

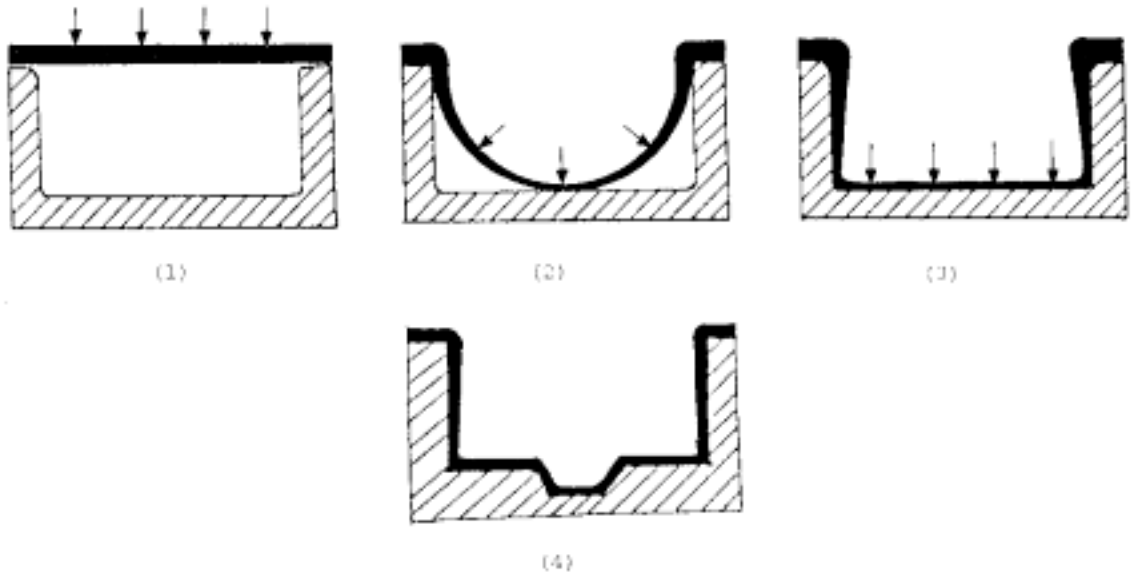

Figure 1-1 Schematic of Simple Female Forming [1]

1.2.1.2 Female Drape Forming

This process consists of bulge forming a sheet into a female mould in which one or more male details are placed, as shown in Figure 1-2. Deformation of the sheet during bulging ceases when the polar region comes in contact with the male tool. Continued application of the forward forming pressure will drape the forming sheet, forcing it to take the shape of the male details. This process results in a relatively uniform thickness distribution in the regions of the sheet covering the male tooling. This process is preferred when dimensional tolerances of the concave surface of the finished component are important. However, this process is limited to parts with relatively low aspect ratio besides involving higher wastage of material.

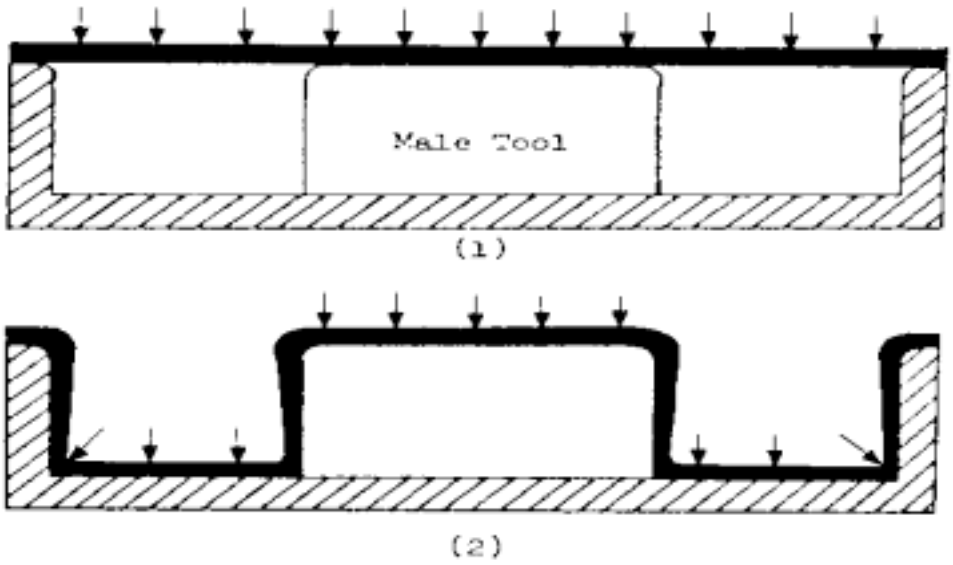

Figure 1-2 Schematic of Female Drape Forming [1]

1.2.1.3 Reverse Bulging

In reverse bulging, the sheet to be formed is first blown away from the female mould into which it will eventually be formed. After producing the initial dome, the forming pressure is reversed, forcing the bubble to fold in on itself into a female mould. The plastic flow is concentrated within the zone adjacent to the clamping flange and this results in a much more uniform thickness distribution in the formed shape than could be obtained by simple female forming, as shown Figure 1-3. The height to which the initial bubble is blown should not be more than about 10% greater than the depth of the final formed component. If the height of the bubble is too great then folds or wrinkles are likely to develop in the finished part.

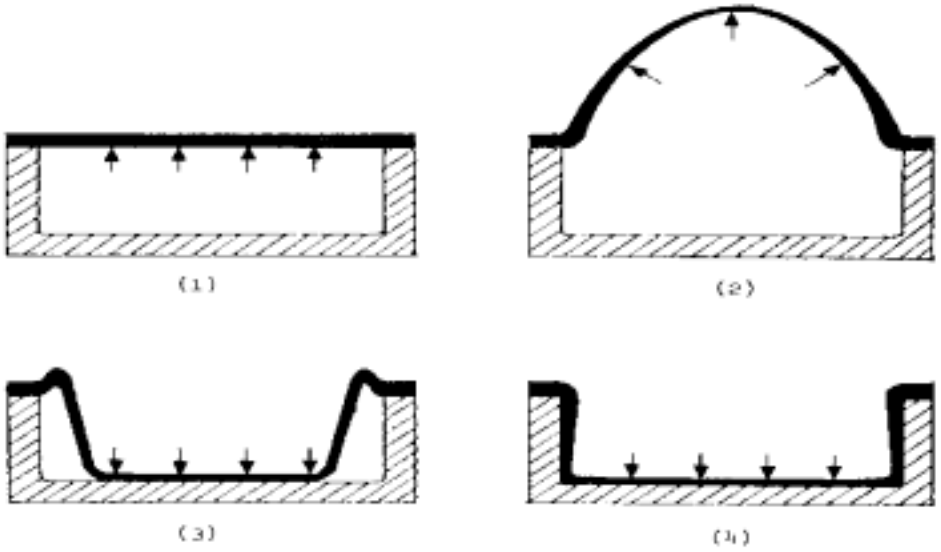

Figure 1-3 Schematic of Reverse Bulging [1]

1.2.1.4 Plug-Assisted Forming

A moving auxiliary tool is used to pre-stretch the areas of the forming sheet, as shown in Figure 1-4. As the tool moves past the starting plane of the forming process, contact is made between the plug and the central regions of that sheet.

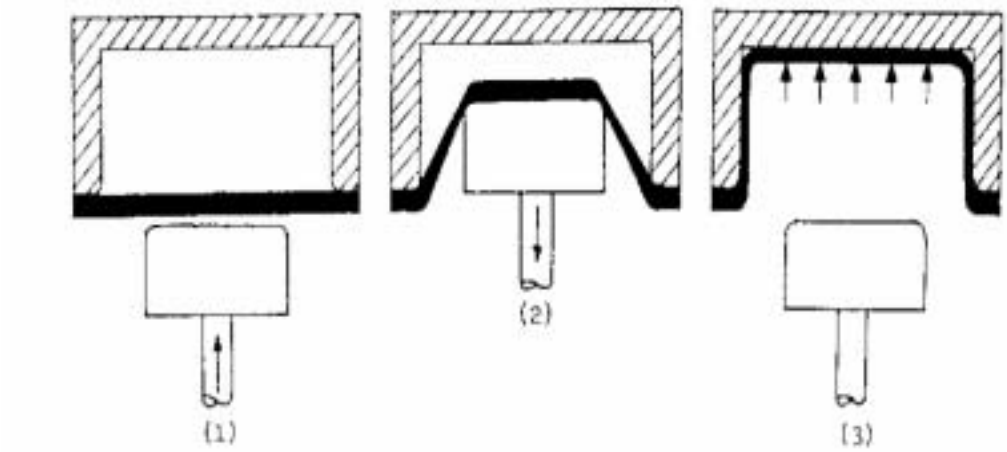

Figure 1-4 Schematic of Plug Assisted Forming [1]

Frictional forces prevent any significant stretching of those areas of the sheet in contact with plug and deformation is transferred to the annular zone between the plug and the clamping flange. After pre-stretching, the plug is withdrawn and the gas pressure is used to complete the female forming process.

1.2.1.5 Snap-Back Forming

It is the male forming equivalent of plug-assisted forming, the plug defining the final form of the component, as shown in Figure 1-5. The sheet to be formed is first blown into a bubble away from the male tool. Once the bubble has formed, the tool is moved up into the bubble. As the male plug continues to move into the bubble, the forming pressure is reversed forcing the bubble to collapse onto the plug. A combination of friction and forming pressure lock the sheet in contact with the tool and effectively prevent any further deformation. Snap back forming is of two types: Vacuum snap-back forming and Pressure snap-back forming. This process is excellent for deep parts because the pre-stretching prior to being formed distributes the material more evenly allowing for better wall thickness.

1.3 General Aspects of Superplastic Deformation

Deformation during SPF is generally affected by several factors including - strain rate sensitivity, temperature, grain size and cavitation. Strain rate sensitivity (m) is an important parameter in superplasticity, which represents the capacity of the material to resist necking and thereby influences the overall deformation and stability during SPD. Higher the value of m, higher is the resistance to neck growth. The magnitude of m increases with increasing temperature and decreasing grain size. The boundaries of SP interval (region II) are usually determined starting from the empirical condition of $m > 0.3$. The strain-rate sensitivity index (m) is not a material constant and it depends on a number of factors like: strain rate, strain, temperature, grain size etc.

Another important aspect is the role of microstructure during SPD. Superplasticity is generally exhibited by materials with a fine grain size (< 10 microns). It is imperative that this

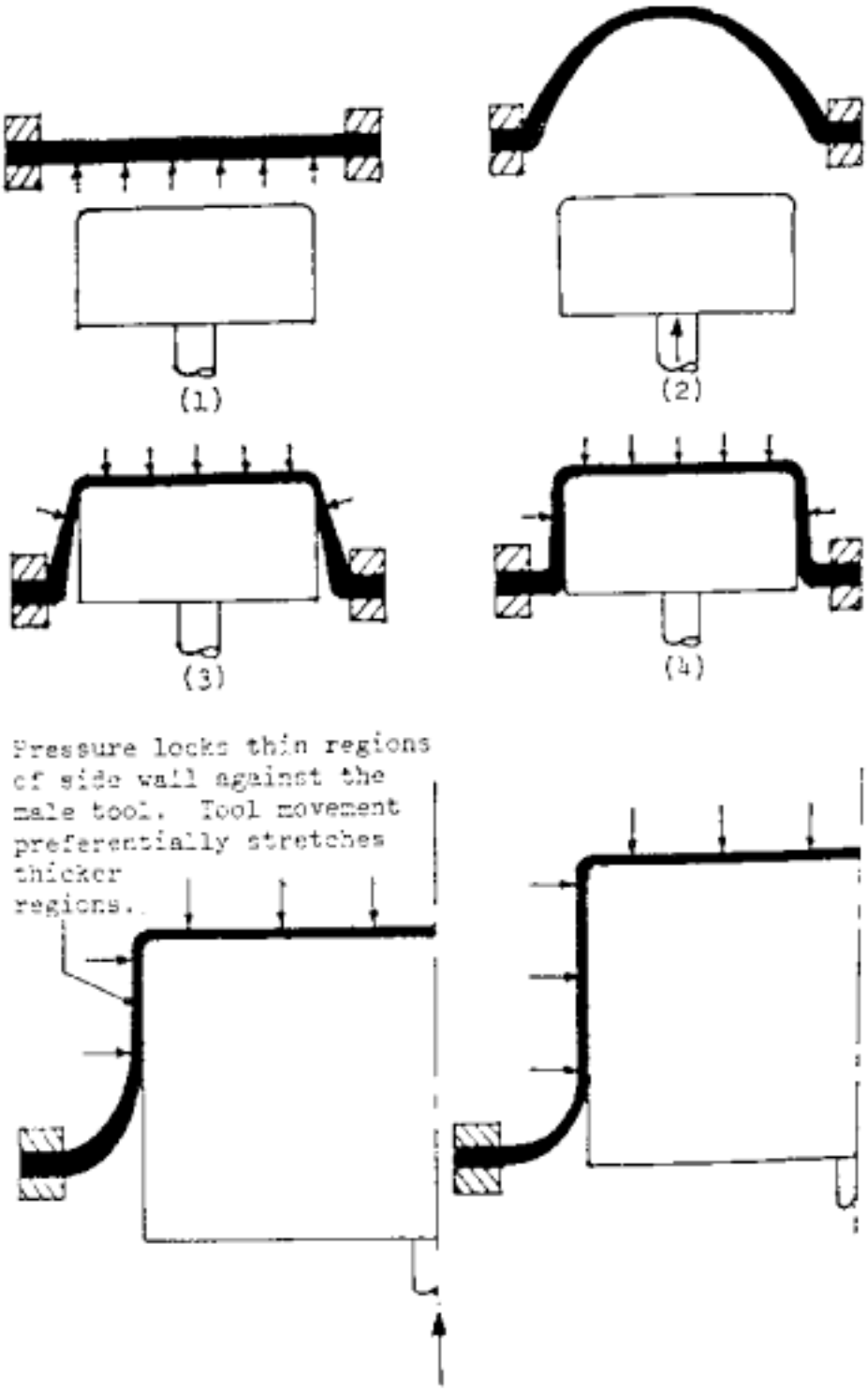

Figure 1-5 Schematic of Snap-Back Forming [1]

fine-grained nature of superplastic materials be maintained during SPF operations even at elevated temperatures. This has been achieved by developing quasi-single phase alloys in which grain boundaries are pinned by intergranular second-phase particles, or by developing microduplex alloys in which grain growth is restricted markedly as a result of frequent interphase grain contacts [20]. The distinct phenomenon of the average grain aspect ratio being much less than the corresponding macroscopic dimensional ratio at very high strains is attributed to the role of grain boundary sliding (shearing on grain boundaries). The dominant deformation mechanism in SP region is believed to be extensive grain boundary sliding (GBS) accompanied by diffusional flow or slip [8, 9, 10]. Thus, the grain shape is preserved during SPF. SPD is often accompanied by grain growth, the rate of which depends on both strain and strain-rate and is usually in excess during the deformation [11].

Microstructural features like: precipitates and particles at grain boundaries, grain boundary ledges, grain size and grain size distribution, and the presence of amorphous phase at interfaces, play an important role in cavitation [12]. It has been well-established that most SP materials exhibit cavitation during deformation and extensive cavitation during deformation would cause premature failure of the materials besides having deleterious effect on post-forming properties and severely restricting the applications of the formed product [13]. Cavitation can be characterized into three phases: nucleation, growth and coalescence. A detailed description of these aspects is dealt in chapter 2.

1.4 Problem Definition and Motivation:

On account of several advantages offered by SPF, it is considered as a viable, efficient and often better route to manufacture a growing range of products. However, the widespread industrial use of SP alloys is hindered due to a number of issues including low production rates, expensive and extensive pre-forming steps and limited predictive capabilities of stability during deformation and failure. In order to achieve maximum ductility, the part has to be formed at relatively low strain rates, i.e., slow forming - causing low production rate, which would adversely affect the overall economy. Forming at higher strain rates, though would decrease the forming time, it would affect the maximum attainable ductility. Hence it puts forth a challenge of

forming the components as rapidly as possible while maintaining the required quality/ductility of the formed parts, such as eliminating localized thinning and rupture. The other significant limitation is the lack of appropriate predictive models of failure during SPD. Though the subject of SPF has been studied extensively over the past few decades, the available failure criteria are either based on geometrical instabilities (necking) or microstructural aspects (cavitation). However, it has been commonly observed that SP alloys fail under the influence of both modes of failure. The contribution of each failure mode to the overall deformation behavior depends on material parameters such as composition and microstrutural aspects as well as on the process parameters such as strain-rate and temperature.

There has been not much work done in order to develop a stability model that accounts for both geometrical instabilities and microstructural aspects including cavitation and grain growth. Ding et. al. [14] had attempted to combine the effects of necking and grain growth and thereby develop a stability criterion for SP materials, in order to predict failure during SPD that accounts for both necking and grain growth. Optimum variable strain rate paths were generated using the developed stability criterion. However, this model did not take account the important microstructural aspect of cavitation, which has a significant adverse effect on the formability and final applications of the finished product. Thus, in order to predict the actual deformation and failure during SPF; it is imperative for the model to account for cavitation besides grain growth and necking.

The present work gets its motivation from the fact that there are no stability models accounting for both modes of failure and thus aims to develop a multiscale stability criterion for SPD, for different loading conditions. The effects of cavity nucleation, cavity growth and anisotropy must also be taken into consideration while developing a stability criterion for SP materials, in order to predict deformation and failure more closely to the conditions generated during actual forming operations. Addressing the above said issues is the main motive behind this research.

1.5 Research Objectives

The main goal of this research is to investigate certain fundamental issues relating to analyzing and modeling of SPF, that have not been addressed much in literature. One such aspect is the study involving the combined effect of geometrical instabilities (necking) and microstructural aspects including grain growth and cavitation. Cavitation has been an important consideration in fabricating complex metal parts by SPF. The basic processes leading to cavitation failure at working conditions are nucleation, growth and coalescence of cavities. Among these processes, the nucleation and growth aspects are especially important for fabricated components since they usually contain cavitation of less than 5% [15, 20]. At such levels the cavity coalescence aspect is almost negligible. Also most of the models and criteria developed are based on simple uniaxial loading case, assuming isotropic conditions, although it has been a common observation that sheet metals often exhibit plastic anisotropy during large deformations. And there no stability criteria available in literature that take into account all the above aspects. Based on a detailed literature review on these issues, it was identified that the following aspects require a detailed study and thus are framed as the main objectives of the present research:

1. Develop a multiscale stability criterion accounting for both modes of failure, incorporating both nucleation and growth of cavities, for a simple uniaxial loading condition.

2. Extend the above model to account for various loading conditions as encountered during actual forming operations.

3. Generate Optimum Variable Strain-Rate Forming Paths for different SP alloys using the above developed stability criteria and study the effect of various aspects like: strain rate sensitivity, initial grain size, initial levels of cavitation and nucleation strain on the optimum forming paths.

4. Incorporate the effect of anisotropy into the stability model and study its effect on the deformation and failure during SPF.

1.6 Thesis Layout

A detailed review of various aspects dealing with mechanical behavior of SP materials is presented in Chapter 2. It includes a thorough review of important parameters that influence the superplastic deformation as well as constitutive models describing the process of SPF. It would also focus on the effect of microstructural features, which include: grain growth and cavitation on SPD. A review of various models for grain growth and cavitation is also included. Finally, an overview of the various stability models proposed based on different failure criteria will be discussed and compared.

Chapter 3 would present the framework of developing a failure criterion for uniaxial loading case, accounting for both geometrical instabilities (necking) as well as microstructural aspects including grain growth and cavitation (nucleation and growth). The effects of constant and continuous nucleation of cavities are incorporated into the model besides plasticity controlled void growth. The effects of strain rate sensitivity, initial grain size, grain growth exponent, initial levels of cavitation (including constant and continuous nucleation, and growth of cavities) and nucleation strain on the optimum forming paths of different SP alloys is studied

Since biaxial stretching is the dominant stress state in the superplastic sheet blow forming processes, a two dimensional analysis of the localization behavior of the sheet is more appropriate for predicting failure and stability during SPD [16]. In stretching, all strain components in the plane of the sheet are tensile in nature and so are the stress components. Chapter 4 presents the framework of developing a multiscale stability criterion for biaxial stretching of thin sheets of viscoplastic metals under plane stress conditions, using a linear stability analysis. The effects of constant and continuous nucleation of cavities are also incorporated into the model. The effects of strain rate sensitivity, initial grain size, grain growth exponent, initial levels of cavitation (including constant and continuous nucleation, and growth of cavities), nucleation strain and stress state (or strain rate ratio) on the optimum forming paths of SP copper alloy are presented.

Chapter 5 would present the framework of extending the model to account for anisotropy, isotropic hardening and kinematic hardening. The model enables to study the effect of

anisotropic parameters and hardening besides above mentioned parameters, on the optimum forming paths of SP alloys.

Finally, Chapter 6 would discuss the important conclusions drawn from the research and also suggest future recommendations. This chapter would give an incite into the importance of optimum forming paths and its application to form various components using different SP alloys. The future recommendations would suggest the scope of further development on this subject to improvise the model and its applications, thus enable faster rates of production using SPF techniques and thereby make SPF an efficient and economic forming practice.

Chapter 2 Characteristics and Elements of Modeling Superplastic Deformation

The main features to be considered in order to characterize SP deformation include – characteristic aspects like high strain rate sensitivity of flow stress, microstructural aspects like grain size and cavitation, and accurate microstructure based constitutive equations to predict deformation process and thereby enhance the performance of superplastic forming operations.

2.1 Strain rate sensitivity (m)

Superplastic materials exhibit large tensile elongations to failure due to phenomenal resistance to necking during superplastic deformation (SPD) caused by strain rate hardening. Strain rate sensitivity (*m*) represents the capacity of the material to resist necking and thereby influences the overall deformation and stability during SPD [1].

Strain rate sensitivity of metals arises from viscous nature of the deformation process. This viscosity is a result of the resistance offered by internal obstacles within the material [10,17]. In dislocation glide and climb processes, the obstacles are a fine dispersion of second phase particles within the grain interior between which the dislocations are bent around and moved [18]. High diffusivities around grain boundary regions can lead to grain boundary sliding, at high homologous temperatures. The overall strain rate sensitivity of a material is a result of the rate sensitivities of the grain boundary and the grain interior, and can change from a high value (as high as ~ 1) at lower strain rates to a low value (~0.2-0.3) at higher strain rates. Higher the value of *m*, higher is the resistance to neck growth. This neck resistance scales with strain rate sensitivity and originates from an exceptional sensitivity of the flow stress to strain rate. Thus the most important mechanical characteristic of a superplastic material is the high strain rate sensitivity of the flow stress which is expressed by strain-rate sensitivity index referred to as '*m*' and is defined as:

$$m = \frac{d \log \sigma}{d \log \dot{\varepsilon}} \qquad \text{Eq. 2.1}$$

For SP behavior, *m* would be greater than or equal to 0.3 and for the majority of superplastic materials *m* lies in the range of 0.4-0.8 (typically observed in SP region II, as shown in Fig. 2a) subject to tensile straining leads to a locally high strain rate and, for a high value of m, to a sharp increase in the flow stress within the necked region. Hence the neck undergoes strain rate hardening which inhibits its further development. Thus high strain rate sensitivity confers a high resistance to neck development and results in the high tensile elongations-characteristic of SP materials. In the absence of the effect of cavitation damage, high *m* – values generally result in large elongations by decreasing the growth rate of an incipient neck that grows during deformation. It has been also used as a means to assess proposed mechanism of superplastic deformation by using the following constitutive equation:

$$\sigma = K \dot{\varepsilon}^m \qquad \text{Eq. 2.2}$$

where *K* is a material constant and *N* (*=1/m)* is the stress exponent. It should be noted that *m* is not a constant over more than one decade of strain-rate and increases with increasing forming temperature (T) and decreasing grain size (d) [19,20]. Thus a specific value of *m* is not characteristic of the material and only serves as an index of the rate effect on flow stress at a particular testing condition and microstructure employed.

Strain rate or velocity jump tests are used for the determination of *m* [5]. Stress relaxation tests are also used to measure strain rate sensitivity index [21]. The procedure involves the plastic deformation of the solid to some chosen stress level followed by stopping the cross head and observing the continuity in the stress as a function of time. Typical values of strain rate sensitivity [1] for different SP alloys are: (a) aluminum: 0.4-0.6, (b) titanium: 0.6-0.8 (c) copper: 0.35-0.5 (d) nickel alloys: 0.4-0.65.

2.2 Grain Size

The degree of superplasticity in engineering alloys is influenced by grain size and grain size distributions as grain boundary sliding accompanied by diffusion or dislocation glide is

believed to be the dominant mechanism in the superplastic region II. For metals and their alloys to exhibit superplastic phenomenon, a fine grain size of approximately 5 to 10 microns is necessary [22]. However, superplasticity is still observed in metals for grain sizes up to 20 microns and a grain size of less than 1 micron is typical in case of ceramics exhibiting superplasticity. In the presence of a suitable microstructure, superplasticity occurs over a narrow range of temperatures which generally is ~$0.5T_m$ [1]. A significant amount of grain growth during SPD can lower a material's strain rate sensitivity of flow stress and may result in premature failure [23]. The strain rate during SPD increases as grain size decreases when grain-boundary sliding (typical for region II) is the rate controlling process. The strain rate is generally inversely proportional to the grain size to the second or third power [3], i.e.,

$$\dot{\varepsilon} \propto d^{-p} \qquad \text{Eq. 2.3}$$

where *p* (grain growth exponent = 2 or 3) is a characteristic of micromechanism of deformation. It is the inverse exponent of grain size, suggesting that the grain size has an inverse proportionality with flow stress. When the grain size is large, p takes very small values (~ 0) [24]. Higher the value of p, more is the resistance offered to necking and thus higher is the stable deformation.

Grain growth in SP materials is driven by a decrease in surface energy and accommodated by grain boundary migration. The rate at which a grain boundary migrates depends on the mobility of the grain boundary and on the magnitude of the driving force. The gradient in chemical potential across a grain boundary acts as the driving force for grain growth. The system energy decreases and the grain size increases when atoms diffuse to the lower potential. The energy may be categorized as stored energy (cold work induced dislocations), elastic strain and grain boundary curvature [25].

2.2.1 Grain Growth Modeling

Based on grain boundary sliding accompanied by diffusion and / or dislocation glide mechanisms, several models [5,26,27] were proposed. A combination of these mechanisms was

developed to account for the increase in grain anisotropy at higher strain rates and is assumed that the combination controls the relatively narrow range in strain rate between the two extremes. These models not only predicted the resulting final microstructure but also could predict the stress-strain rate response. Investigations lead to the conclusion that static grain growth does not account for all of the microstructural evolution occurring during SPD [25]. Clark and Alden [28] proposed the "excess vacancy" model which suggests that grain boundary sliding during SPD will increase the concentration of vacancies on the boundary. These additional vacancies increase the diffusivity of solute atoms along the boundary migration rate. They could observe consistent equiaxed grain morphology throughout SPD. Several studies also suggest that concurrent grain growth during SPD is significantly more rapid than static grain growth [10,28,29,30]. Strain induced grain growth generally causes strain hardening which, in addition to high strain rate sensitivity, also provides an increased resistance to strain localization and thus may lead to increased ductility.

Two basic models of grain growth have been considered during this project. One of which is a simple linear relationship accounting for only dynamic grain growth (d) with strain (ε), as proposed by Caceres and Wilkinson [31] for copper alloys was used. They proposed that grain boundary sliding creates damaged zones, and that the grain boundary migrates to consume these regions leading to grain growth. The same model was also used by Li et al [30] to account for grain growth in aluminum alloys. Several other studies also suggested that concurrent/dynamic grain growth is significantly more rapid than static grain growth [10, 28].

$$d = d_o + c\varepsilon \qquad \text{Eq. 2.4}$$

where, "c" is an empirical constant obtained by fitting the model to experimental data and d_o is the initial grain size. This model was used in our study while developing the stability criterion for Copper and Aluminum alloys. The other grain growth model was proposed by Hamilton [32], which suggests that the total grain growth kinetics ($\dot{d}$) results from static grain growth rate ($\dot{d}_S$) and the deformation enhanced grain growth rate ($\dot{d}_d$). The static grain growth is assumed to follow the kinetics of particle stabilized growth rates [8] and is used to account for thermal exposure during SPF process. Clark and Alden [28] proposed a model for the deformation

enhanced grain growth kinetics, which assumes that the grain boundary mobility is increased due to an increase in the grain boundary vacancy concentration resulting from grain boundary sliding. The total grain growth rate can thus be expressed as:

$$\dot{d} = \dot{d}_s + \dot{d}_d = \frac{B}{d^q} + \frac{k_4(1-e^{-t/\tau})}{d^q}\dot{\varepsilon} \qquad \text{Eq. 2.5}$$

where q is a constant, B is a function of temperature; k_4 represents the vacancy generation rate and τ is the vacancy relation time.

2.3 Cavitation and Its Modeling

Cavitation is the phenomenon of internal void formation, which generally occurs within metallic materials during secondary working and superplastic deformation. Most of the SP materials exhibit this phenomenon and these include alloys of aluminum, copper, iron, lead, silver, titanium and zinc [1,12]. It has been postulated that internal imperfections (cavities) in solids are generated by the nucleation and growth of voids. Cavitation is considered to be an application limiting factor for the products manufactured by SPF technology, as excessive cavitation not only leads to premature failure but also adversely affects the mechanical properties of the final product, particularly in certain high strength applications[10, 33].

The morphology of cavities formed during SPD depends upon the type of material being considered and also the strain rate at which they are deformed. In general, three types of cavities have been observed in SP materials, which include:

1. Spherical voids with radii up to ~ 100 microns
2. Elliptical voids elongated parallel to the tensile axis with lengths up to ~ 50microns and aspect ratios from 2:1 to10:1
3. Groups of angular or crack like cavities, each up to 10 microns in length, interlinked around clusters of grains.

Cavitation occurs in three phases: nucleation, growth of existing and nucleating cavities and coalescence. Most of the cavitation models related to the above processes were originally developed for the prediction of creep life in coarse microstructures. However, creep concepts cannot be used to model SP cavitation, due to vast difference in deformation conditions between creep and SP deformation. The extent of cavitation is characterized by the sum of the growth of pre-existing cavities and growth of nucleating cavities during deformation. It depends on several factors which include strain-rate, temperature, strain, stress state, besides several metallurgical factors [20, 31].

2.3.1 Cavity Nucleation

Strain is accumulated during SPD deformation primarily as a result of grain boundary sliding (GBS) [1]. Cavities nucleate when the kinetic of accommodating GBS fail to match the requirements imposed by the deformation rate, as the stresses developed do not relax sufficiently fast. Presence of microstructural defects such as grain boundary ledges, triple points and intergranular particles, contribute substantially in raising the stress level local to the sliding grain boundaries. Nucleation of cavities is related to debonding along certain particle-matrix interfaces and is strain controlled. Debonding between particle and matrix can occur during heavy cold rolling to produce sheet. Possible cavity nucleation mechanisms include: (a) intragranular slip interactions with non-deformable second phase particles and grain boundaries, (b) continuous condensation of vacancies on grain boundaries which experience a normal tensile stress and (c) by vacancy clustering due to the stress concentration on grain boundary inclusions produced by strain incompatibility and GBS [20,33]. Factors which influence cavity nucleation include: grain size, type, volume fraction and distribution of hard particles, the proportions and physical properties of the major phases besides strain, strain rate, temperature and stress state.

Most studies consider a constant nucleation rate or a constant number of nucleating cavities during the deformation [1, 33, 34]. The cavity nucleation rate is generally bracketed between 10^4 and 10^6 cavities/mm^3/unit strain increment. However, it is often found that the population density of cavities increases with strain [35,36,37]. This phenomenon is termed as

“continuous nucleation”. The number of cavities is generally found to increase at higher strain rates and at lower test temperatures [20]. This is due to the higher flow stresses, reduced strain rate sensitivity and poorer diffusional accommodation process.

However, it should be noted that the even though cavities may be nucleating immediately after the deformation begins, they become optically resolvable only after certain strain. It was observed [20] that newly emerging cavities begin to appear after an initial strain of ~ 0.2 in aluminum alloys. Once the deformation surpasses this strain level, the number of cavities steadily increases with strain under all test conditions. This initial strain value emerges by achieving decohesion at the particle-matrix interface in the early stage. The number of cavities nucleating depends on the size of the constrained zone of plastic deformation near the particle interface and is a function of particle size [36]. Larger particles and larger interface defects induce more rapid decohesion with increasing strain, while smaller particles have a smaller constrained zone and thus require more strain to produce complete debonding. Another aspect of nucleation: the cavity formation frequency increases with increasing strain-rate. This strain-rate effect on continuous nucleation is directly related to a higher strain rate for constrained plasticity near the particle interface, which is believed to be related to higher deformation stresses in the matrix. This condition also reduces the strain-rate sensitivity and diffusional accommodation process at the particle-matrix interfaces, thereby assisting interface debonding.

2.3.2 Cavity Growth

Cavity growth is a result of diffusion controlled mechanism and/or plasticity controlled mechanism [38]. According to the existing models for cavity growth, growth by diffusion of vacancies along grain boundaries into the cavity is believed [39] to occur in early stages. It is observed that subsequent growth of cavities occurs by plastic deformation of the surrounding matrix [40,44], or by a coupled diffusion-plasticity process [35] . Cavities growing by diffusional growth mechanism will be rounded while those growing by a power-law growth mechanism tend to be elongated along the tensile axis [12]. However, it is established that diffusional growth dominates when the cavity size is small (below 1 micron). As the cavity size increases,

diffusional growth decreases very sharply and plastic flow of the surrounding matrix becomes the dominant cavity growth mechanism. From an engineering stand point, due to large deformations associated with SPD, plasticity controlled growth is of greater interest [1,33,41,42, 43]. Growth of an interface defect by plasticity controlled mechanism is a preferred concept for cavity formation because (a) it is energetically more favorable than breaking atomic bonds under high hydrostatic tension, and (b) debonding occurs only at a limited number of particles, while the development of hydrostatic tension is expected to affect all particle interfaces. Also, at higher test temperatures, cavitation tendency of the material is reduced rather than increased as predicted by the diffusional growth mechanism [14]. Thus, plasticity controlled model for the void growth of an isolated, noninteracting cavity under uniaxial tensile deformation is given by:

$$f_a^P = f_{ao}^P \exp(\eta\varepsilon) \qquad \text{Eq. 2.6}$$

where, f_a^P is the current/instantaneous area fraction of pre-existing cavities, f_{ao}^P is the initial area fraction of pre-existing cavities and η is the void growth parameter which is given as follows [44]:

$$\eta = \left(\frac{m+1}{m}\right)\sinh\left(\frac{2(2-m)}{3(2+m)}\right) \qquad \text{Eq. 2.7}$$

The above relation between η and m was derived by Cocks and Ashby [44] for a planar array of spherical, noninteracting, grain boundary cavities under tensile straining conditions. Studies on modeling cavity growth deduced the following observations [45]: the growth of the cavity is related to the strain and strain rate sensitivity only, greater the strain rate sensitivity, slower is the cavity growth, the radius of a cavity increases with increase in strain and the variation of the radius or volume growth of a separate cavity during SPD follows an exponential law. They also suggested that the difference between experimental and theoretical values was due to the interaction effects between the adjacent cavities. It should also be noted that there are numerous

voids having extremely small size in the superplastically deformed materials. Hence this may also be responsible to the discrepancy between the experimental and predicted values.

2.3.3 Cavity Coalescence

Cavity coalescence is the interlinkage of neighboring cavities due to a microscopic flow-localization process within the material ligament between them [1,33]. An interesting aspect of SP materials is the apparent resistance to cavity interlinkage, enabling these materials to tolerate considerable cavitation, on account of high strain rate sensitivity associated with SP materials. When two or more voids coalesce the void produced is larger than either of its constituent voids [46]. However, the effect of a sudden increase in the growth rate of a number of isolated voids on the rate of increase of the total void volume fraction is offset by a decrease in the total number of voids. Hence there would be no net change in the rate of increase in the total void volume fraction with strain. Mean void growth rate increases with void coalescence, as large isolated cavities which are most likely to have an adverse effect on the post forming mechanical properties of SP alloys are created by void coalescence. Coalescence can occur along both longitudinal and transverse directions; with the latter being the more important one as it eventually leads to failure.

Factors on which coalescence during SPD depends include: size of cavities, number of cavities per unit density (population density) and the spatial distribution of the cavities within the material. At low fractions of cavities, cavity coalescence has a negligible effect on the mean cavity growth rate, but becomes much more significant with increase in fraction of cavities. However, it is not possible to calculate the variation of the volume fraction (or area fraction) of cavities with strain without a quantitative understanding of the functions describing the distribution of void sizes, the overall population density of cavities and their variation with strain. Several studies attempted to model cavity coalescence [1,46], by considering a distribution of stationary, randomly located cavities of various sizes which grow with strain. Further studies were carried to model cavity coalescence process within a tensile specimen through an analysis of (a) the temporal and spatial location of cavities inside the specimen, and

(b) the temporal cavity radius [47]. They assumed coalescence to occur as soon as the material ligament between two neighboring cavities was exhausted. The new cavity radius was calculated by assuming conservation of volume.

$$r_c^3 = r_i^3 + r_j^3 \qquad \text{Eq. 2.8}$$

in which r_c represents the radius of the cavity formed by coalescence of cavities with radii r_i and r_j.

X-ray microtomography was used for 3D characterization of the coalescence process [48]. They variation of number of cavities in the investigated volume with strain was used as a parameter to characterize the coalescence process during SPD. A significant interlinkage between the cavities was confirmed from the continuous decrease in the number of cavities after surpassing a certain strain value (~ 1.1). They observed the formation of a single cavity due to interlinkage which represented up to 75% of the total volume fraction of cavities. The ratio between the volume of the largest cavity in the investigated volume and the corresponding total volume fraction of cavities called the “Interlinkage” parameter was defined to describe the coalescence process.

2.4 Constitutive Models

For SPF to emerge as an efficient manufacturing technology there is a need for accurate numerical models to describe the deformation during SPF and also to investigate the stability during SPD. Simple and accurate constitutive models which can describe deformation under multi-axial loading conditions as encountered during real forming operations are required [49]. Thermomechanical constitutive equations of SP materials should describe the relationship between flow stress, strain, strain-rate, temperature and other microstructural quantities which include grain size and cavitation [50]. Thus in case of SP materials, a relation involving $\sigma - \dot{\varepsilon} - \varepsilon$, taking into account temperature, strain hardening/softening, grain growth (static and dynamic), cavitation (nucleation, growth and coalescence), deterioration in post-deformed

thermo-mechanical properties, is necessary to model the deformation. Constitutive equations for SP materials can be broadly classified into two categories: (a) Phenomenological constitutive equations and (b) Physical or microstructure based constitutive equations [51]. Phenomenological equations are formulated based on a given set of experimental data to describe stress-strain curve within the area of their applicability, without considering the micro-mechanisms of SPD. Standard power law model, Polynomial models, Smirnov's model, Mechanistic model etc. qualify under phenomenological models. Physical constitutive equations are models characterizing SP flow by considering microstructural parameters (Burgers vector, GBS etc). Amongst several models which qualify under this category, the models proposed by Hamilton [32] and Ghosh [52] are the most common and standard models to describe SPD. SPD models are also classified based on either continuum mechanics or atomistic mechanics. Continuum mechanics based models are of two types: (1) one which considers macroscopic response of SP materials to mechanical forces and (2) one which accounts for measured values of activation energy of flow. Atomistic models are classified into four types: (1) diffusion creep models, (2) modified dislocation creep models, (3) grain boundary deformation models and (4) multi-mechanism models [53]. A basic review of some of the important models is included below.

Flow of polycrystalline or multi-phase solids at elevated temperatures in terms of a non-Newtonian viscous matrix that contains a dispersion of plate-like flaws was modeled by Hart [54]. Combining the matrix and the flaws in a parallel format the following expression was developed:

$$\sigma = \sigma_o \left(y - (1-y)z\right)\dot{\varepsilon}^{\mu} \qquad \text{Eq. 2.9}$$

where σ_o and μ are phenomenological constants depending on the composition and temperature, y is the proportion of the material deforming in a non-Newtonian viscous manner and z is the stress ratio carried by the Newtonian and the non-Newtonian viscous elements respectively.

Ashby and Verall [27] developed a constitutive relation for SPD from basic energy balance principles. They combined observations of grain switching with experiments in bubble motion and developed a geometric model of the form, shown below:

$$\dot{\varepsilon} = \frac{K}{d^2}\left(\sigma - \frac{0.72\Gamma}{d}\right) D_L \left[1 + \left(\frac{3.35}{d} \cdot \frac{D_{gb}}{D_L}\right)\right] \qquad \text{Eq. 2.10}$$

They then expanded the model to include three basic regions (I, II, III) of superplasticity. This equation quantifies regions I and II. At higher strain rates, SPD of region II transitions to power law creep (PLC)-region III. Ashby and Verall proposed the following relation to quantify region III:

$$\dot{\varepsilon}_{PLC} = A \cdot \frac{D_L G b}{kT}\left(\frac{\sigma}{G}\right)^n \qquad \text{Eq. 2.11}$$

Avery and Backofen [55], combined the movement of dislocations across the grains and vacancy migration within the grains leading to viscous flow, to express the strain rate as follows:

$$\dot{\varepsilon} = A \sinh(Bq) + C\sigma \qquad \text{Eq. 2.12}$$

where A, B and C are material constants. However, the drawback of this model is its applicability to a small range of strain rates. This model was then modified to describe SPD over a wider range of strain rates by including a term accounting for grain-size dependence. The expression can be expressed as:

$$\dot{\varepsilon} = \frac{A'\sigma^2}{d^3} + B'\sigma^2 \sinh\left(\beta'\sigma^{5/2}\right) \qquad \text{Eq. 2.13}$$

where $A', B' \text{and} \beta'$ are material constants and d is the average grain size. The first term in the above expression accounts for grain boundary migration. This is more significant at low stresses.

The second term accounts for dislocation climb controlled creep and is more significant at high stress and high strain rates.

Mukherjee [56] proposed a model for steady state strain-rate, accounting for activation energy and temperature, as expressed below:

$$\dot{\varepsilon}_s = C\left(\frac{\sigma}{G}\right)^n \exp\left(-\frac{Q}{RT}\right) \qquad \text{Eq. 2.14}$$

where C is a constant, G is the shear modulus, n is an exponent, Q is the activation energy, R is Boltzman's constant and T is the absolute temperature. Suery and Baudelet [57] incorporated rheological and metallurgical relations describing SPD, to develop a more generalized model, as expressed below:

$$\dot{\varepsilon}_s = C'\left(\frac{\sigma-\sigma_o}{d^a}\right)^n \exp\left(-\frac{Q}{RT}\right) \qquad \text{Eq. 2.15}$$

where σ_o is the threshold stress, d is the initial grain size and a is an adjustable exponent. They extended the present model to accommodate for structural changes during SPD, by introducing functions representing deformation-enhanced grain growth.

Investigators like Hamilton et al [32], developed constitutive models by combining mechanical parameters with microstructural aspects to describe SPD based on sigmoidal curve shown in Figure 2-1.a. The constitutive relation developed was based on the assumption that independent deformation mechanisms may act within superplastic strain rate region II and power-law creep region III and the total strain rate is therefore the sum of these [27], which is expressed as follows:

$$\dot{\varepsilon}_{Tot} = \dot{\varepsilon}_s + \dot{\varepsilon}_c \qquad \text{Eq. 2.16}$$

where $\dot{\varepsilon}_{Tot}$ is the total observed strain rate, $\dot{\varepsilon}_s$ is the superplastic strain rate corresponding to region II and $\dot{\varepsilon}_c$ is the creep strain rate, corresponding to region III. Both components are

functions of stress, temperature, diffusivity and material parameters. Thus, the final form of the model assuming grain boundary diffusion and isothermal deformation can be expressed as:

$$\dot{\varepsilon}_{Tot} = \frac{K_2 (\sigma - \sigma_o)^{1/m}}{d^p} + K_3 \sigma^n \qquad \text{Eq. 2.17}$$

where σ_o is the threshold stress, m is the strain rate sensitivity, n is the stress exponent, p is the grain growth exponent, and K_2 and K_3 are material constants. It can be seen that the first term accounts for grain growth unlike the creep strain rate component. The above model accounts for all three regions of the sigmoidal curve.

Ghosh [52], proposed a new approach to describe SPD based on grain boundary sliding via grain mantle deformation. The accommodation of stress concentration at grain boundary ledges, particles and triple points is believed to occur by dislocation creep involving glide and climb. It was assumed that the overall that the overall superplastic creep strain rate is the sum of mantle and core deformation and is expressed as:

$$\dot{\varepsilon} = \dot{\varepsilon}_m + \dot{\varepsilon}_c \qquad \text{Eq. 2.18}$$

$$\dot{\varepsilon} = \frac{A}{d^2}(\sigma - \sigma_o)^{1+q} + \left(1 + \frac{A}{d^3}\right)\sigma^n \qquad \text{Eq. 2.19}$$

where A, q, A_1, n are material constants and are generally evaluated from macro-experiments, while suffixes m and c correspond to the mantle and core regions. The model could accurately predict stress-strain rate characteristics of metals with fully and partially recrystallised microstructures and strain hardening characteristics. The details of grain growth kinetics and flow stability were also simulated well.

Caceres and Wilkinson [58], suggested a simple constitutive expression for describing SPD. It can expressed as follows:

$$\dot{\varepsilon} = K\sigma^{n} d^{-p} \qquad \text{Eq. 2.20}$$

where σ is the flow stress required to produce the desired strain rate, d is the grain size, while K, n, p are material constants. This expression suggests that grain growth during deformation results in an increase on flow stress. Understanding the significance of cavitation and its ability to restrict the applications of SPF products, they incorporated the level of cavitation into the constitutive expression, which can be expressed as:

$$\dot{\varepsilon} = K\left(\frac{\sigma}{(1-f_a)}\right)^{n} d^{-p} \qquad \text{Eq. 2.21}$$

where f_a refers to area fraction of cavities, which has its own evolution equation.

Khaleel et al [59] proposed a viscoplastic model for describing deformation and damage during SP flow, based on a continuum mechanics approach. The model includes the effect of strain hardening, strain rate sensitivity, dynamic and static recovery, nucleation and growth of voids. They also compared their predicted values with those obtained experimentally. They proposed the following simple expression for overstress function (f):

$$f = \left(\frac{J-(k_o+R)}{C(T)}\right)^{1/m} \quad , \text{for } J > K = k_o + R$$
$$f = 0 \quad , \text{for } J \le K \qquad \text{Eq. 2.22}$$

where k_o+R represents a reference stress whose variable part R represents isotropic hardening, m, C, k_o are material constants and T is absolute temperature. The evolution equation of R included hardening, dynamic recovery and static recovery terms. Using the definition of effective strain rate, the above equation can be rewritten as:

$$\dot{\bar{\varepsilon}} = \left(\frac{J - K}{\hat{C}} \right)^{1/m} \qquad \text{Eq. 2.23}$$

The overstress function (f) was modified to account for a voided material and is expressed as follows:

$$f = \left(\left(J - K\right)\left(1 - \xi^{1/2}\right) / C(T)\left(1 - \xi^{1/2}\right) \right)^{1/m} \qquad \text{Eq. 2.24}$$

where ξ is the volume void fraction parameter and its evolution equation accounted for both nucleation and growth of voids.

2.5 Stability Analysis of SPD

The widespread industrial application of SPF components is limited and hindered due to a number of issues including low production rate and limited predictive capabilities of stability during deformation and failure. In order to achieve maximum ductility, the part has to be formed at relatively low strain rates, i.e., slow forming - causing low production rate, which would adversely affect the overall economy. Forming at higher strain rates, though would decrease the forming time, it would affect the maximum attainable ductility. Hence it puts forth a challenge of forming the components as rapidly as possible while maintaining the required quality of the formed parts, such as eliminating localized thinning and rupture. The other significant limitation is that the available failure criteria for SP materials in the literature are either based on macroscopic geometrical instabilities or microstructural aspects. However, it is commonly observed that SP alloys fail under the influence of both modes of failure. The contribution of each failure mode to the overall deformation behavior depends on material parameters such as composition and microstructural features as well as on the process parameters such as strain rate and temperature. Thus in order to make SPF process a viable and a better route to manufacture a growing range of products, a detailed analysis on the stability and failure during SPD has to be carried out. Some of the studies which focused on this area are mentioned below, starting with

those which are based only on geometric considerations, followed by those based only on microstructural aspects.

Stability Analysis based on Geometrical considerations only:

Hart [60] presented a phenomenological theory of tensile deformation, including both the onset of unstable deformation and the rate of development of necking instabilities. He examined the stability of the deformation by describing the growth of an inhomogeneity in the unstable deformation regime. It was assumed that at any stage of deformation true stress (σ) is dependent on the previous strain history, and that small changes in σ depend linearly on the corresponding small changes of plastic strain (ε) and plastic strain rate $(\dot{\varepsilon})$. Thus, a possible constitutive equation in differential form as shown below was proposed:

$$d\sigma = \sigma_{\varepsilon}\, d\varepsilon + \sigma_{\dot{\varepsilon}}\, d\dot{\varepsilon} \qquad \text{Eq. 2.25}$$

The coefficients in the above expression are considered to be material parameters that depend on the specimen history and vary with deformation. The deformation was defined to be stable if the magnitude of the cross-section difference existing in the sample does not increase during the course of deformation. It is suggested that high ductility can be seen in materials which exhibit stable deformation. Hart defined the condition for stable deformation as follows:

$$\left(\dot{dA}/dA\right) \leq 0 \qquad \text{Eq. 2.26}$$

where $\dot{dA}$ is the variation in the incremental area rate and dA is the variation in cross-sectional area. Assuming constancy of volume and that the stress is a function of strain and strain rate only (not accounting for microstructural evolution), he derived the following stability criterion for stable deformation of SP materials for a uniaxial loading case:

$$\gamma + m \geq 1 \qquad \text{Eq. 2.27}$$

$$\gamma = \frac{1}{\sigma}\left(\frac{\partial \sigma}{\partial \varepsilon}\right)_{\dot{\varepsilon}} \qquad \text{and} \qquad m = \frac{\dot{\varepsilon}}{\sigma}\left(\frac{\partial \sigma}{\partial \dot{\varepsilon}}\right)_{\varepsilon}.$$

The first term in the above equation represents strain hardening exponent and the second term represents the strain rate sensitivity. Hart showed that the local nonuniformity in area is caused by uniform, uniaxial straining in the incipient neck and showed that onset of instability occurs when:

$$\gamma + m = 1 \qquad \text{Eq. 2.28}$$

The above equation allows one to consider Newtonian-viscous material $(\gamma = 0, m = 1)$ to represent the limiting form of "stable flow".

Duncombe [61] defined plastic instability as the growth of a locally thinned region or neck in a material upon application of stresses. The study analyzed groove type instability using linearization techniques. The effects of strain hardening, strain rate sensitivity and material anisotropy were included. This geometrical stability criterion analyzed both the onset and the rate of development of local thickness inhomogeneities under biaxial loading, based on the following definition of instability:

$$\delta\left(\dot{A}/A\right) = 0 \qquad \text{Eq. 2.29}$$

That is, the point at which the variation in strain rate starts to increase was chosen as the point of onset of instability. For a uniaxial, isotropic case, his theory suggests, the onset of instability occurs when:

$$\gamma = 1 \qquad \text{Eq. 2.30}$$

The above expression predicts that the beginning of instability is totally independent of strain rate sensitivity.

Ghosh [62] analyzed tensile instability based on maximum load consideratio. He defined tensile deformation as stable, as long as it is accompanied by a load rise, even though an imperfection in it may be growing during this stage. The onset of instability is therefore at the maximum load, which, for a perfect specimen deforming at constant strain-rate occurs when the well-known Considere condition ($\gamma = 1$) is satisfied. However, for tests at constant crosshead speed, maximum load for perfect specimens is satisfied when the following condition is satisfied:

$$\gamma - m = 1 \qquad \text{Eq. 2.31}$$

The above model suggests that the onset on instability depends on "m". Thus the effect of m on the strain to reach instability may be beneficial, detrimental or consequential depending on one's choice of definition. The above equation is less general, as it strictly applies to a constant extension rate tensile test.

Nichols [63] presented a unified survey, considering both geometric and pre-straining types of necks and also included the aspects of both onset of instability and the rate of propagation of instabilities. The criteria developed on the basis of Hart's was appropriate for ascertaining the onset of uniaxial tensile instabilities in various types of tests on isotropic tensile bars using the long-wavelength, uniaxial stress approximation and can be expressed as:

$$\delta\dot{A} = -\frac{\dot{\varepsilon}}{m}(\gamma + m - 1)\,\delta A - \frac{\gamma f\,\dot{A}}{m} \qquad \text{Eq. 2.32}$$

Swift [64] and Hill [65] introduced instability criteria for diffuse and local instability respectively. Though these criteria present an insight into the gross limits of sheet metal formability, they are incapable of describing the rate of flow localization following instability and are applicable only when the imposed strain path is such that $\rho^* \leq 0$ (where $\rho^* = d\varepsilon_2/d\varepsilon_1$).

The famous M-K [66] analysis deals with strain paths characterized by $\rho^* > 0$ representing the stretching regime of the forming limit diagram. They postulated the presence of a material imperfection at which a shift in strain rate from $\rho^* > 0$ to $\rho^* = 0$ occurs and hence permit a localized neck to form. They could formulate and visualize the growth of a geometric imperfection by considering material related imperfection like variation in hardness, strain hardening index etc. However the forming limit diagrams predicted by M-K analysis is strictly applicable to a sheet deformed/stretched in a plane and not punch stretched. Storen and Rice [67] analysis does not postulate the imperfection but treated the onset of localized necking for $\rho^* > 0$ as a bifurcation problem that occurs as a result of development of a corner or vertex on the yield locus.

Stability analysis based on Microstructural aspects:

Several studies [68,69,70] have suggested that ductile materials fail due to the growth of holes/voids. It was observed that the fracture due to growth of holes becomes dominant when the size of inclusions becomes large enough to be observed under a microscope. In ductile fracture by the growth of holes, changes in size, shape, and spacing of the holes will depend on the entire history of stress, strain and rotation [71].

McClintock [71] assumed that the material contains three mutually perpendicular sets of cylindrical holes of elliptical cross section with axes parallel to the principal directions of the applied stress and strain increment. It was also assumed that most of the applied strain occurs while the holes are still small enough so that their interactions with each other may be neglected. Thus the problem was reduced to a generalized plane strain deformation of a void in an infinite medium. He then derived a fracture criterion for an elliptical hole under the condition of constant stress ratio as follows:

$$F = \frac{R}{R^o}\frac{\left(1+m'\right)}{\left(1-m'^o\right)}e^{-\varepsilon} \qquad \text{Eq. 2.33}$$

where F is the relative hole growth factor, R [= (a+b)/2] is the mean radius of an elliptical hole and m′ [= (a-b)/(a+b)] is the eccentricity of the elliptical hole and the superscript 'o' depicts when the holes are initially round. He further extended the criterion for the case of varying stress ratios.

Void nucleation and growth are commonly observed in processes which are characterized by large local plastic flow, such as ductile fracture [72]. Gurson, A.L. [73] developed an approximate yield criteria and flow rules for porous (dilatant) ductile materials, showing the role of hydrostatic stress in plastic yield and void growth. The yield criteria were approximated through an upper bound approach. Different void geometries like circular and elliptical are considered while developing the model. In a subsequent paper he proposed a model which accounts for void nucleation, plastic flow and hardening behavior in ductile materials.

Perzyna [74] described ductile fracture as the final stage of necking process and is preceded by the nucleation of voids at the second phase particles , growth of voids due to plastic deformation and yield stress state and also interlinkage of voids. He proposed a simple model for an elastic-viscoplastic solid with internal imperfections. The developed model was within the internal state variable structure as well as within the rate type structure. The symmetric rate of deformation tensor **D** was postulated as:

$$\begin{aligned} \mathbf{D}^{e} &= \mathbf{D} - \mathbf{D}^{p} \\ \mathbf{D}^{e} &= \frac{1}{2G}\left[\hat{\sigma} - \frac{\upsilon}{1+\upsilon}\mathrm{tr}\hat{\sigma}\mathbf{I}\right] \\ \mathbf{D}^{p} &= \frac{\gamma_{o}}{\varphi}\left\langle \phi\left(\frac{f\left(J_{1}, J_{2}', J_{3}', \xi\right)}{\kappa}\right) - 1\right\rangle \partial f \end{aligned} \qquad \text{Eq. 2.34}$$

where $\hat{\sigma}$ denotes the symmetric rate of change of the Cauchy stress tensor σ, G is the shear module, υ is the Poisson ratio, γ_o is the viscosity constant, φ is interpreted as the control function. $\kappa = \hat{\kappa}(\xi)$ denotes a material function, where ξ denotes the imperfection internal state

variable which is interpreted as the void volume fraction parameter. The evolution equation of ξ is assumed to be of the form as shown below:

$$\dot{\xi} = \dot{\xi}_{\text{transport}} + \dot{\xi}_{\text{nucleation}} + \dot{\xi}_{\text{growth}} \qquad \text{Eq. 2.35}$$

The transport phenomena in solids are important only at elevated temperatures; nucleation of voids is connected with the inelastic power and with the rate of the first invariant of the stress tensor while the growth of voids during the inelastic flow process is mainly implied by the inelastic strain rate.

Stability analysis based on Geometrical and Microstructural aspects:

Limited studies are found in literature which focuses on developing a stability criterion incorporating both geometrical and microstructural aspects of failure. Even in these limited studies not all important aspects of failure are incorporated. Some of these studies are discussed below:

Jonas and Baudelet [75] proposed a generalized equation of plastic stability that is valid in presence of mechanical and machining defects. Mechanical defects include work hardening due to mechanical damage while machining defects refer to geometric faults due to machining variations. The analysis was later extended to include the generation of spherical and planar defects during straining, as they could lead to more rapid flow localization which increases the tendency towards tensile instability. The form of the expression they developed can be expressed as:

$$m\left(\frac{\partial \ln \dot{A}}{\partial x}\right)_t = \left(\frac{\partial \ln A}{\partial x}\right)_t [\gamma + m - 1] - \gamma \frac{d \ln A_o}{dx} \qquad \text{Eq. 2.36}$$

However, it should be noted that the above model does not account for grain growth which has been experimentally proved to have a significant influence on the stability and failure during SPD.

Ding et al [14] modified Hart's stability criterion in order to account for grain growth besides geometrical instabilities. They accomplished the task by considering a microstructure based constitutive equation (Eq. 2.17) as proposed by Hamilton et al [32] coupled with a grain growth equation accounting for both static and dynamic components of grain growth as expressed by Eq. 2.5. The modified stability criterion for SP materials at the onset of instability is developed following Hart's [54] methodology and it is be expressed as follows:

$$\gamma' + m' = 1$$
$$\gamma' = \frac{\dot{d}}{\dot{\varepsilon}^2}\left(\frac{\partial \dot{\varepsilon}}{\partial d}\right)_{\sigma} \quad \text{and} \quad m' = \frac{\sigma}{\dot{\varepsilon}}\left(\frac{\partial \dot{\varepsilon}}{\partial \sigma}\right)_{d} \qquad \text{Eq. 2.37}$$

where γ' represents strain hardening due to grain coarsening and m' represents inverse of the strain rat sensitivity (m). However, it should be noted that the above model for SP materials, does not account for cavitation which is an important and possible mode of failure in SP materials.

2.6 Optimum Forming Paths for SP materials

In order to make SPF an economically viable manufacturing process, rate of production must be increased without sacrificing the ductility of the material as well as maintaining the required quality of the product, like eliminating localized thinning and rupture [14,76]. Several factors which affect the quality of the formed parts, like – material flow properties, process parameters, geometry and friction effects, must be considered in practical forming operations. This led to an increased interest in numerical models which could predict the forming characteristics and establish forming parameters, such as gas pressure application to control strain rate and eventually optimize the forming process.

Hamilton et al [32] found quite different elongations are often found for different strain rate paths for the same initial strain rate. Thus, superplastic ductility was found to depend on the strain rate path. Ren et. al [77] have shown that by designing a strain rate path based on

experimentally measured strain and strain rate parameters, a significant reduction in time for deformation to a relatively high strain could be achieved compared to constant strain rate forming, for Al-Li . Thus, a possible solution to the challenge of increasing the production rate while maintaining the desired material and mechanical properties - is to develop Optimum Variable Strain Rate Forming paths. This would mean to start forming at higher strain rates at initial strains as the effect of grain growth and cavitation are very small at low strains and thereafter form at reduced strain rates as the effect of microstructural aspects becomes dominant at higher strains. The optimum path would represent the upper bound/limit of strain rate at any given strain for stable deformation, i.e., the path represents the onset of instability for any strain value.

Johnson [25] developed optimum variable strain rate forming paths for SP Ti-6Al-4V alloy, by incorporating a microstructure based constitutive equation (Eq. 2.17) coupled with a grain growth equation accounting for both static and dynamic aspects (Eq. 2.5) into Hart's analysis and hence proved that a significant reduction in deformation time could be achieved when compared with constant strain rate forming. However the optimum paths designed did not account for cavitation.

The above review clearly suggests the significance of optimum variable strain rate forming paths in increasing the rate of production of components using SPF while maintaining the desired ductility. It also, indicates the lack of suitable model to generate these paths (in literature). This forms the prime basis of this research - to develop a multiscale stability criterion accounting for both geometrical and microstructural aspects of failure and thereby generate optimum variable strain rate forming paths for different SP alloys.

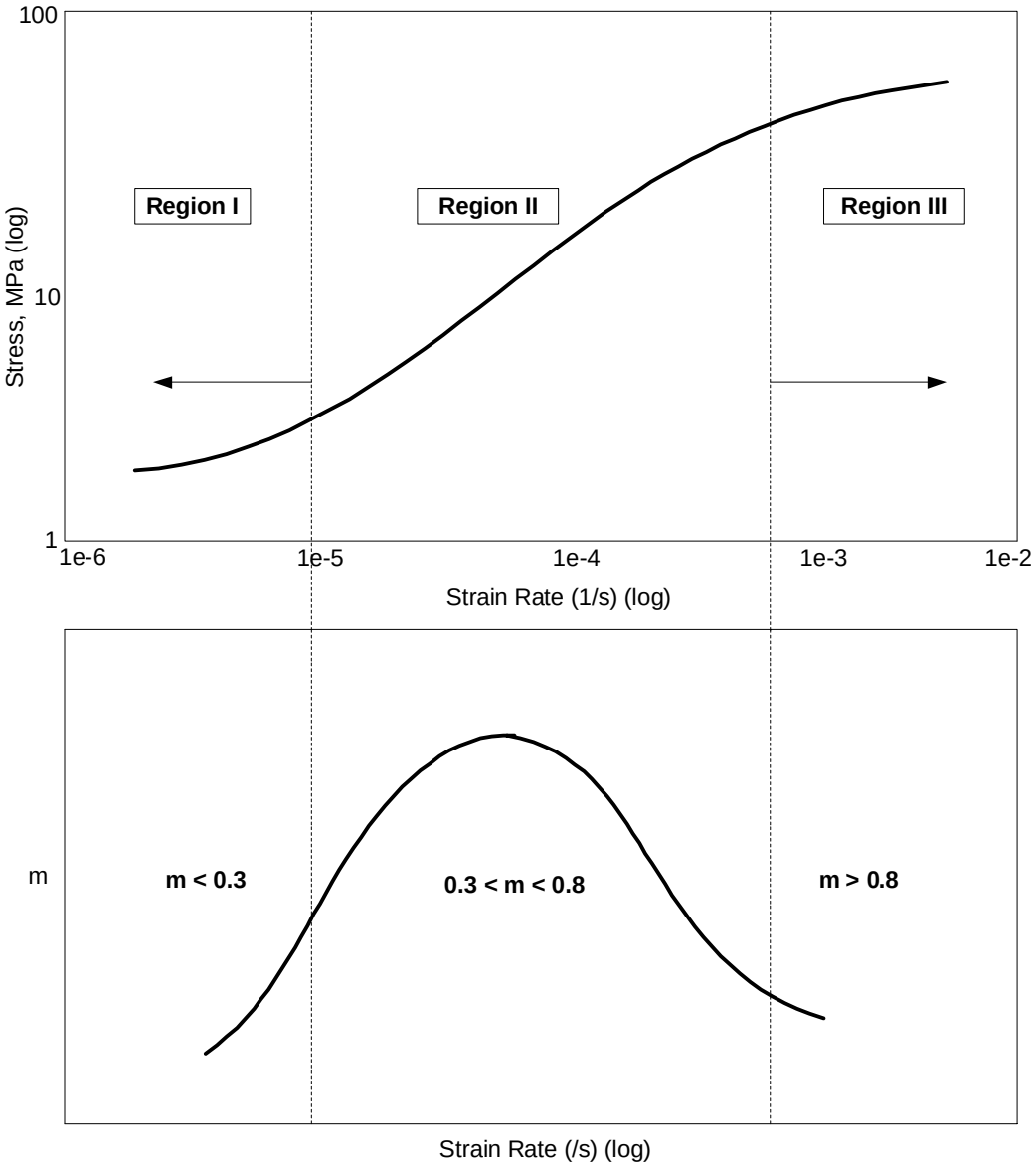

Figure 2-1 Typical Stress Strain rate relation for SP materials. Dependence of (a) flow stress, and (b) strain rate sensitivity index on strain rate

Chapter 3 Multiscale Stability Analysis and Optimization of SPF under Uniaxial Loading

Ability to form complex and intricate shapes makes SPF a better manufacturing route than most conventional forming methods which have proven to be inadequate in forming complicated shapes. SPF is typically conducted at high temperature and under controlled strain rate, can give a ten-fold increase in elongation compared to conventional room temperature processes. Because the forming temperature is above the annealing temperature, SPF components are dimensionally stable and free from residual stresses. To date, this forming technique has been applied most effectively in the aerospace industry were the high premium on structural optimization has justified the high cost of SPF-grade alloys, the long forming times associated with low allowable strain rates, and the lengthy trial-and-error process that is often used to develop a workable forming cycle. The development of low cost SPF alloys and the optimization of forming cycles through process simulation are critical factors in bringing SPF to wider application in different industries. Numerical modeling to predict deformation and failure characteristics like localized thinning and rupture during superplastic deformation has gained immense prominence. Modeling is also mainly used to predict forming parameters like the gas pressure application to control strain rate, study the effect of microstructural parameters on the stable deformation and eventually optimize the process. Thus, a major challenge is to form the products as rapidly as possible while maintaining the quality of the formed products. To this end, a possible solution is to design a variable strain rate forming path [14].

The main objective of the current work is to develop a multiscale stability criterion accounting for both geometrical instabilities (necking) as well as microstructural aspects including grain growth and cavitation, under uniaxial loading condition. This is achieved by incorporating a modified microstructure based constitutive model coupled with grain growth and cavitation evolution equations into Hart's [60] stability analysis.

3.1 Model Development

The model development is based on the frame work of Hart's stability analysis. Hart [54] developed a tensile stability criterion for materials exhibiting strain hardening and strain rate hardening. Hart used a simple constitutive equation (as discussed in chapter 2) in which the flow stress was a function of strain and strain rate only was used in developing the stability criterion.

If a load P is supported by a specimen of length L and A be the cross section area at any instant during deformation, then the stress (σ) is expressed as follows:

$$P = \sigma * A \qquad \text{Eq. 3.1}$$

Thus, time rate of change of load can be expressed as:

$$\dot{P} = \dot{\sigma}A + \sigma\dot{A} \qquad \text{Eq. 3.2}$$

Since the load P is same at all points and does not vary, rate of change of load would be zero. Thus the left hand side of the above equation becomes "0". Incremental change in strain and strain rate can be expressed as follows:

$$\delta\varepsilon = -\left(\frac{\delta A}{A}\right) \text{ and } \delta\dot{\varepsilon} = -\delta\dot{A}/A + \left(\dot{A}/A\right)\left(\delta A/A\right) \qquad \text{Eq. 3.3}$$

where δA is the variation in the cross-sectional area and $\delta\dot{A}$ is the variation in the area increment rate.

The functional form of constitutive equation for SP materials is an expression in which the superplastic strain rate is a function of flow stress (σ), strain (ε), grain size (d) and cavitation (e.g. area fraction of cavities f_a), and is given as:

$$\dot{\varepsilon} = f\left(\sigma, \varepsilon, d, f_a\right) \qquad \text{Eq. 3.4}$$

Differential form of the above equation can be expressed as:

$$d\dot{\varepsilon} = \left(\frac{\partial \dot{\varepsilon}}{\partial \sigma}\right)_{d,f_a} d\sigma + \left(\frac{\partial \dot{\varepsilon}}{\partial d}\right)_{\sigma,f_a} dd + \left(\frac{\partial \dot{\varepsilon}}{\partial f_a}\right)_{\sigma,d} df_a \qquad \text{Eq. 3.5}$$

It should be noted that the strain and grain size are interchangeable parameters in the model, as the effect of strain is implicitly accounted for through he grain growth model.

A simple form of the constitutive equation for SP materials, accounting for grain growth and cavitation is given by [31,41,7]:

$$\dot{\varepsilon} = \frac{k}{d^p}\left(\frac{\sigma}{(1-f_a)}\right)^{1/m} \qquad \text{Eq. 3.6}$$

where $\dot{\varepsilon}$ is the superplastic strain rate, σ is the superplastic flow stress, d is the grain size, m is the strain rate sensitivity, p is the grain size exponent, f_a is the area fraction of cavities and k is a material constant.

However, the deformation in some of the SP materials is better described by a constitutive equation that accounts for deformation in SP and creep regions. Hamilton [32] formulated a microstructure-based constitutive equation for SP materials based on the assumption that independent deformation mechanisms may act within the superplastic region II and the power law creep region III, as follows:

$$\dot{\varepsilon} = \frac{k_2}{d^p}[\sigma - \sigma_o]^{1/m} + k_3[\sigma]^n \qquad \text{Eq. 3.7}$$

where σ_o is the threshold stress, m is the strain rate sensitivity, n is the stress exponent, p is the grain growth exponent, and k_2 and k_3 are material constants. The above equation is formulated by incorporating the effect of grain-growth and threshold stress. The effect of strain hardening is embedded into this model as the effect of grain coarsening as predicted by the grain growth kinetics. Incorporating the effect of cavitation (as suggested in [31]), the above equation can be modified [76] as follows:

$$\dot{\varepsilon} = \frac{k_2}{d^p}\left[\left(\frac{\sigma}{(1-f_a)}\right) - \sigma_o\right]^{1/m} + k_3\left(\frac{\sigma}{(1-f_a)}\right)^n \qquad \text{Eq. 3.8}$$

The degree of superplasticity in engineering alloys is influenced by grain size and grain size distributions It is well known that concurrent/dynamic grain growth during SPD is significantly more rapid than static grain growth [10,28]. This strain-induced grain growth generally leads to strain hardening, which provides increased resistance to strain localization, and thus results in higher ductility. A possible model to account for grain growth in superplastic materials has the following simple form [30,31,76]:

$$d = d_o + c\varepsilon \qquad \text{Eq. 3.9}$$

where d represents dynamic grain growth, c is an empirical which depends on strain rate and ε is the superplastic strain. The differential form of the grain growth equation can be expressed as:

$$dd = c\,d\varepsilon \qquad \text{Eq. 3.10}$$

Alternatively, some of the studies indicate the importance of considering both static and dynamic aspects of grain growth [32, 52] into consideration, while accounting for the effects of grain growth on the stable deformation of SP materials. The total grain growth kinetics ($\dot{d}$) results from static grain growth rate ($\dot{d}_s$) and the deformation enhanced grain growth rate ($\dot{d}_d$). The static grain growth is assumed to follow the kinetics of particle stabilized growth rates [78] and is used to account for thermal exposure during SPF process. Clark and Alden [28] proposed a model for the deformation enhanced grain growth kinetics, which assumes that the grain boundary mobility is increased due to an increase in the grain boundary vacancy concentration resulting from grain boundary sliding. The total grain growth rate can thus be expressed as:

$$\dot{d} = \dot{d}_s + \dot{d}_d = \frac{B}{d^q} + \frac{k_4(1-e^{-t/\tau})}{d^q}\dot{\varepsilon} \qquad \text{Eq. 3.11}$$

where q is a constant, B is a function of temperature; k_4 represents the vacancy generation rate and τ is the vacancy relation time. Differential form of the above equation can be expressed as:

$$dd = \frac{k_4}{d^q}d\varepsilon \qquad \text{Eq. 3.12}$$

The evolution equation for the total area fraction of cavities (f_a^{Tot}) is a function of cavity area fraction due to nucleation $\left(f_a^N\right)$, cavity area fraction due to pre-existing voids $\left(f_a^P\right)$ and strain (ε) [59,73,74], and is expressed as:

$$f_a^{Tot} = f(f_a^N, f_a^P, \varepsilon) \qquad \text{Eq. 3.13}$$

The term representing the nucleation is different for constant nucleation and continuous nucleation cases, while the term representing the growth remains the same in both cases and is a function of strain rate sensitivity (m) and superplastic strain (ε). Thus the evolution equation for cavitation accounting for constant nucleation and growth is represented by the following equation:

$$f_a^{Tot} = f_{ao}^N \exp[\eta * (\varepsilon - \varepsilon_n)] + f_{ao}^P \exp(\eta\varepsilon) \qquad \text{Eq. 3.14}$$

Differential form of the above equation can be represented as:

$$df_a^{Tot} = f_a^{Tot}\, \eta\, d\varepsilon \qquad \text{Eq. 3.15}$$

In constant nucleation case, the effect of nucleation would come into account, only after the strains reached are greater than the nucleation strain. Once strains attained are more than the nucleation strain, a certain fixed number of cavities come into existence and they grow along with the pre-existing cavities.

The evolution equation accounting for continuous nucleation case and growth can be expressed as follows:

$$f_a^{Tot} = f_{ao}^N * (1 + \langle \varepsilon - \varepsilon_n \rangle) \exp[\eta * (\varepsilon - \varepsilon_n)] + f_{ao}^P \exp(\eta\varepsilon) \qquad \text{Eq. 3.16}$$

Differential form of the above equation can be expressed as follows:

$$df_a^{Tot} = \left(f_a^{Tot}\, \eta + f_{ao}^N \exp[\eta(\varepsilon - \varepsilon_n)]\right) d\varepsilon \qquad \text{Eq. 3.17}$$

The above model suggests that a certain number of cavities nucleate after reaching a certain critical strain and also that their number increases with an increase in strain. Thus, the model in total accounts for continuously nucleating cavities, their subsequent growth as well as the growth of pre-existing cavities. The term $\left(1+\left\langle \varepsilon-\varepsilon_n \right\rangle\right)$ in the evolution equation for continuous nucleation accounts for the increase in the area fraction of nucleating cavities with strain, hence incorporating the effect of continuous nucleation. However, the increase in area fraction of nucleating cavities takes place only after the strains reached exceed the nucleation strain. Mathematically, this condition can be expressed as:

$\left\langle \varepsilon-\varepsilon_n \right\rangle = 0, \qquad$ if $\varepsilon \le \varepsilon_n$

$\left\langle \varepsilon-\varepsilon_n \right\rangle = \varepsilon-\varepsilon_n, \quad$ if $\varepsilon > \varepsilon_n$

It is assumed that the area fraction of cavities due to constant nucleation of cavities is zero, until the term $\left\langle \varepsilon-\varepsilon_n \right\rangle$ becomes a positive value, while it is assumed to be zero until the term $\left(1+\left\langle \varepsilon-\varepsilon_n \right\rangle\right)$ becomes greater than zero, in case of continuous nucleation. Terms, f_{ao}^{N} is the initial area fraction of nucleating cavities, ε_n is the nucleating strain i.e., the strain from which the nucleation of cavities can be observed and hence measured, η is the void growth parameter which is a function of strain rate sensitivity and is given by the following expression [43]:

$$\eta = \left(\frac{m+1}{m}\right)\sinh\left(\frac{2(2-m)}{3(2+m)}\right) \qquad \text{Eq. 3.18}$$

By substituting the differential form of the strain rate increment (Eq. 3.3), differential form of grain growth (Eq.3.10 or Eq. 3.12) and differential form of cavitation (Eq.3.15 or Eq.3.17) into the differential form of the functional representation of the constitutive equation (Eq.3.5), we arrive at:

In case of Constant Nucleation:

$$-\frac{d\dot{A}}{dA}+\left(\frac{\dot{A}}{A}\right)\left(\frac{dA}{A}\right)=\sigma\left(\frac{\partial\dot{\varepsilon}}{\partial\sigma}\right)_{d,f_a^{Tot}}\frac{\partial\sigma}{\sigma}+c\left(\frac{\partial\dot{\varepsilon}}{\partial d}\right)_{\sigma,f_a^{Tot}}d\varepsilon+f_a^{Tot}\eta\left(\frac{\partial\dot{\varepsilon}}{\partial f_a^{Tot}}\right)_{\sigma,d}d\varepsilon \qquad \text{Eq. 3.19}$$

In case of Continuous Nucleation:

$$-\frac{d\dot{A}}{dA}+\left(\frac{\dot{A}}{A}\right)\left(\frac{dA}{A}\right)=\sigma\left(\frac{\partial\dot{\varepsilon}}{\partial\sigma}\right)_{d,f_a^{Tot}}\frac{\partial\sigma}{\sigma}+c\left(\frac{\partial\dot{\varepsilon}}{\partial d}\right)_{\sigma,f_a^{Tot}}d\varepsilon+\left(f_a^{Tot}\eta+f_{ao}^{N}\exp[\eta(\varepsilon-\varepsilon_n)]\right)\left(\frac{\partial\dot{\varepsilon}}{\partial f_a^{Tot}}\right)_{\sigma,d}d\varepsilon$$

Eq. 3.20

Hart [60] defined the condition for the deformation to be stable, if in the course of deformation the variation in the magnitude of the cross-sectional area does not increase, i.e.,

$$\left(\frac{d\dot{A}}{dA}\right)_p\le 0 \qquad \text{Eq. 3.21}$$

Applying this condition of stability to Eq. 3.19 or Eq. 3.20, the new multiscale stability criterion describing the condition for onset of instablity during deformation of SP materials, under uniaxial loading can be expressed as:

$$\gamma'+m'+\zeta'=1 \qquad \text{Eq. 3.22}$$

where

$$\gamma'=\frac{\dot{d}}{\dot{\varepsilon}^2}\left(\frac{\partial\dot{\varepsilon}}{\partial d}\right)_{\sigma,f_a^{Tot}},$$

$$m'=\frac{\sigma}{\dot{\varepsilon}}\left(\frac{\partial\dot{\varepsilon}}{\partial\sigma}\right)_{d,f_a^{Tot}} \text{ and}$$

$$\zeta'=\frac{f_a^{Tot}\eta}{\dot{\varepsilon}}\left(\frac{\partial\dot{\varepsilon}}{\partial f_a^{Tot}}\right)_{\sigma,d} \qquad \text{Constant Nucleation}$$

(or)

$$\zeta'=\frac{\left(f_a^{Tot}\eta+f_{ao}^{N}\exp[\eta(\varepsilon-\varepsilon_n)]\right)}{\bar{\varepsilon}}\left(\frac{\partial\dot{\varepsilon}}{\partial f_a^{Tot}}\right)_{\sigma,d} \qquad \text{Continuous Nucleation}$$

The first term in the above equation accounts for strain hardening due to grain coarsening, second term accounts for the effect of strain rate sensitivity and the third term accounts for cavitation effects. It should be noted that the above equation reduces to the basic Harts' criterion, when grain growth and cavitation effects are neglected (assuming no strain hardening and no cavitation).

3.2 Results and Discussions

Variable strain rate forming paths offer an optimum solution to form the components at a faster rate without compromising on the quality or strength of the formed components. Optimum forming paths are developed by simultaneously solving the stability criterion (Eq. 3.22) along with the microstructure based constitutive equation (Eq. 3.6 (or) Eq. 3.8) and the evolution equations for grain growth (Eq.3.9 (or) Eq. 3.11) and cavitation (Eq. 3.15 (or) Eq. 3.17). The partial differentials in the stability criterion are evaluated from the constitutive equation with respect to one factor, keeping the other two factors constant (from the three factors: stress, grain size and cavitation). This would evolve a critical strain at a particular constant strain rate. This critical strain would indicate the maximum strain that can be attained at a particular strain rate, initial grain size and initial levels of cavitation. The process is repeated for several constant strain rates and the corresponding critical strains are determined. The loci of these points would yield an optimum forming path for SP materials, which suggests that forming along or below the curve would ensure uniform and stable deformation. Effects of initial grain size, initial levels of cavitation, strain rate sensitivity, nucleation strain, and grain growth exponent on the optimum forming paths can be investigated. The proposed model can be applied to any SP material, provided the required parameters can be obtained from experimental studies. For the purpose of this study, primarily commercial SP copper alloy Coronze CDA 638 is chosen because of extensive cavitation exhibited by this alloy. In order to show the applicability of the model and stability criterion, optimum variable strain rate forming paths for SP titanium and aluminum alloys are also developed.

A) Superplastic Titanium alloys

Ti-6Al-4V alloy at 900°C exhibits SP properties. It's a common alloy used in the aircraft industry besides in dental implants and in submarine industries, on account of its high strength to

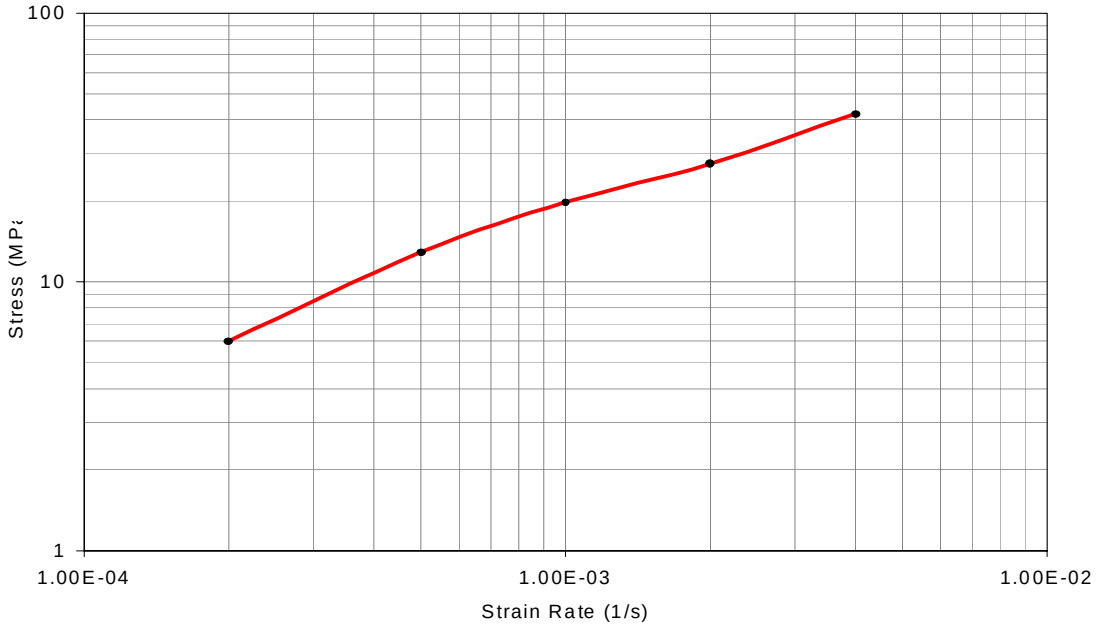

Figure 3-1 Stress vs.- Strain rate curves for SP Ti-6Al-4V @ 900°C in region II

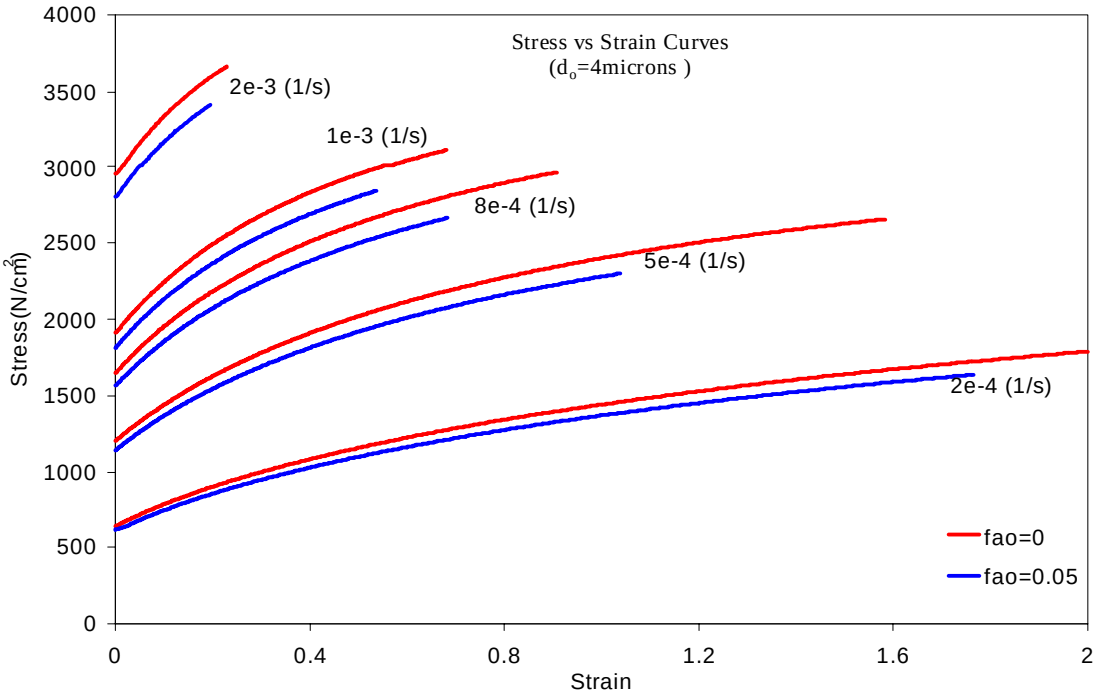

Figure 3-2 Stress vs.- Strain curves for SP Ti-6Al-4V @ 900°C in region II

weight ratio, excellent mechanical properties, resistance to erosion and corrosion, ability to withstand a wide range of temperatures, hard and smooth surface that limits the adhesion of foreign materials. However, high material and fabrication costs limit the application of titanium alloys. Thus, the optimization technique proposed in this study may offer a suitable solution to minimize the cost of production by increasing the rate of production. The typical sigmoidal shaped stress vs. - strain rate curve for SP materials in region II is shown in Figure 3-1. Stress-strain curves for different constant strain rates with (f_{ao}=0.05) and without (f_{ao}=0) cavitation are shown in Figure 3-2.The curves are plotted only up to the point of onset of instability, i.e., till the onset of necking, hence they depict the variation of stress with strain during the stable and uniform deformation. The curves accounting for cavitation terminate before the ones which do not account for cavitation, indicating that the instability creeps in earlier due to the presence of cavities in the material. The parameters of the constitutive equation and grain growth are obtained from literature [14,25].

B) Superplastic Aluminum alloys

Aluminum alloys are the most extensively used SP alloys for various applications, including – automotive body panels, airframe control surfaces, structural elements, gate panels, ticket vending machines, architectural and marine applications. AA 5083 and AA 7475 are the commonly used aluminum alloys which exhibit SP behavior at elevated temperatures (~500^{o}C). Good corrosion resistance, medium strength, good weldability and increased fracture toughness are responsible for the successful application of SP aluminum alloys for various applications [79]. Figure 3-3 denotes the stress strain behavior of SP AA 5083 alloy (~500^{o}C) for different constant strain rates. The parameters of the constitutive equation are determined by fitting the model (lines) to the experimental (dots) values obtained from literature [41]. Grain growth model was fitted to experimental data [41] on grain growth with strain and the required parameters of grain growth model were determined, as shown in Figure 3-4.

C) Superplastic Copper Alloys

Several copper based alloys like- aluminum bronze, Cu-Zn-Ni alloys and commercial Coronze CDA 638 alloy, have been found to exhibit SP behavior at elevated temperatures (~550^{o}C). Coronze CDA 638 alloy has been one of the prime alloys for studying the cavitation

behavior in SP alloys, as it has been observed that excessive cavitation takes place during the deformation of this alloy and as a result of which the maximum stable elongations

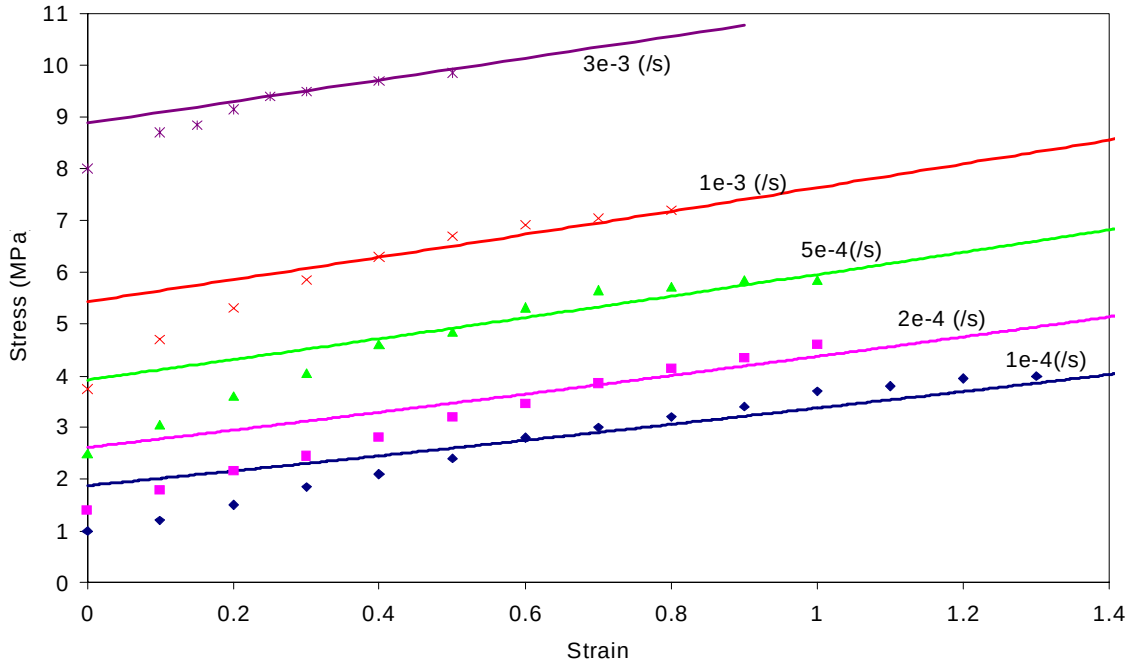

Figure 3-3 Stress vs.-Strain curves for AA 5083 [Fitting the model (line) to experimental values (dots)

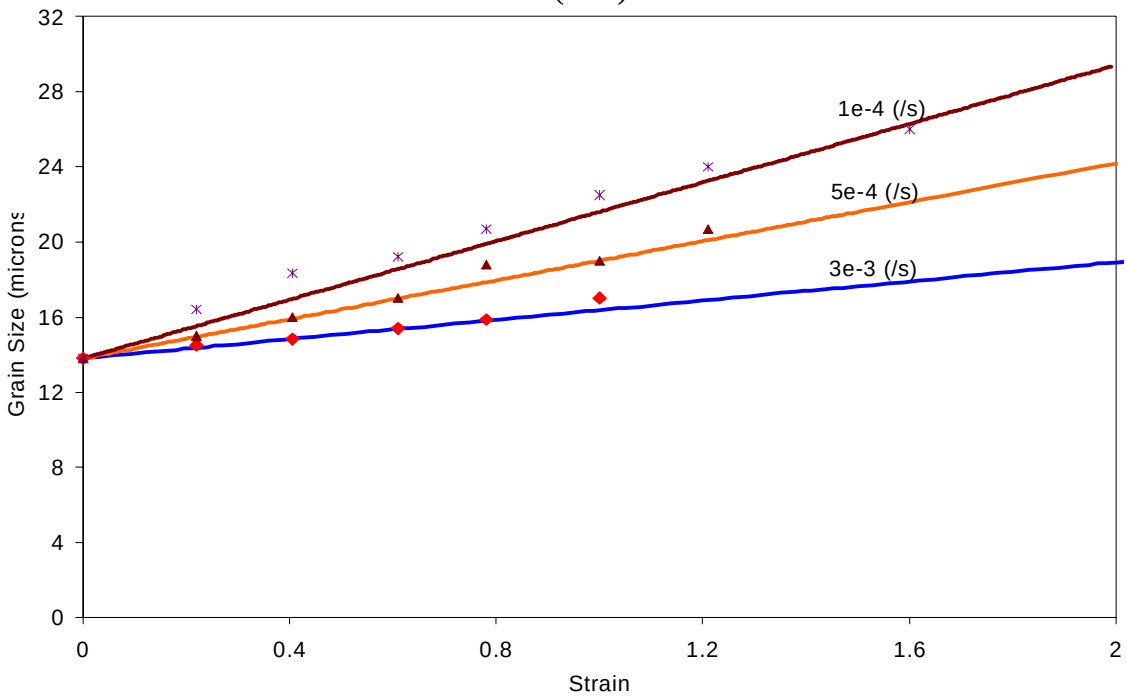

Figure 3-4 Fitting grain growth model to experimental data [41] for AA 5083

have been found to be less than 500%, inspite of the strain rate sensitivity being around 0.5 [1,12]. Coronze CDA 638 with a composition of Cu-2.8%Al-1.8%Si-0.4%Co is a commercial copper alloy developed as a high strength, high oxidation resistant material and essentially contains a solid solution copper matrix with a dispersion of Co-rich phase. The fine dispersion of cobalt silicide particles restricts the grain growth during SP deformation even at elevated temperatures [12,80].

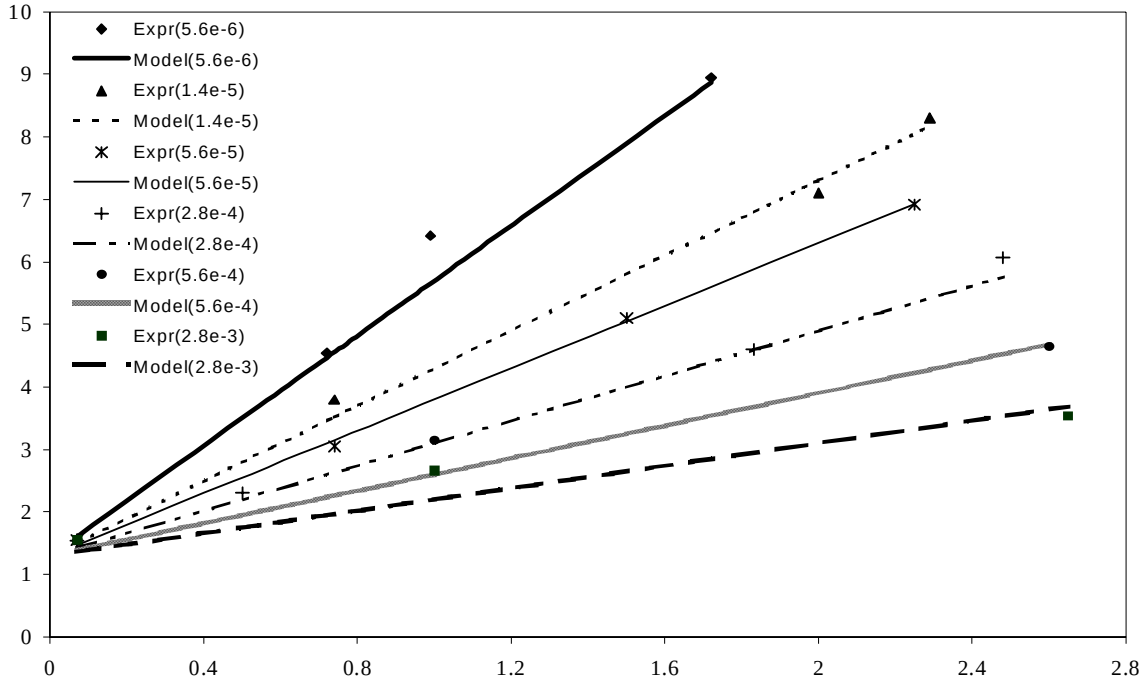

Figure 3-5 Fitting grain growth model to experimental data [31] for CDA 638

Figure 3-5 illustrates the capability of the grain growth model to predict the increase in grain size with strain at different constant strain rates. The empirical constant (c) which is a function of strain rate is determined by fitting the grain growth model to experimental data [31].

3.2.1 Effect of Initial Grain size and Grain Growth on the Optimum Forming Paths:

Figure 3-6, depicts the significance of accounting for grain growth while modeling stability and uniform deformation of SP materials. The maximum attainable strain at any

particular strain rate is significantly reduced when grain growth is accounted [7]. An initial grain size of 4 microns, grain growth exponent 'p'=0.3 and a strain rate sensitivity 'm'= 0.6-0.7 (typical for SP Ti6Al4V alloy @ 900^{o}C [1,14]) were used during the modeling. Effect of initial grain size accounting for growth of pre-existing cavities only on the optimum variable strain rate forming paths for Ti6Al4V and AA 5083 are shown in Figure 3-7 and Figure 3-8, respectively. In case of both SP alloys, more stable deformation is achieved at a comparatively faster rate for fine grain size. With the increase in the initial grain size, the maximum attainable strains for uniform deformation are reduced significantly. This is in agreement with the established fact that fine and stable grain size yields more stable and uniform deformation [1,10]. However, it must

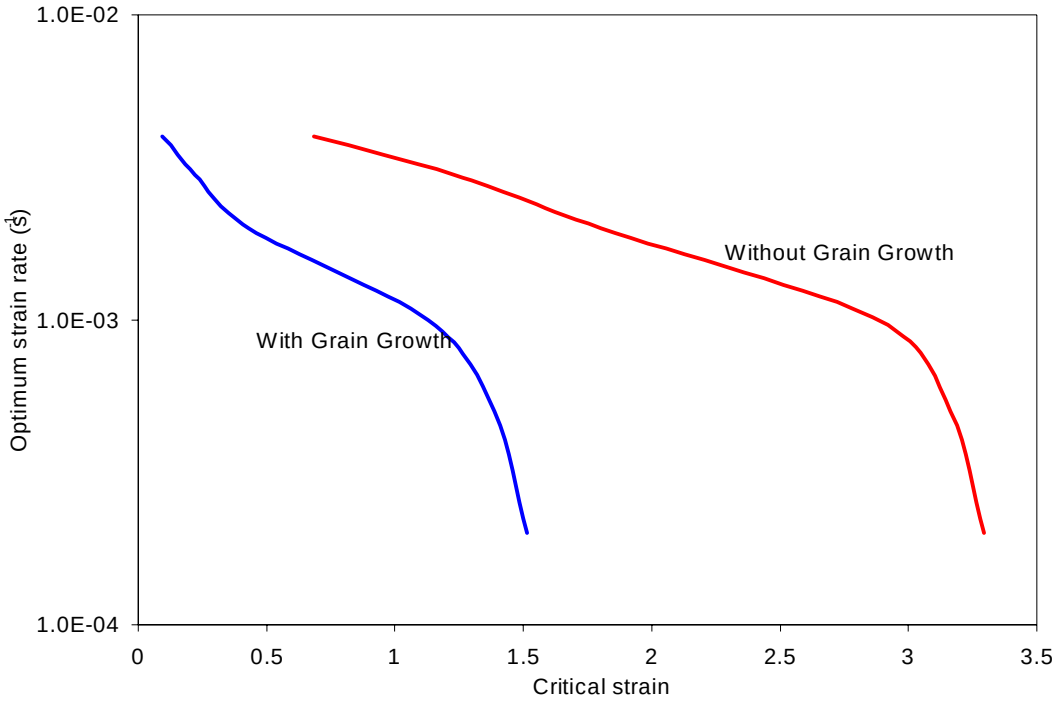

Figure 3-6 Effect of grain growth on the Optimum Forming path of SP Ti6Al4V @ d_o= 4mic, p=3.0, f_{ao}^{p}=0.01, m=0.6-0.7

be noted that the trend and slopes of the curves differ from alloy to alloy. In case of Ti6Al4V, the maximum attainable strains without any instability seem to be less affected by the increase in the initial grain size when compared to the strains attained in case of AA 5083, as the grain size increases. This can be attributed to the material behavior and typical initial grain sizes considered. Since, cavitation (mainly nucleation) is more pronounced in copper alloys [12], the

effect of initial grain size is studied by accounting for the growth of both pre-existing cavities (f_{ao}^{p}) and nucleating (f_{ao}^{N}-constant/continuous). Effect of initial grain size on the optimum forming paths for CDA 638 accounting for constant nucleation + pre-existing cavities and continuous nucleation + pre-existing cavities is shown in Figure 3-9 and Figure 3-10, respectively.

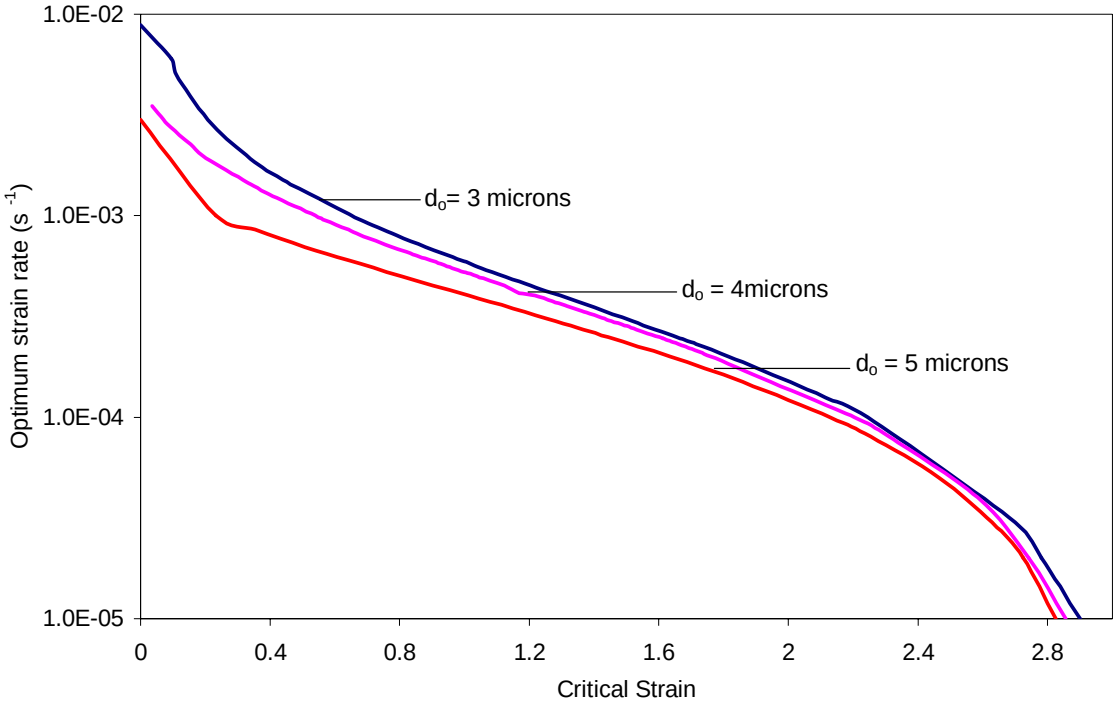

Figure 3-7 Effect of initial grain size on the Optimum forming paths of SP Ti6Al4V @ m=0.6-0.7, f_{ao}^{p}=0.05, p=3.0

It should be noted that the net effect of reduction in maximum stable strains attained with an increase in the initial grain size remains the same even in case of SP copper alloy, but the trend and slope of the curves for CDA 638 differs from SP titanium and aluminum alloys. It should also be noted that the maximum strain attained for any particular initial grain size is less in case of continuous nucleation in comparison to the constant nucleation case. This is explained based on the fact that in the former case, the numbers of cavities nucleating increase with strain there by increasing the adverse affects of cavitation, as against a constant number of cavities nucleating after surpassing the nucleation strain in the later case. This clearly indicates the importance of accounting for continuous nucleation of cavities.

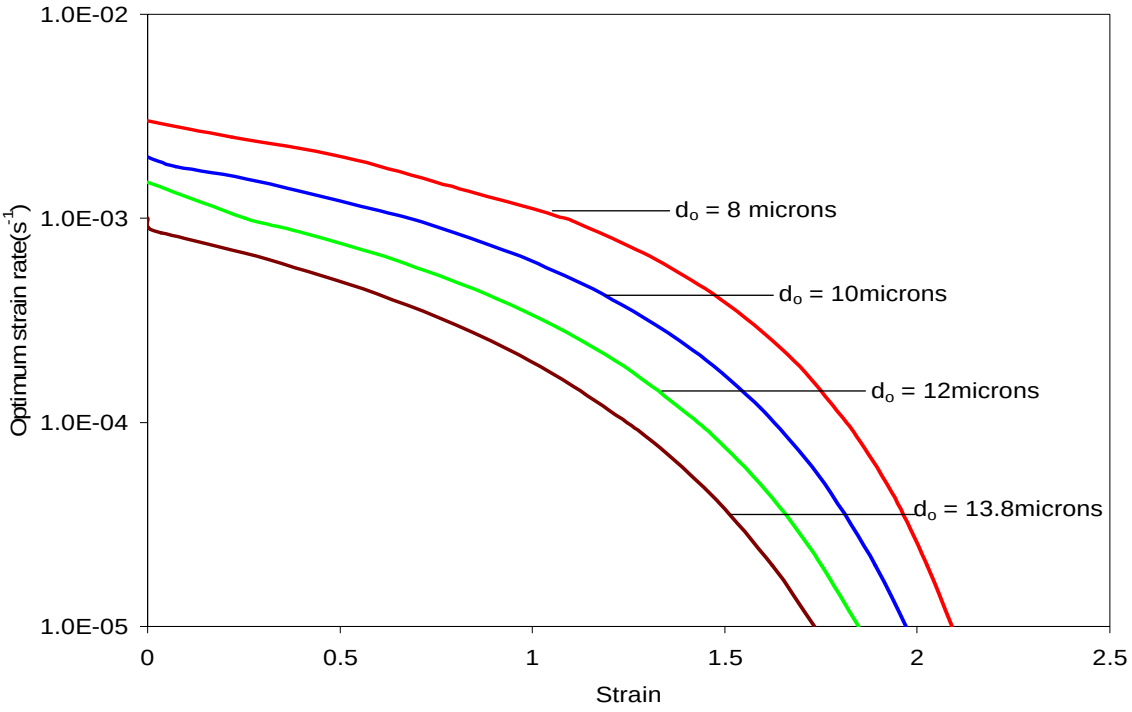

Figure 3-8 Effect of initial grain size on the Optimum forming paths of SP AA 5083 @ m=0.6, f_{ao}^{p}=0.01, p and c are evaluated as function of strain rate

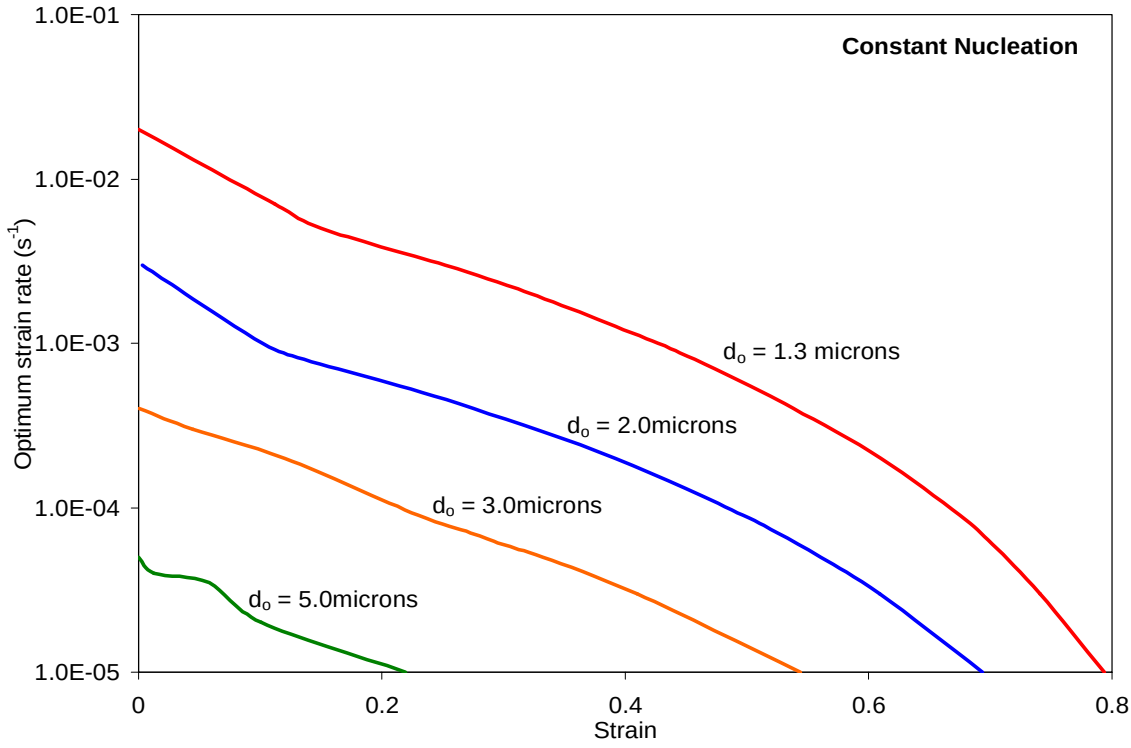

Figure 3-9 Effect of initial grain size on the Optimum forming paths of SP CDA 638 @ p=2.4,m=0.45, f_{ao}^{p}=0.03, ε_n=0.1 and f_{ao}^{N}=0.05

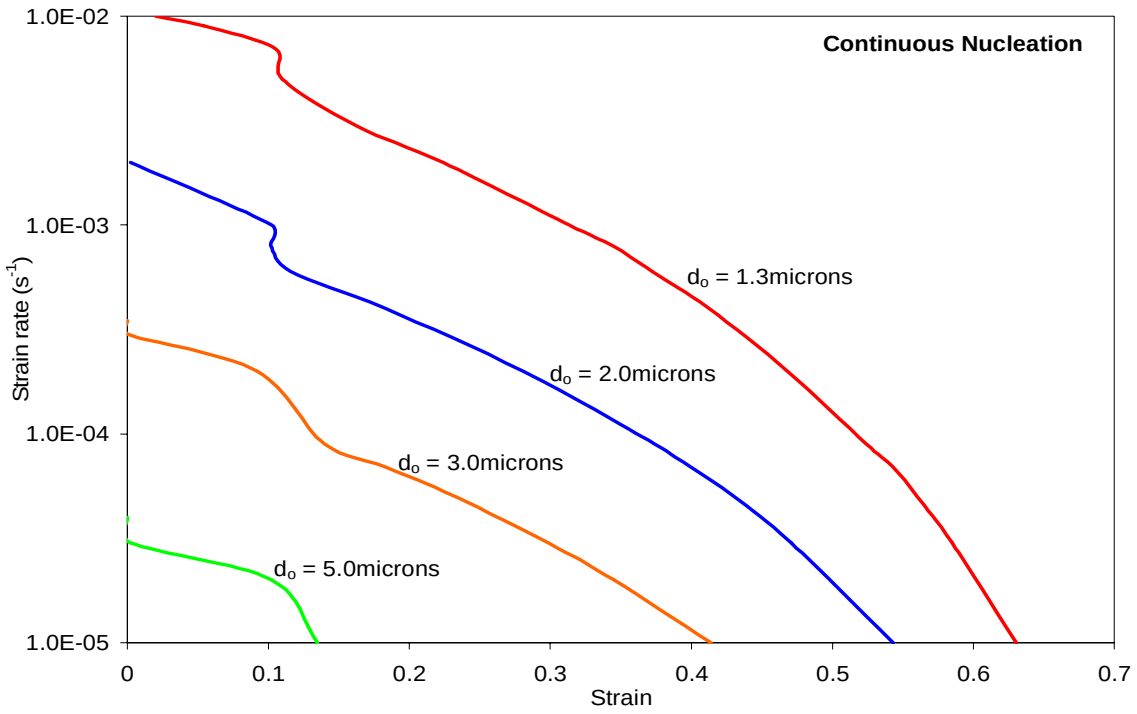

Figure 3-10 Effect of initial grain size on the Optimum forming paths of SP CDA 638 @ p=2.4,m=0.45, f_{ao}^{p}=0.03, ε_n=0.1 and f_{ao}^{N}=0.05

In both constant nucleation & continuous nucleation case, the pre-existing cavities start growing soon after the deformation starts to take place and continue to grow further with strain, while the nucleating cavities come into picture only after the strains attained are more than the nucleation strain (which differs from material to material). A sudden drop in the curve can be seen at a strain of 0.1, where the newly emerging cavities make an appearance and begin to grow along with the pre-existing cavities. The effect is more pronounced in continuous nucleation case, as the number continues to increase with strain, after surpassing the nucleation strain.

3.2.2 Effect of Pre-existing cavities on the Optimum Forming Paths:

Certain cavities are believed to pre-exist even before the material is deformed to produce the desired final shape. These voids are generally created during the thermomechanical

processing of the materials, which is done in order to develop fine grain size for the material to exhibit superplasticity [1]. The effect of initial area fraction of pre-existing cavities and their

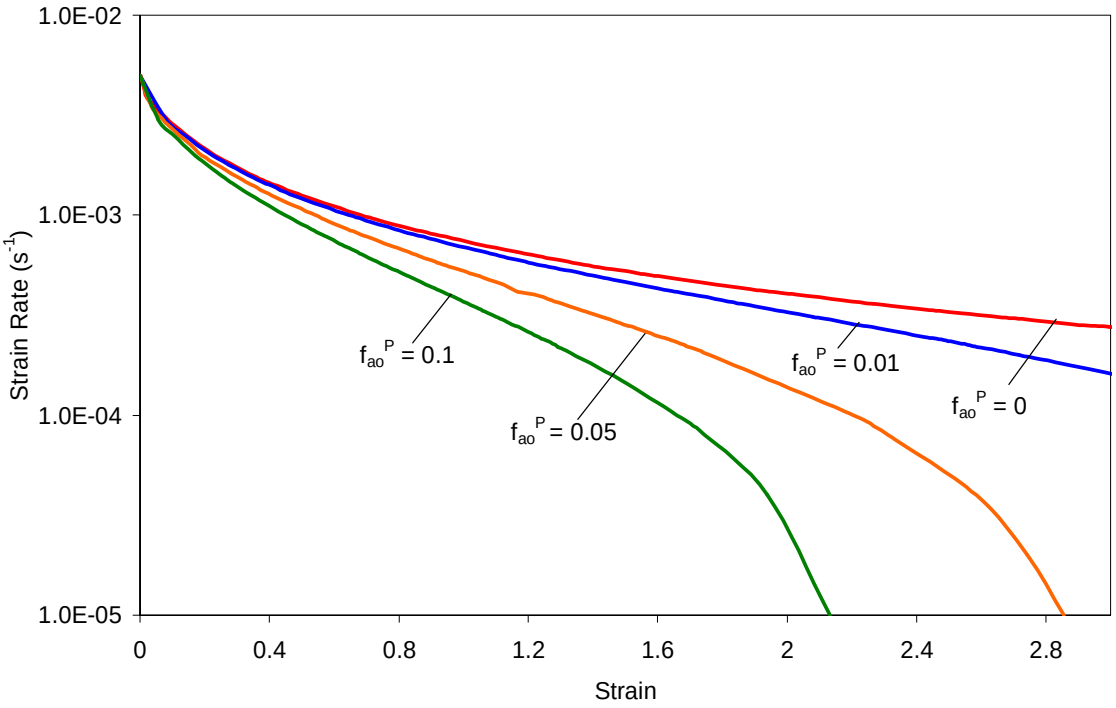

Figure 3-11 Effect of Pre-existing cavities on the Optimum Forming paths of SP Ti6Al4V @ d_o=4microns, m=0.7, p=3.0

growth during deformation along with grain growth on the stable deformation of Ti6Al4V @ 900^{o}C is clearly shown in Figure 3-11. It can be observed that the maximum critical strain attained significantly decreases with an increase in the percentage of cavities. It should also be noted that the slopes of these curves decrease with an increase in the initial area fraction of pre-existing cavities. Similar phenomenon is observed in case superplastic AA 5083 (Figure 3-12) and CDA 638 (Figure 3-13) alloys when deformed at their respective elevated temperatures. However the slopes of these curves not only differ with a change in initial area fraction of cavities but also differ with material. This clearly shows the significance of accounting for pre-existing cavities and also the ability of the model to predict the effect of pre-existing cavities on the optimum variable strain rate path, for different SP alloys.

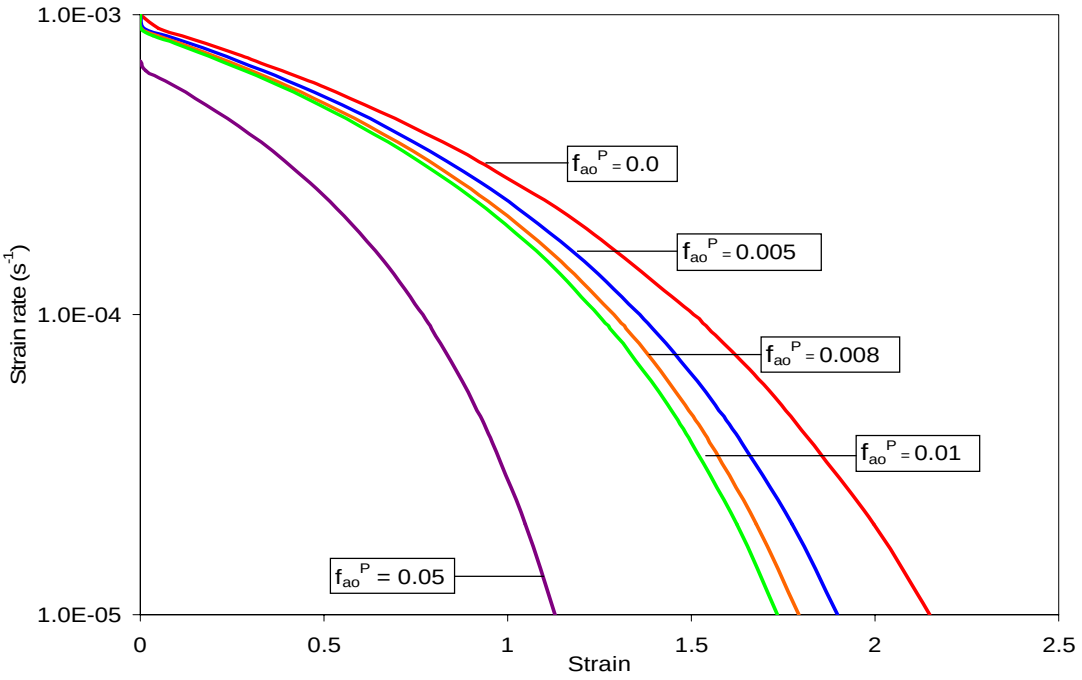

Figure 3-12 Effect of Pre-existing cavities on the Optimum Forming paths of SP AA 5083 @ d_o=13 microns and m=0.6

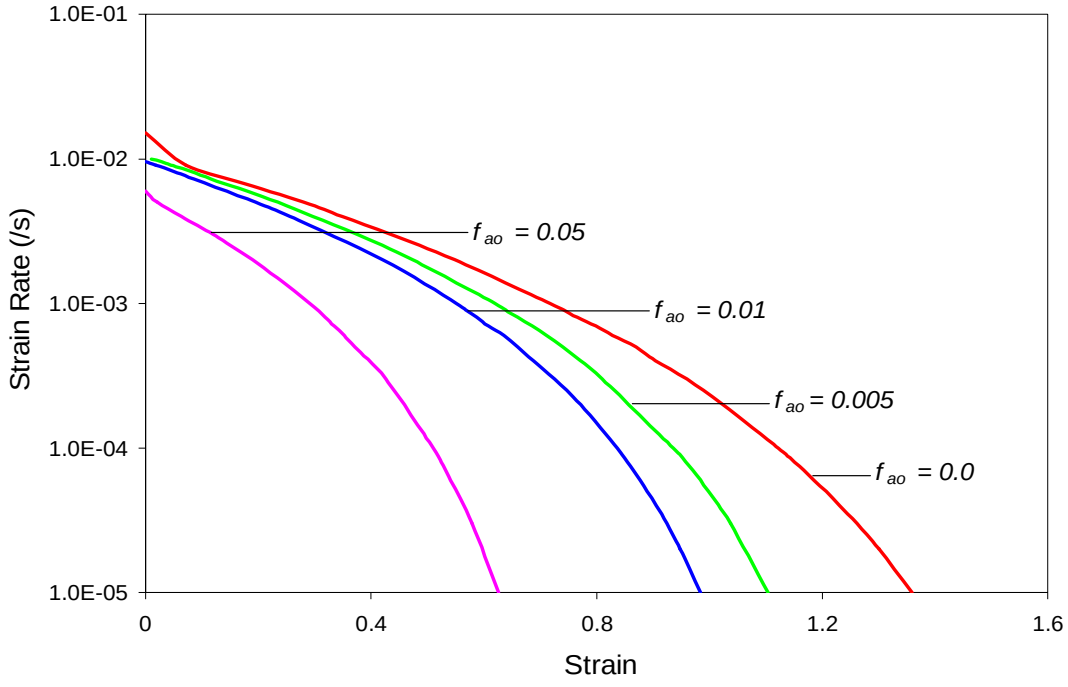

Figure 3-13 Effect of Pre-existing cavities on the Optimum Forming paths of SP CDA 638 @ d_o=1.3microns, p=2.4 and m=0.45

3.2.3 Effect of Strain rate sensitivity (m):

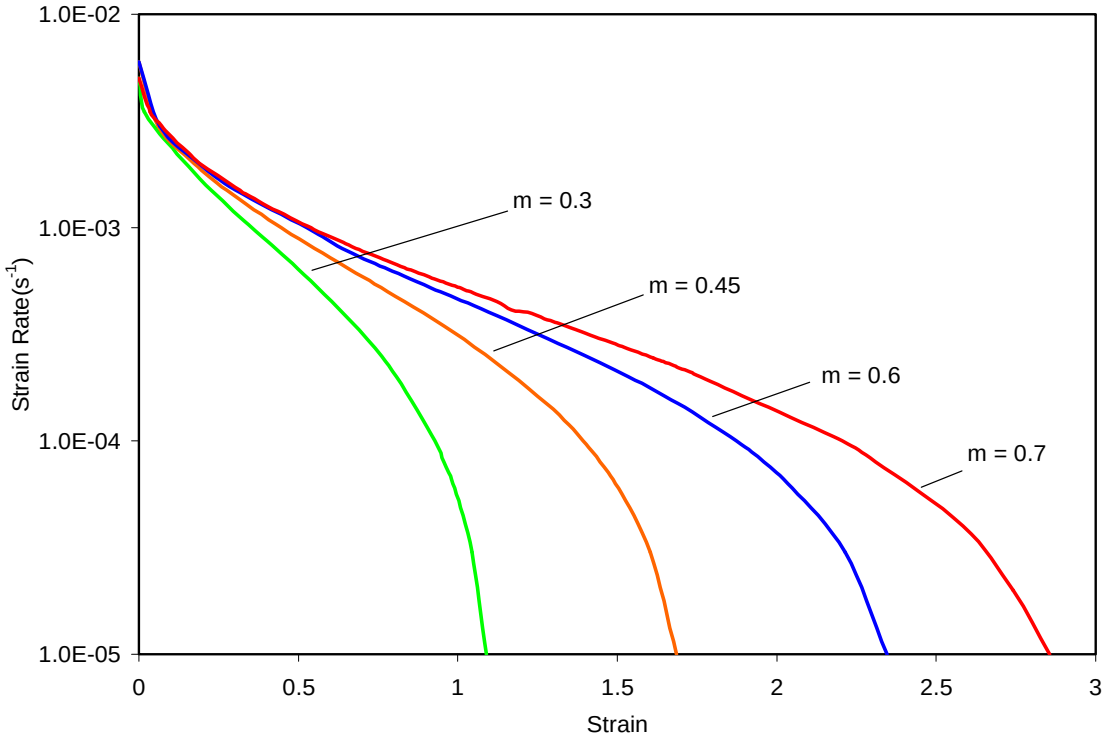

Figure 3-14 Effect of 'm' on the Optimum Forming paths of SP Ti6Al4V @ d_o=4μ, f_{ao}^{P}=0.05

Strain rate sensitivity is an important characteristic of SP materials. The effect of 'm' on the optimum forming paths of different SP alloys has been investigated. A constant strain rate sensitivity 'm' was assumed all through the deformation and the effect of varying 'm' from 0.3 to 0.7 for SP Ti6Al4V is shown in Figure 3-14. With an increase in 'm' value, it can be seen that more stable deformations can be achieved at a much higher strain-rate. Thus, an alloy with higher 'm' value would offer faster rate of production without compromising on the ductility of the material. This is an experimentally established fact [1]. Similar phenomenon is observed in case of SP CDA 638, as shown in Figure 3-15 – for constant nucleation and Figure 3-16 – for continuous nucleation. The maximum strains attained increase with an increase in strain rate sensitivity, but the increase is less in case of continuous nucleation, in comparison to the constant nucleation case. This reiterates the significance of accounting for continuous nucleation while modeling stability and failure during SPD.

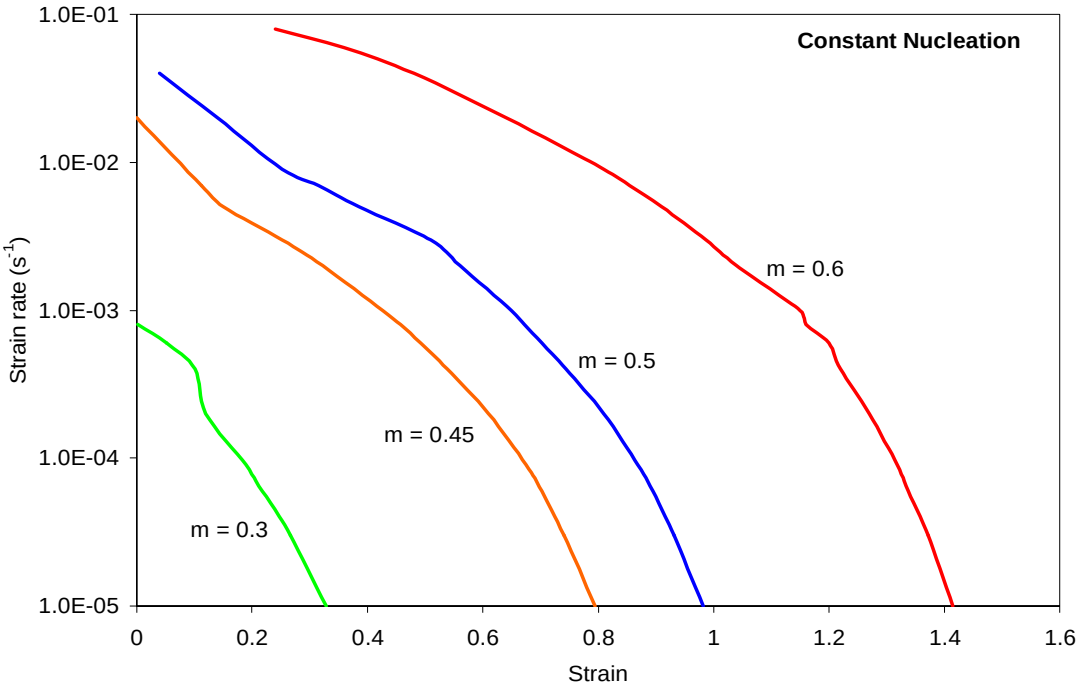

Figure 3-15 Effect of 'm' on Optimum Forming paths of CDA 638 @ d_o=1.3μ, p=2.4, ε_n = 0.1, f_{ao}^P=0.05 and (constant nucleation) f_{ao}^N=0.03

However, it has been observed that the strain rate sensitivity varies during the superplastic deformation [1,41]. This effect is accounted by assuming strain rate sensitivity as a function of strain rate, based on the experimental data obtained from Iwasaki et al [41] for SP AA 5083 alloy. A simple functional form was proposed and incorporated into the stability model such that 'm' varies with strain during deformation. Figure 3-17 indicates the effect of varying initial area fraction of cavities coupled with variation in the strain rate sensitivity during deformation as a function of strain rate sensitivity. It should be noted that though the phenomenon is same as in case of other alloys, the slopes of the curves are significantly different, as they are accounting for variation of strain rate sensitivity with deformation. Thus, the model could also successfully predict the effect of varying 'm' during deformation.

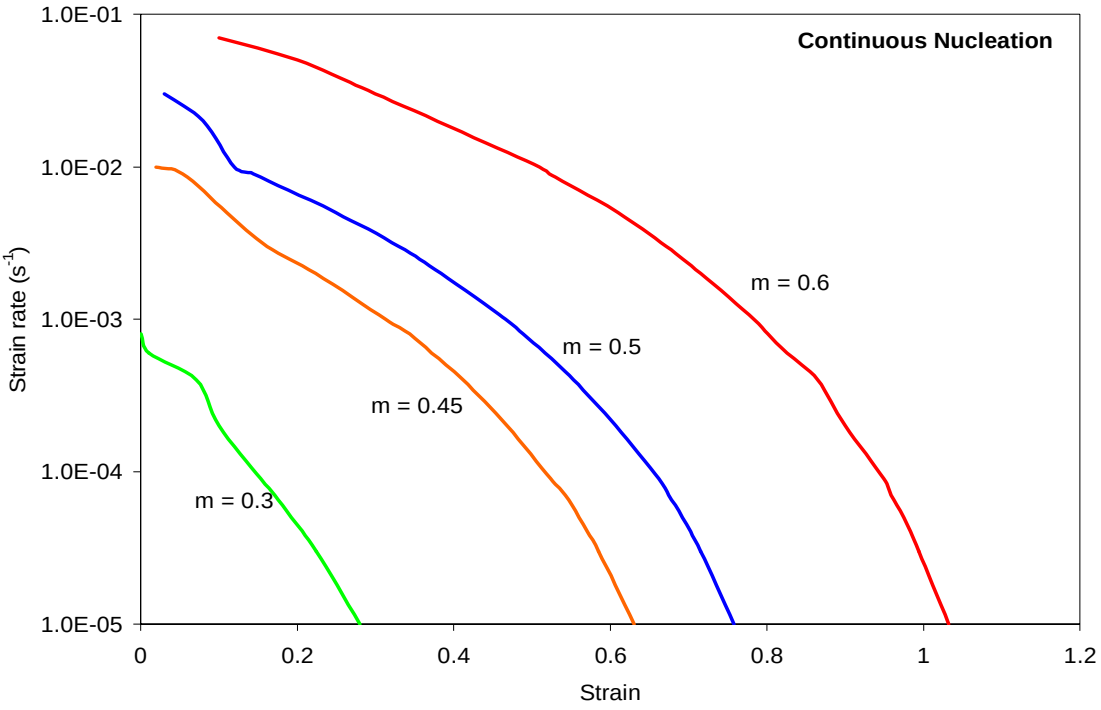

Figure 3-16 Effect of 'm' on Optimum Forming paths of CDA 638 @ d_o=1.3μ, p=2.4, ε_n = 0.1, f_{ao}^{P}=0.05 and (continuous nucleation) f_{ao}^{N}=0.03

3.2.4 Effect of Nucleating cavities on the Optimum Forming Paths:

Besides the cavities that pre-exist in a material, general cavitation in superplastic metals occurs after an appreciable strain [20] (nucleating strain which may vary from material to material). Once voids are nucleated, they expand/grow along with the pre-existing cavities through plastic deformation, which would lead to void coalescence and eventually to ductile failure [81]. The nucleation of the cavities is addressed under two categories: Constant and Continuous nucleation (the description of each has been dealt in chapter 2). However, it has been established that continuous nucleation of cavities [12,20,35] is more practical in most SP alloys. But some studies [1,33] have also considered constant nucleation, mainly for the ease of modeling it. Thus, in this study we deal with both the approaches and clearly indicate the difference of their (constant and continuous nucleation case) effect on optimum forming paths. We chose copper alloy to demonstrate this effect, since copper alloys are one among the SP alloys that are highly prone to the adverse effects of nucleation of cavities [12].

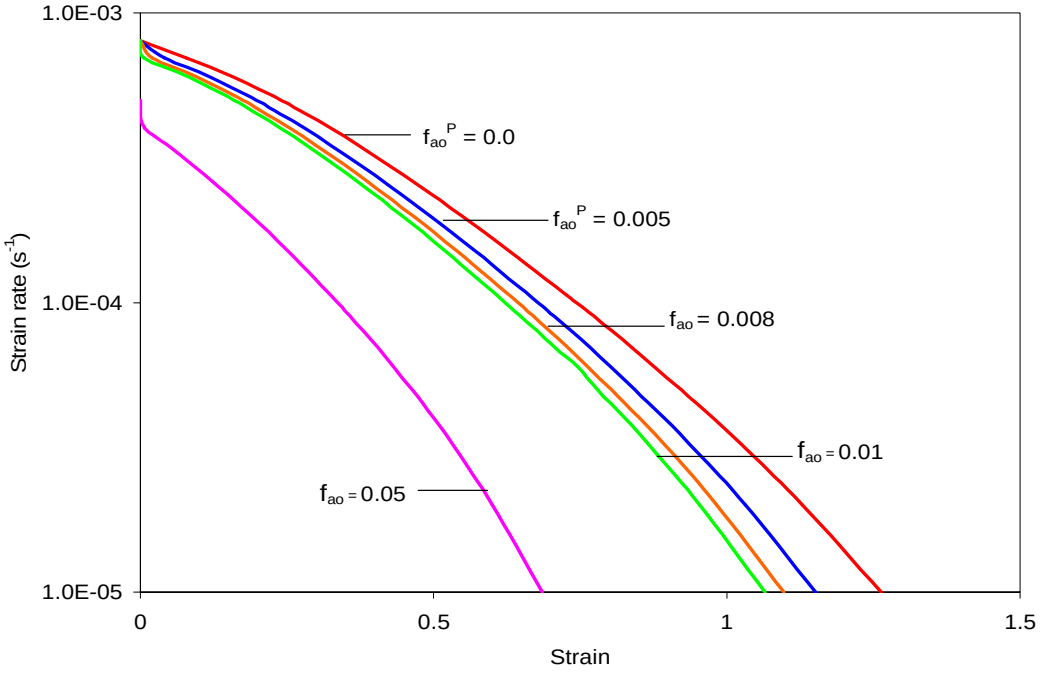

Figure 3-17 Effect of varying f_{ao}^{p} on Optimum Forming paths with 'm' varying during deformation as a function of $\dot{\varepsilon}$

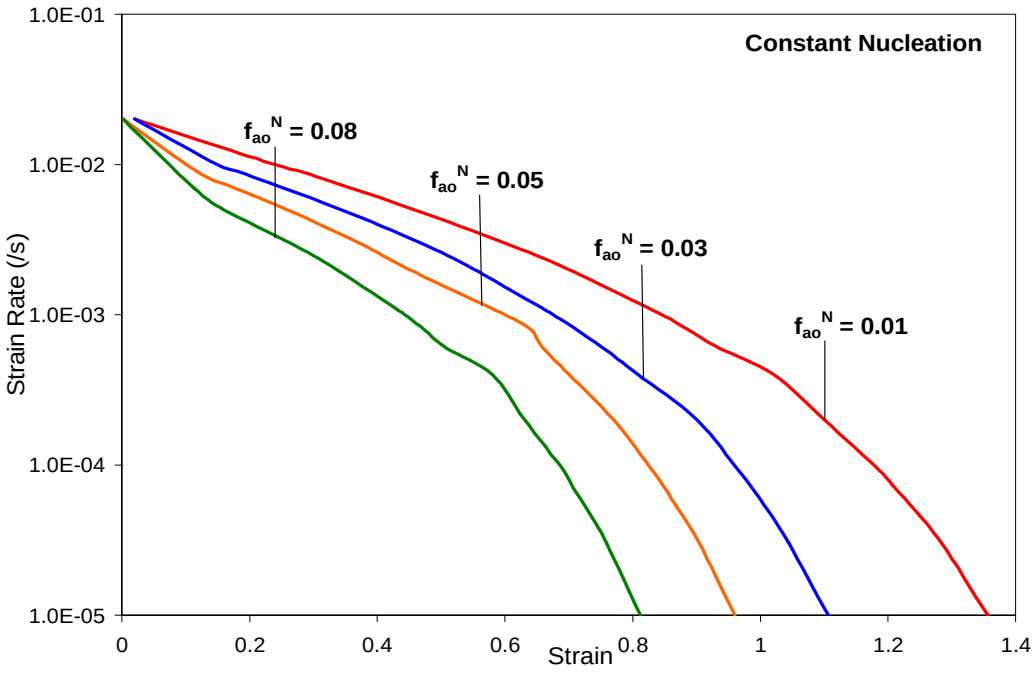

Figure 3-18 Effect of Nucleating (constant) cavities on the Optimum Forming paths of SP CDA 638 @ d_o=1.3microns, ε_n =0.1, p=2.4, f_{ao}^{P} =0 and m=0.45

The effect of only constant and continuous nucleation of cavities (without considering the pre-existing cavities, f_{ao}^{P}) for a given initial grain size (d_o) of 1.3 microns, grain growth exponent (p) of 2.4, nucleation strain (ε_n) of 0.1 and strain rate sensitivity (m) of 0.45, on the optimum forming paths of SP CDA 638 is shown in Figure 3-18 and Figure 3-19 respectively. It can be clearly seen that maximum critical strains attained for any particular condition is always less in case of continuous nucleation in comparison to the constant nucleation case. For instance, the maximum critical strain reduces from 0.8 in case of constant nucleation to 0.58 in case of continuous nucleation, when the initial area fraction of nucleating cavities is 0.08. This can be explained based on the fact that the number of cavities increase continuously with strain in case of continuous nucleation, as a result of which the effective strains are still further reduced. However, the effect of accounting for both pre-existing cavities along with nucleating (constant and continuous) on the optimum paths is depicted below. Firstly, the effect of varying initial area fraction of pre-existing cavities at a given initial area fraction of nucleating cavities, on the optimum forming paths is considered. Figure 3-20, shows the combined effect of the pre-existing cavities and their growth with strain along with nucleating (constant) cavities followed by their growth with strain.

In comparison to Figure 3-18, it should be noted that the maximum critical strains for same initial area fraction of nucleating cavities and all other conditions remaining same, decrease significantly when pre-existing cavities are also considered in addition to the nucleating cavities. Same phenomenon is observed in case of continuous nucleation case also, as shown in Figure 3-19 and Figure 3-21 respectively. Comparison between Figure 3-20 and Figure 3-21 shows the significant difference in the effect of constant vs. continuous nucleation case - on the optimum forming paths. The sharp drop in the curves seen in Figure 3-21 at a strain of 0.1, clearly indicate the beginning of nucleation effect on the optimum paths. It should be noted that this effect is more significant in case of continuous nucleation when compared to constant nucleation.

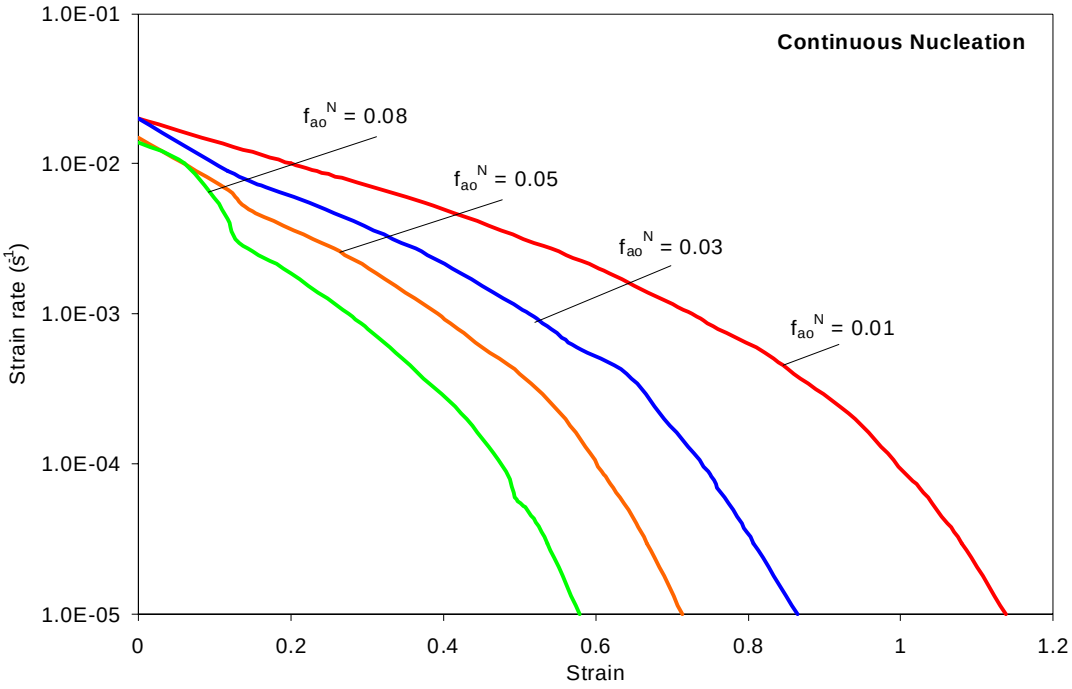

Figure 3-19 Effect of Nucleating (continuous) cavities on the Optimum Forming paths of SP CDA 638 @ d_o=1.3microns, ε_n =0.1, p=2.4, f_{ao}^{p} =0 and m=0.45

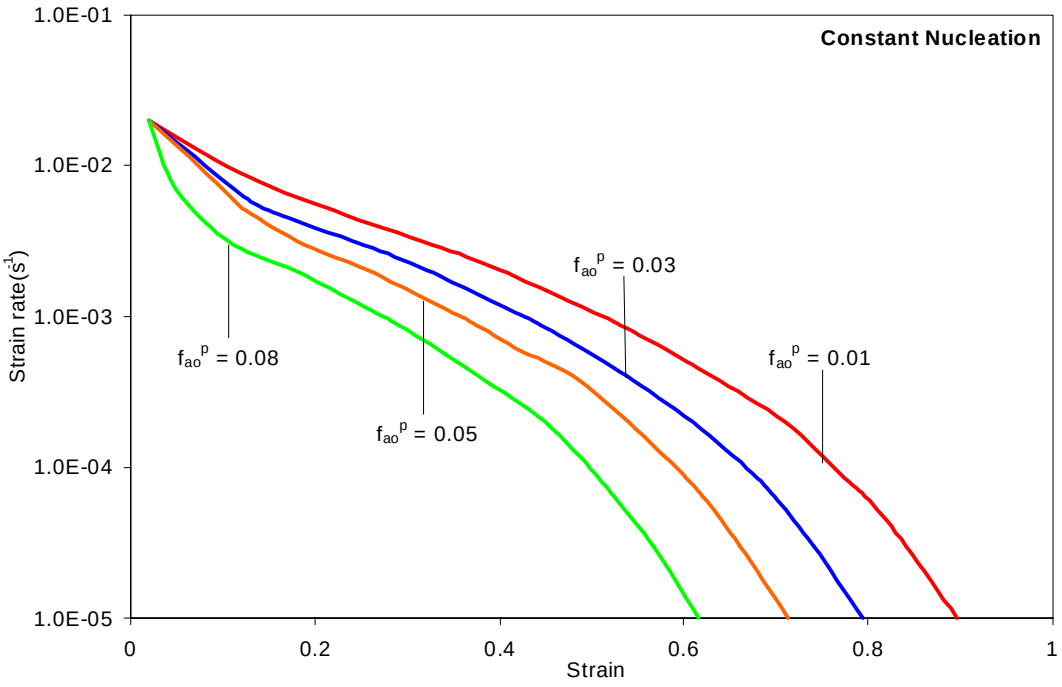

Figure 3-20 Effect of varying Pre-existing + Nucleating (constant) cavities on the Optimum Forming paths of SP CDA 638 @ d_o=1.3mic, ε_n =0.1, p=2.4, f_{ao}^{N} =0.05 & m=0.45

Secondly, the effect of varying initial area fraction of nucleating cavities given a certain initial area fraction of pre-existing cavities on the optimum forming paths of SP CDA 638 alloy was investigated. With all other parameters remaining the same, and assuming an initial area fraction of pre-existing cavities to be 0.05, it can be observed that with an increase in the initial area fraction of nucleating cavities, the attainable maximum strains decrease significantly. Same phenomenon is observed in case of both continuous and constant nucleation cases. However, as observed in previous results, the reduction in maximum strains attained is more when accounting for continuous nucleation in comparison to the constant nucleation case. The sharp drop seen in the curves at a strain of around 0.1, marks the beginning of the effect of nucleating cavities (as the nucleation strain was assumed as 0.1).

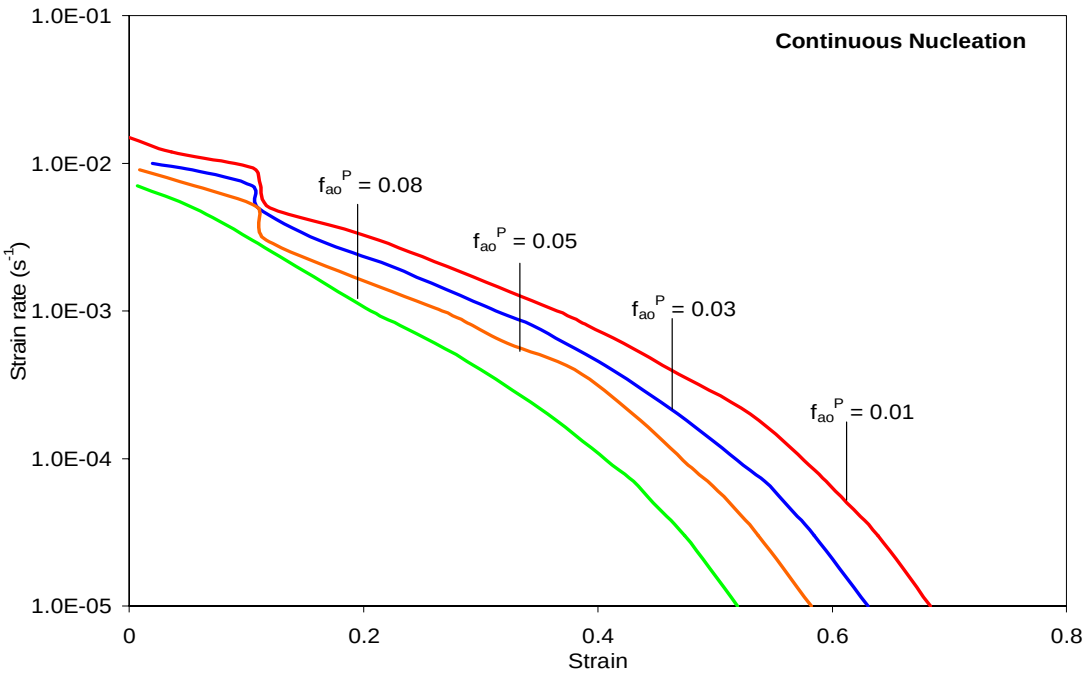

Figure 3-21 Effect of varying Pre-existing + Nucleating (continuous) cavities on the Optimum Forming paths of SP CDA 638 @ d_o=1.3microns, ε_n =0.1, p=2.4, f_{ao}^N =0.05 & m=0.45

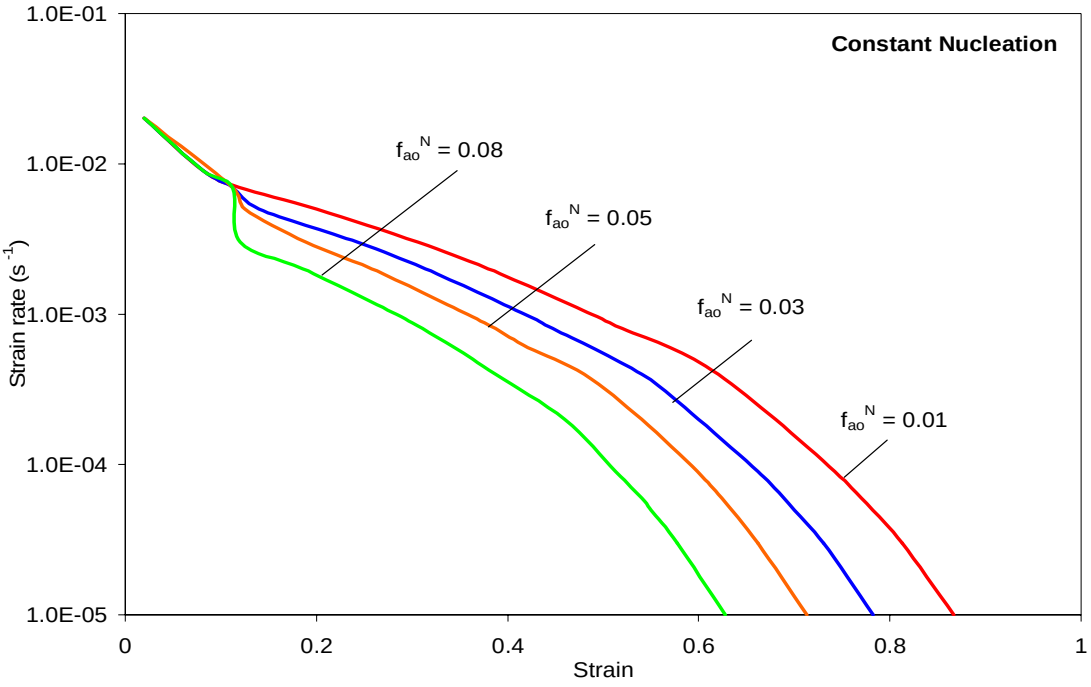

Figure 3-22 Effect of Pre-existing + varying Nucleating (constant) cavities on the Optimum Forming paths of SP CDA 638 @ d_o=1.3microns, ε_n =0.1, p=2.4, f_{ao}^{P} =0.05 & m=0.45

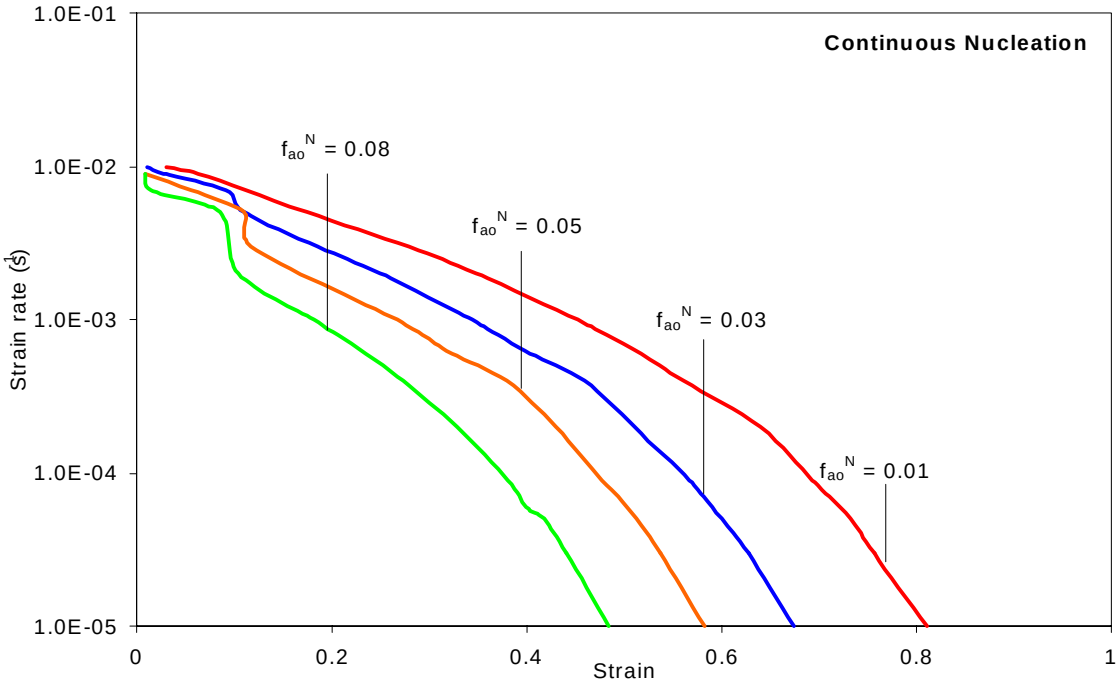

Figure 3-23 Effect of Pre-existing + varying Nucleating (continuous) cavities on the Optimum Forming paths of SP CDA 638 @ d_o=1.3microns, ε_n =0.1, p=2.4, f_{ao}^{P} =0.05, m=0.45

3.2.5 Effect of Nucleation Strain (ε_n) on Optimum Forming paths:

Excluding the cavities that pre-exist in a material, most cavities come into existence only after the material has undergone some amount of deformation [12,20]. However, it is difficult to ascertain if the cavities truly nucleated from zero size or they pre-existed and became visible only after growing to a reasonable size. Nucleation strain (ε_n) is thus defined as the strain at which new cavities begin to appear and continue to grow along with the pre-existing cavities. The value of nucleation strain may differ from material to material and also may depend on the conditions at which the alloy is being deformed. It is generally in the range of ~ 0.2 [20]. The effect of nucleation strain on the optimum forming paths, under the conditions of constant and continuous nucleation for SP CDA 638 alloy has been studied and presented in Figure 3-24 and Figure 3-25 respectively. The sharp drop in the curves at the corresponding nucleation strain is due to the nucleation of new cavities in addition to the pre-existing ones. Lower the nucleation

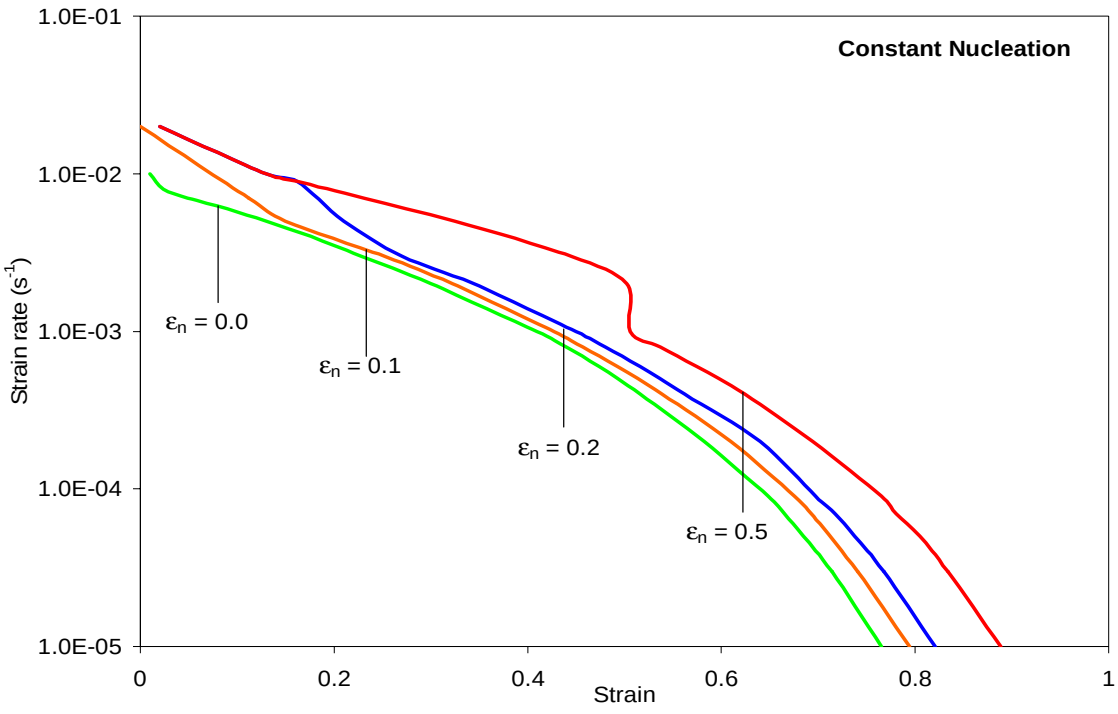

Figure 3-24 Effect of Nucleation strain (ε_n) on the Optimum Forming paths of CDA 638 @ d_o= 1.3μ, m=0.45, p=2.4, $f_{ao}{}^P$=0.03 and $f_{ao}{}^N$=0.05 (constant nucleation case)

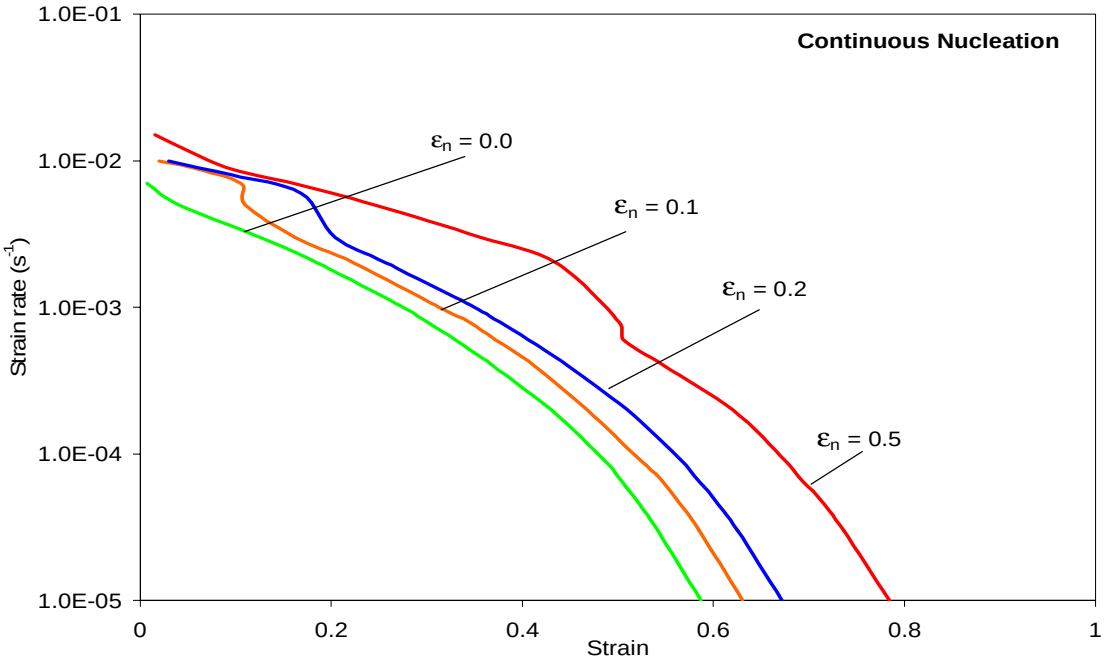

Figure 3-25 Effect of Nucleation strain (ε_n) on the Optimum Forming paths of CDA 638 @ d_o= 1.3μ, m=0.45, p=2.4, f_{ao}^{P}=0.03 and f_{ao}^{N}=0.05 (continuous nucleation case)

strain lesser is the stable deformation, as more cavities come into existence if the nucleation strain is low, thus adversely affecting the stable deformation of SP alloys. The maximum strains attained under continuous nucleation framework are considerably less than those attained under constant nucleation framework.

3.2.6 Effect of Grain Growth Exponent (p) on the Optimum Forming Paths:

The activation energy for flow in SP region II is generally similar to that for grain boundary diffusion and the flow stress is grain size dependent (p = 1.6 to 3) [1, 41]. Iwasaki et al [41], suggested that 'p' value can be determined for a particular strain rate, from the stress and 'm' values by using the constitutive equation. The effect of varying 'p' on the optimum forming paths of SP CDA 638 alloy under uniaxial deformation is shown in Figure 3-26 for constant nucleation case and Figure 3-27 for continuous nucleation case. It can be seen that more stable deformation at much faster rate is possible for a higher value of 'p'. As seen in other cases, the maximum strains attained are more in case of constant nucleation in comparison to those obtained in case of continuous nucleation case, for a particular set of conditions.

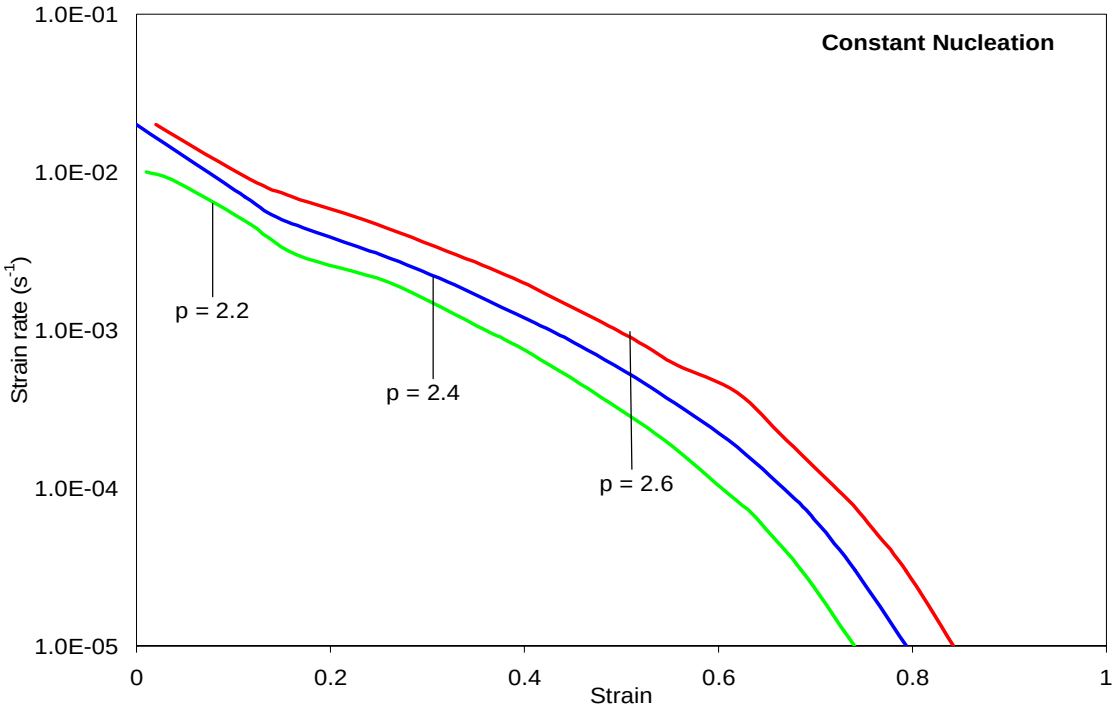

Figure 3-26 Effect of 'p' on the Optimum forming paths of SP CDA 638 @ d_o= 1.3μ, m=0.45, ε_n =0.1, f_{ao}^P=0.03 and f_{ao}^N=0.05 (constant nucleation case)

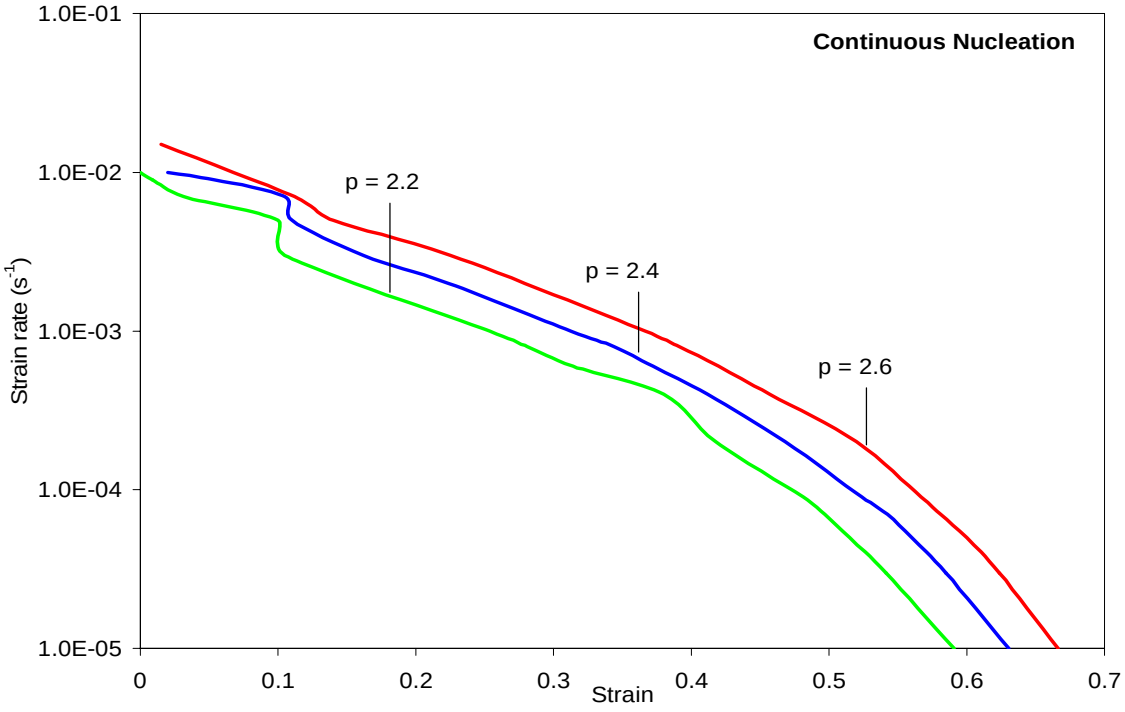

Figure 3-27 Effect of 'p' on the Optimum forming paths of SP CDA 638 @ d_o= 1.3μ, m=0.45, ε_n =0.1, f_{ao}^P=0.03 and f_{ao}^N=0.05 (continuous nucleation case)

3.2.7 Effect of Void Growth Parameter (η) on the Optimum Forming Paths:

Void growth parameter is a function of strain rate sensitivity and is a single entity in the cavitation evolution equation which varies with the loading condition. The effect of varying the void growth parameter on the optimum forming paths of SP CDA 638 under constant and continuous nucleation case is shown in Figure 3-28 and Figure 3-29 respectively. Increasing the void growth parameter decreases the maximum strains attained and also adversely affects the stable deformation. Same phenomenon is observed in case of constant and continuous nucleation cases, though maximum strains attained are lower in the latter in comparison to the former. Effect of nucleation strain seems to be more pronounced in case of continuous nucleation case, for a given set of conditions, specially for higher η values.

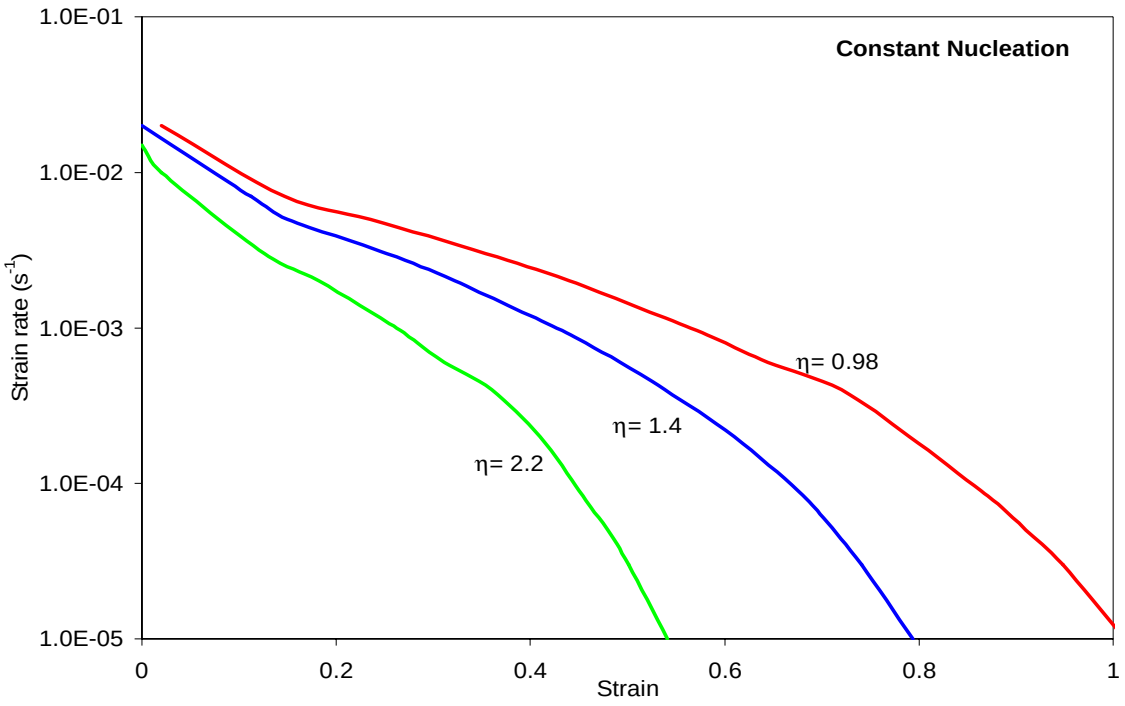

Figure 3-28 Effect of void growth parameter on the optimum forming path of CDA 638 @ d_o= 1.3μ, m=0.45, p=2.4, ε_n =0.1, f_{ao}^{P}=0.03 and f_{ao}^{N}=0.05 (constant nucleation case)

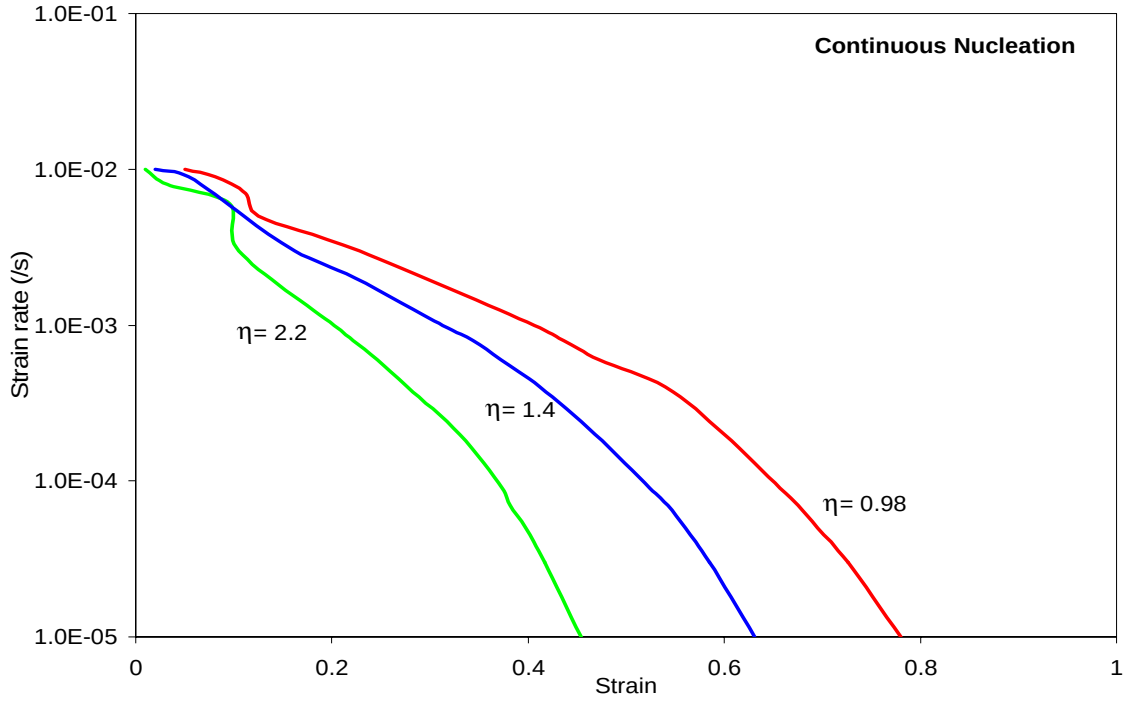

Figure 3-29 Effect of void growth parameter on the optimum forming path of CDA 638 @ d_o= 1.3μ, m=0.45, p=2.4, ε_n =0.1, f_{ao}^P=0.03 and f_{ao}^N=0.05 (continuous nucleation case)

3.3 Conclusion:

Optimization of SPF can be achieved by using variable strain rate forming paths that reduce the production time without scarifying the ductility of SP materials. A multiscale microstructure based stability criterion for SP materials under uniaxial loading condition is developed, by using a modified constitutive equation along with the evolution equations of grain growth and cavitation. The stability model is then used with the modified microstructure based constitutive and evolution equations for different SP alloys and optimum forming paths are developed. The effect of initial grain size, strain rate sensitivity, only pre-existing cavities, only nucleating cavities, pre-existing + nucleation (constant and continuous), nucleation strain, grain growth exponent and void growth parameter on the optimum forming paths of different SP alloys, under uniaxial loading condition has been studied. The effect of constant and continuous nucleation case for each and every condition considered on the optimum forming paths of CDA 638 alloy are also presented. The importance of accounting for both geometrical instabilities and

microstructural aspects (including grain growth and cavitation) while modeling SPD and predicting optimum variable strain rate forming paths for uniaxial loading condition, has been clearly demonstrated.

Chapter 4 Multiscale Stability Analysis and Optimization of SPF under Various Loading conditions

SPF of most industrial components would require different loading conditions / complex stress states and not just uniaxial loading [82]. Biaxial stretching is considered to be a dominant stress state in superplastic sheet blow forming processes [14]. A two dimensional analysis of the localization behavior of the sheet under plane stress condition is carried out to develop optimum variable strain rate paths, similar to the procedure suggested by Ding et al [14]. Ding developed an instability criterion for biaxial stretching under the assumption that localized necking initiates along the direction perpendicular to the major principal stress direction, by employing a linear stability analysis similar to that used by Zbib & Aifantis [83] and Zhu et al [84]. A modified microstructure - based constitutive equation for superplastic deformation (SPD) is combined with grain and cavitation evolution equations. These equations are then incorporated into the framework of Hart's stability analysis [60] which is based only on geometrical considerations. The result is a new multiscale stability criterion which accounts for geometrical instabilities, grain and cavitation evolutions for various stress states. The proposed criterion is then used to design optimum forming profiles based on variable strain rate loading paths. The effects of cavitation and biaxiality ratio on the stability of deformation are investigated besides the effect of initial grain size and strain rate sensitivity. The effects of constant and continuous nucleation on the optimum forming paths developed by using the above stability criterion are also investigated.

4.1 Model Development:

It has been experimentally observed that a localized neck forms perpendicular to the loading axis, in tension tests [25,53]. Thus, in order to develop a stability criterion for SP materials accounting for different stress states, the analysis is simplified by assuming a priori that the neck is normal to the maximum principal stress and follow the procedure analogues to that proposed by Marciniak and Kuczynski [85].

The condition for equilibrium across the neck for in-plane stress condition, as suggested by Storen and Rice [67], can be expressed as follows:

$$\frac{\partial}{\partial x_i}\left(\Delta\dot{\sigma}_{ij} + \sigma_{ij}\,\Delta D_{33}\right) = 0 \qquad \text{Eq. 4.1}$$

where Δ represents the difference between the values of field variables inside and outside the neck and $D_{33} = \Delta\dot{H}/\Delta H$, which represents the difference in thickness strain rate inside and outside the neck. The equilibrium equation can be expressed in terms of principal axes as [14]:

$$\Delta\dot{\sigma}_1 + \sigma_1\Delta\dot{\varepsilon}_3 = 0 \qquad \text{Eq. 4.2}$$

The condition for local necking, based on the incompressibility condition can be expressed as:

$$\sigma_1 = \frac{\Delta\dot{\sigma}_1}{\Delta\dot{\varepsilon}_1} \text{ (or) } \sigma_1 = \frac{\Delta\sigma_1}{\Delta\varepsilon_1} \text{ (or) } \sigma_1 = \frac{\delta\sigma_1}{\delta\varepsilon_1} \qquad \text{Eq. 4.3}$$

Expression similar to Eq.3.3, can be expressed as follows:

$$\delta\varepsilon_1 = -\frac{\delta A}{A_o}e^{\varepsilon_1} \text{ and } \delta\dot{\varepsilon}_1 = -\frac{\delta\dot{A}}{A_o}e^{\varepsilon_1} - \frac{\delta A}{A_o}\dot{\varepsilon}_1 e^{\varepsilon_1} \qquad \text{Eq. 4.4}$$

where A_o represents initial area of cross-section and A is the instantaneous cross-section area in the major principal direction. Assuming proportional loading, the state of the sheet metal at the onset of necking can be characterized by the ratio (ρ) between the principal strains ε_1 and ε_2, which can be expressed as follows:

$$\rho = \frac{\varepsilon_2}{\varepsilon_1} = \frac{\dot{\varepsilon}_2}{\dot{\varepsilon}_1} \qquad \text{Eq. 4.5}$$

Similarly, Ding et al [14] suggested that the stress ratio (α) can be expressed as a function of the strain ratio (ρ), as shown below:

$$\alpha = \frac{\sigma_2}{\sigma_1} = \frac{1+2\rho}{2+\rho} \qquad \text{Eq. 4.6}$$

The von Mises equivalent values of stress $\bar{\sigma}$, strain $\bar{\varepsilon}$ and strain rate $\dot{\bar{\varepsilon}}$ can be expressed in terms of principal values as follows:

$$\bar{\sigma} = b\sigma_1,\ \bar{\varepsilon} = a\varepsilon_1,\ \dot{\bar{\varepsilon}} = a\dot{\varepsilon}_1 \qquad \text{Eq. 4.7}$$

where a and b are functions of ρ and can be expressed as follows:

$$a \equiv \frac{2}{\sqrt{3}}\left(1+\rho+\rho^2\right)^{1/2} \text{ and } b \equiv \frac{\sqrt{3}}{2+\rho}\left(1+\rho+\rho^2\right)^{1/2} \qquad \text{Eq. 4.8}$$

The effective plastic strain rate ($\dot{\bar{\varepsilon}}$) for SP materials is a function of effective flow stress ($\bar{\sigma}$), effective plastic strain ($\bar{\varepsilon}$), grain size (d) and cavitation and can be expressed as (similar to Eq. 3.4):

$$\dot{\bar{\varepsilon}} = f\left(\bar{\sigma}, \bar{\varepsilon}, d, f_a\right) \qquad \text{Eq. 4.9}$$

Differential form of the above equation can be expressed as:

$$d\dot{\bar{\varepsilon}} = \left(\frac{\partial \dot{\bar{\varepsilon}}}{\partial \bar{\sigma}}\right)_{d,f_a} d\bar{\sigma} + \left(\frac{\partial \dot{\bar{\varepsilon}}}{\partial d}\right)_{\bar{\sigma},f_a} dd + \left(\frac{\partial \dot{\bar{\varepsilon}}}{\partial f_a}\right)_{\bar{\sigma},d} df_a \qquad \text{Eq. 4.10}$$

Constitutive equations for SP materials similar to Eq. 3.6 and Eq. 3.8 for biaxial deformation can be expressed as follows:

$$\dot{\bar{\varepsilon}} = \frac{k}{d^p}\left(\frac{\bar{\sigma}}{\left(1-f_a\right)}\right)^{1/m} \qquad \text{Eq. 4.11}$$

and

$$\dot{\bar{\varepsilon}} = \frac{k_2}{d^p}\left[\left(\frac{\bar{\sigma}}{\left(1-f_a\right)}\right)-\sigma_o\right]^{1/m} + k_3\left(\frac{\bar{\sigma}}{\left(1-f_a\right)}\right)^n \qquad \text{Eq. 4.12}$$

Grain growth evolution equations for biaxial deformation in SP materials can be expressed as (similar to Eq.'s 3.9-3.11):

Simple linear expression for dynamic grain growth can be expressed as:

$$d = d_o + c\bar{\varepsilon} \qquad \text{Eq. 4.13}$$

Differential form of the above equation can be expressed as follows:

$$dd = c\, d\bar{\varepsilon} \qquad \text{Eq. 4.14}$$

Assuming total grain growth kinetics to be the sum of the static and dynamic parts, the evolution equation for grain growth can be expressed as:

$$\dot{d} = \dot{d}_s + \dot{d}_d = \frac{B}{d^q} + \frac{k_4\left(1-e^{t/\tau}\right)}{d^q}\dot{\bar{\varepsilon}} \qquad \text{Eq. 4.15}$$

The differential form of the above equation can be written as:

$$dd = \frac{k_4}{d^q} d\bar{\varepsilon} \qquad \text{Eq. 4.16}$$

The evolution equations for constant and continuous nucleation in SP materials under different loading conditions (similar to Eq.'s 3.14-3.17) can be expressed as follows:

For Constant Nucleation + Pre-existing cavities:

$$f_a^{Tot} = f_{ao}^{N} * \exp[\psi * (\bar{\varepsilon} - \varepsilon_n)] + f_{ao}^{P} \exp(\psi\bar{\varepsilon}) \qquad \text{Eq. 4.17}$$

Differential form of the above equation can be expressed as:

$$df_a^{Tot} = f_a^{Tot} \psi \, d\bar{\varepsilon} \qquad \text{Eq. 4.18}$$

For Continuous Nucleation + Pre-existing cavities:

$$f_a^{Tot} = f_{ao}^{N} * (1 + \langle \bar{\varepsilon} - \varepsilon_n \rangle) \exp[\psi * (\bar{\varepsilon} - \varepsilon_n)] + f_{ao}^{P} \exp(\psi\bar{\varepsilon}) \qquad \text{Eq. 4.19}$$

Differential form of the above equation can be expressed as:

$$df_a^{Tot} = \left(f_a^{Tot}\psi + f_{ao}^{N} \exp[\psi(\bar{\varepsilon} - \varepsilon_n)]\right) d\bar{\varepsilon} \qquad \text{Eq. 4.20}$$

The void growth parameter (ψ) in the above expressions is a function of strain-rate sensitivity, stress state and the extent of grain boundary sliding. It can be expressed as [1,44] :

$$\psi = \left(\frac{m+1}{m}\right) \sinh\left[2\left(\frac{2-m}{2+m}\right)R\right] \qquad \text{Eq. 4.21}$$

where R is defined as the multiaxiality ratio and is expressed as follows:

$$R = \left(\sigma_m \big/ \bar{\sigma}\right) \qquad \text{Eq. 4.22]}$$

where σ_m is the mean stress and $\bar{\sigma}$ is the von Mises equivalent stress. For uniaxial stress state, R is 1/3 and Eq. (4.21) reduces to the familiar equation used in 1-D analysis (Eq. 3.18).

By substituting the differential form of the strain rate increment (Eq. 4.4), differential form of grain growth (Eq.4.14 or 4.16) and differential form of cavitation (Eq.4.18 or Eq.4.20) into the differential form of the functional representation of the constitutive equation (Eq.4.10), we arrive at:

In case of constant nucleation:

$$b\delta\sigma_1 + \frac{\delta\dot{A}}{A_o} e^{\varepsilon_1} a \frac{\partial\overline{\sigma}}{\partial\dot{\overline{\varepsilon}}} = -\frac{\delta A}{A_o} e^{\varepsilon_1} \left[a \frac{\partial\overline{\sigma}}{\partial\overline{d}} \frac{\partial\overline{d}}{\partial\overline{\varepsilon}} + a f_a^{Tot} \psi \frac{\partial\overline{\sigma}}{\partial f_a^{Tot}} + a\dot{\varepsilon}_1 \frac{\partial\overline{\sigma}}{\partial\dot{\overline{\varepsilon}}} \right] \qquad \text{Eq. 4.23}$$

In case of continuous nucleation:

$$b\delta\sigma_1 + \frac{\delta\dot{A}}{A_o} e^{\varepsilon_1} a \frac{\partial\overline{\sigma}}{\partial\dot{\overline{\varepsilon}}} = -\frac{\delta A}{A_o} e^{\varepsilon_1} \left[a \frac{\partial\overline{\sigma}}{\partial\overline{d}} \frac{\partial\overline{d}}{\partial\overline{\varepsilon}} + a \left(f_a^{Tot} \psi + f_{ao}^{N} \exp\left[\psi(\overline{\varepsilon} - \varepsilon_n)\right] \right) \frac{\partial\overline{\sigma}}{\partial f_a^{Tot}} + a\dot{\varepsilon}_1 \frac{\partial\overline{\sigma}}{\partial\dot{\overline{\varepsilon}}} \right]$$

Eq. 4.24

The condition of stability as suggested by Hart [60] is expressed as follows:

$$\frac{\delta\dot{A}}{\delta A} \leq 0 \qquad \text{Eq. 4.25}$$

Applying this stability condition to Eq. 4.23 or Eq. 4.24 as the case may be, the new multiscale stability criterion for SP material under various loading conditions at the onset of instability - can be expressed as:

$$a\gamma^* + m^* + a\zeta^* = 1 \qquad \text{Eq. 4.26}$$

where

$$\gamma^* = \frac{\dot{d}}{\dot{\overline{\varepsilon}}^2} \left(\frac{\partial\dot{\overline{\varepsilon}}}{\partial d} \right)_{\overline{\sigma}, f_a^{Tot}};$$

$$m^* = \frac{\overline{\sigma}}{\dot{\overline{\varepsilon}}} \left(\frac{\partial\dot{\overline{\varepsilon}}}{\partial\overline{\sigma}} \right)_{d, f_a^{Tot}}$$

and

$$\zeta^* = \frac{f_a^{Tot}\,\psi}{\dot{\bar{\varepsilon}}}\left(\frac{\partial\dot{\bar{\varepsilon}}}{\partial f_a^{Tot}}\right)_{\bar{\sigma},d} \qquad \text{Constant Nucleation}$$

(or)

$$\zeta^* = \frac{\left(f_a^{Tot}\,\psi + f_{ao}^{N}\exp\left[\psi\left(\bar{\varepsilon}-\varepsilon_n\right)\right]\right)}{\dot{\bar{\varepsilon}}}\left(\frac{\partial\dot{\bar{\varepsilon}}}{\partial f_a^{Tot}}\right)_{\bar{\sigma},d} \qquad \text{Continuous Nucleation}$$

The first term in the above equation corresponds to strain hardening due to grain coarsening, the second term corresponds to strain rate sensitivity and the third term accounts for cavitation effect. The above criterion reduces to a 1-D stability criterion for ρ = -0.5 [7]. In addition, the above equations reduce to the basic Hart's criterion [60] when grain growth and cavitation are not considered.

4.2 Results and Discussions:

The above developed stability criterion is simultaneously solved along with the constitutive equation, grain growth evolution equation and cavity evolution equation to construct optimum forming paths for SP materials (by following the procedure as described in Chapter 3), under various loading conditions. The stability criterion is applied to examine the stability of SP Coronze CDA 638 alloy, under biaxial loading conditions. The material parameters are determined by fitting the corresponding equations to the experimental data obtained by Caceres and Wilkinson [31]. Effect of initial grain size, stress ratio, grain growth exponent, strain rate sensitivity, pre-existing cavities, nucleation strain and nucleating (constant and continuous) cavities on the optimum forming paths is investigated.

4.2.1 Effect of Initial Grain size on the Optimum Forming paths:

Finer grain sizes in SP alloys ensure more stable deformation [1]. The effect of initial grain size in case of equi-biaxial (ρ=0.5) deformation on the optimum forming paths is shown in

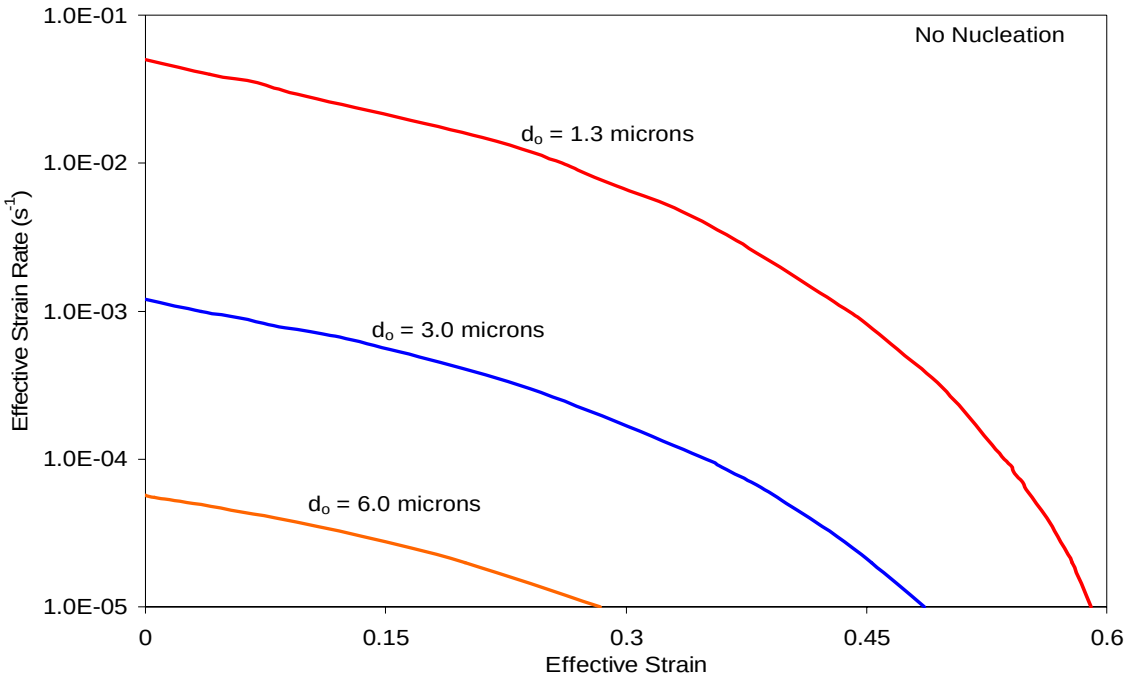

Figure 4-1 Effect of initial grain size on the Optimum forming paths of SP CDA 638 @ m=0.45, p=2.4, f_{ao}^{P} = 0.01, and ρ = 0.5

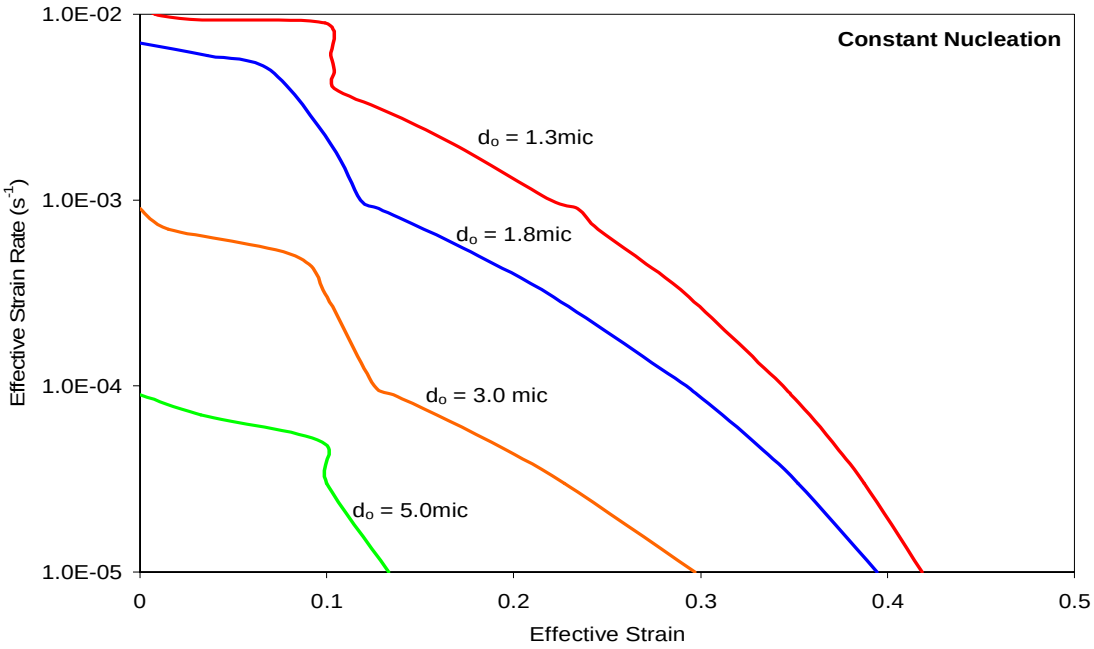

Figure 4-2 Effect of initial grain size on the Optimum forming paths of SP CDA 638 @ m=0.45, p=2.4, ε_n =0.1, f_{ao}^{P} = 0.03, (constant nucleation) f_{ao}^{N} = 0.05 and ρ = 0.5

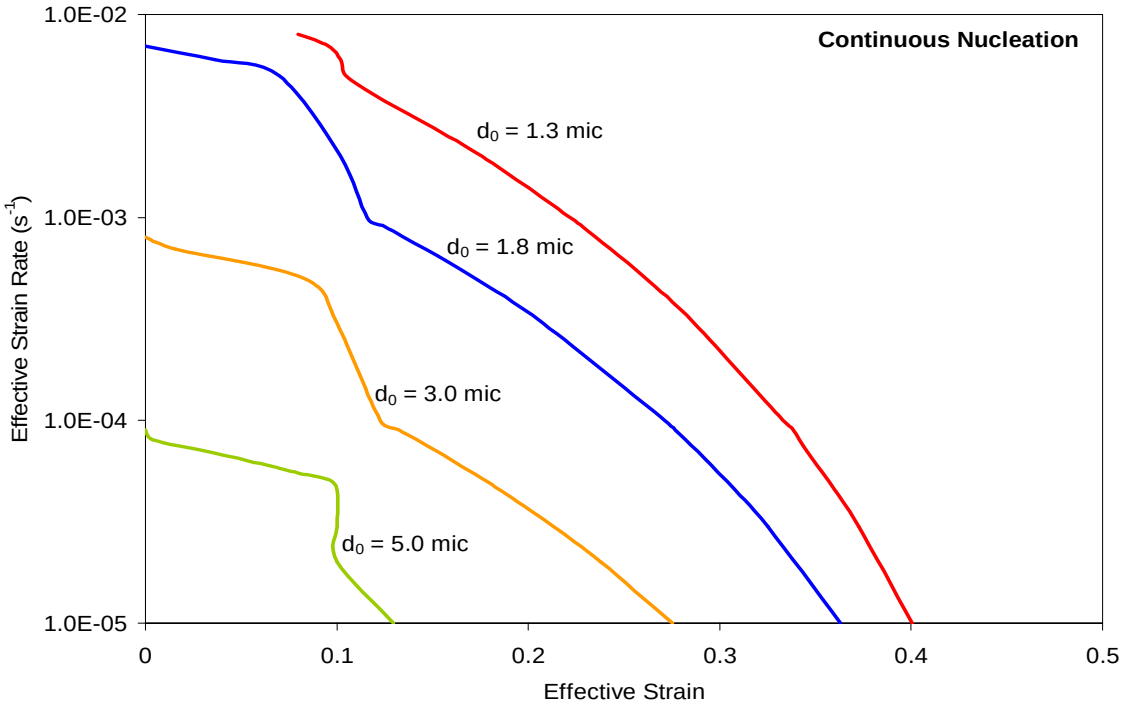

Figure 4-3 Effect of initial grain size on the Optimum forming paths of SP CDA 638 @ m=0.45, p=2.4, ε_n =0.1, f_{ao}^{P} = 0.03, (continuous nucleation) f_{ao}^{N} = 0.05 and ρ = 0.5

Figure 4-1, Figure 4-2 and Figure 4-3 for only pre-existing, pre-existing + constant and pre-existing + continuous nucleation cases, respectively. The plots suggest that finer the grain size more stable is the deformation. With an increase in the initial grain size, the maximum attainable strains without any instability is reduced. Accounting for only pre-existing cavities suggest that more stable deformation is possible for any given condition, when compared to the cases accounting for nucleation and pre-existing cavities. Interestingly, the shape of these curves in case of both constant and continuous nucleation remained the same and the maximum strains attained, though are less in case of continuous nucleation, the difference is not significant. The sudden drop in the curves at a strain of 0.1 indicates the beginning of the effect of nucleating cavities (besides the pre-existing cavities).

4.2.2 Effect of Strain rate sensitivity (m) on the Optimum Forming paths:

Strain rate sensitivity is an important characteristic of SP materials. The effect of ‘m’ on the optimum forming paths of SP CDA 638 alloy considering only pre-existing cavities (without nucleation) are shown in Figure 4-4. As expected, more stable deformation at much faster rate can be achieved in case of the alloy with higher strain rate sensitivity. There is no sudden and sharp decrease in the slope of the curves, since the effect of nucleation is not accounted for.

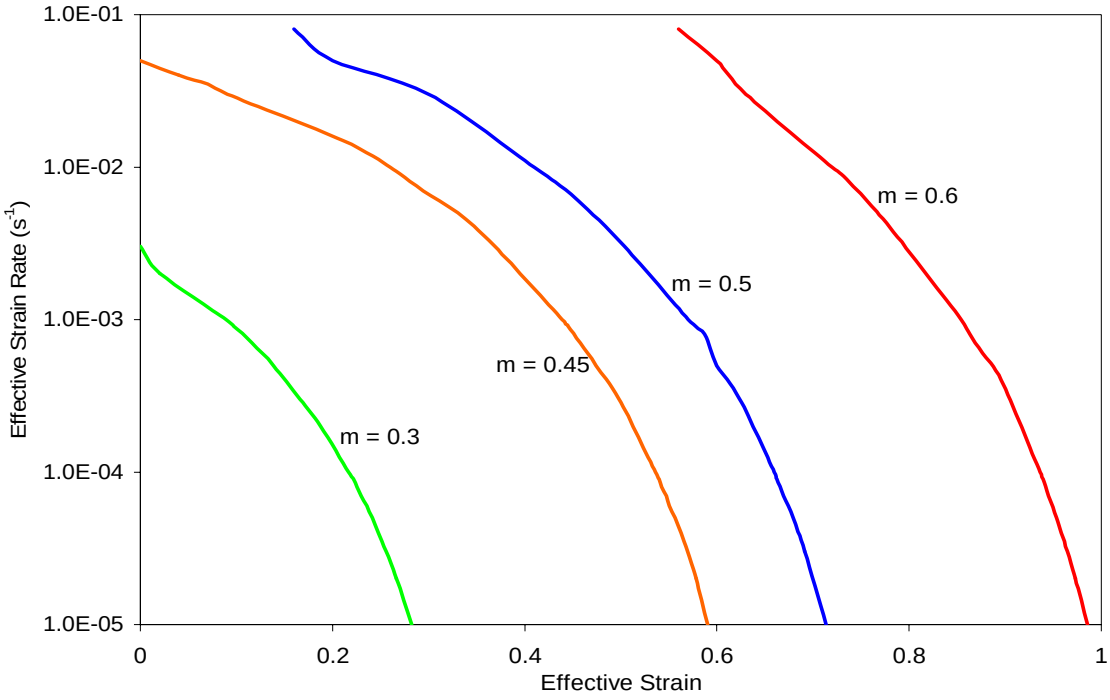

Figure 4-4 Effect of 'm' on the Optimum Forming paths of SP CDA 638 @ d_o =1.3 microns, p=2.4, f_{ao}^{p} = 0.05 and ρ = 0.5

The effect of strain rate sensitivity on the optimum forming paths of SP CDA 638 for a given set of conditions is depicted in Figure 4-5 for constant nucleation case and Figure 4-6 for continuous nucleation case. Large strain rate sensitivity offers more stable deformation and the maximum critical effective strains attained are higher in case of a material with more strain rate sensitivity. As observed in several other cases, the maximum stable deformation attained is less in case of continuous nucleation when compared to the case considering constant nucleation. It should also be observed that there is a sudden drop in the effective strain rate values corresponding to the nucleation strain when the strain rate sensitivity is less. The drop decreases as strain rate sensitivity increases. This phenomenon is seen in both constant and continuous nucleation cases. Thus, higher strain rate sensitivity for a SP alloy is a desirable characteristic to achieve maximum stable deformation, under any loading condition.

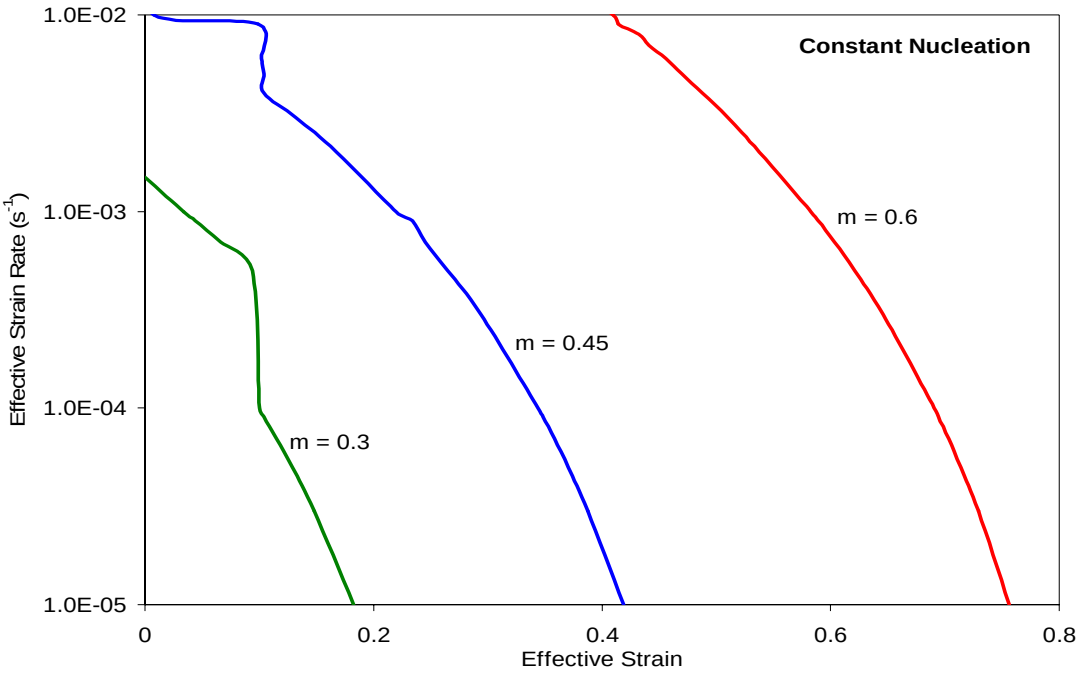

Figure 4-5 Effect of 'm' on the Optimum Forming paths of SP CDA 638 @ d_o =1.3 microns, p=2.4, ε_n =0.1, f_{ao}^P = 0.03, (constant nucleation) f_{ao}^N = 0.05 and ρ = 0.5

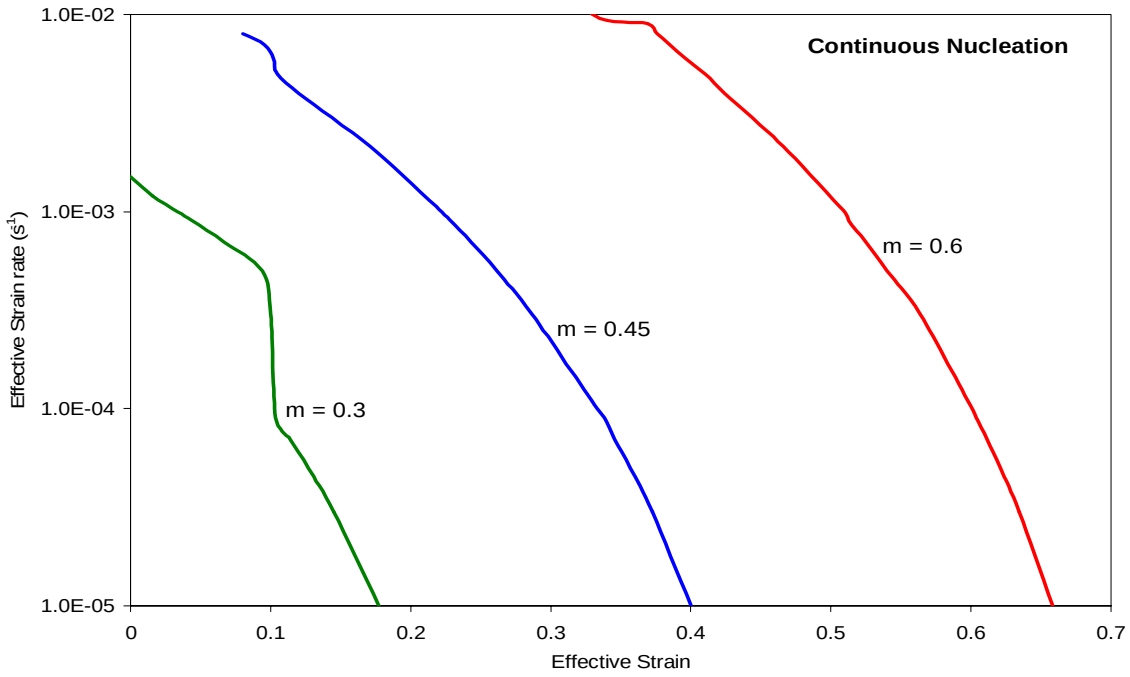

Figure 4-6 Effect of 'm' on the Optimum Forming paths of SP CDA 638 @ d_o =1.3 microns, p=2.4, ε_n =0.1, f_{ao}^P = 0.03, (continuous nucleation) f_{ao}^N = 0.05 and ρ = 0.5

4.2.3 Effect of Pre-existing cavities on the Optimum Forming paths:

It has been demonstrated in the previous chapter that the optimum variable strain rate forming paths for different SP alloys are significantly influenced by the pre-existing cavities and their growth during deformation. Effect of these pre-existing cavities under equi-biaxial loading ($\rho = 0.5$) condition, on the optimum forming paths is shown in Figure 4-7. It is shown, as would be expected that cavitation has adverse effects on deformation stability. The critical strains (that corresponding to the onset of instability) that can be attained are significantly reduced as the initial area fraction of cavities increases. The effect seems to be more pronounced for the biaxial loading case (Figure 4-7) as compared to the uniaxial case (Figure 3-13). For the uniaxial case, the critical strain assuming no cavitation at a strain rate of 10^{-5} s^{-1} is approximately 1.35. This value drops to approximately 1.1 if the initial area fraction of cavities is only 0.5%.For the biaxial case, the critical strain at 0% initial cavitation is about 2.25. The same value drops sharply to a value of about 0.7 if the initial area fraction of cavities is only 0.5%.

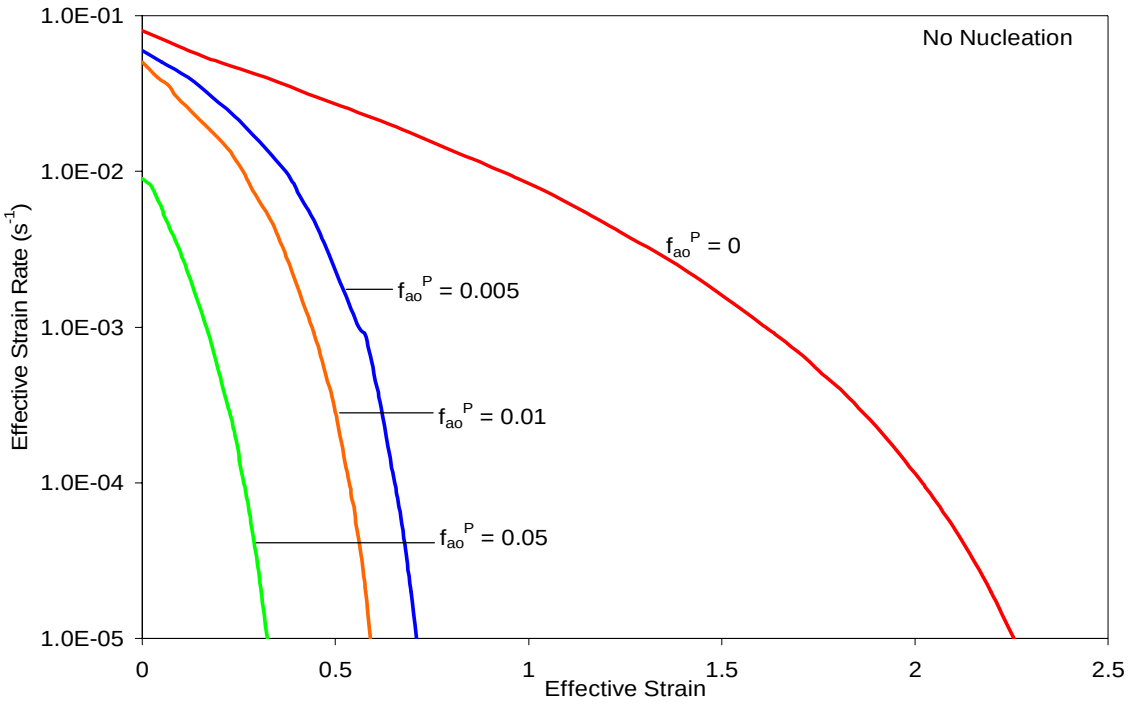

Figure 4-7 Effect of pre-existing cavities on the Optimum Forming paths of SP CDA 638 @ d_o= 1.3microns, p=2.4, m=0.45

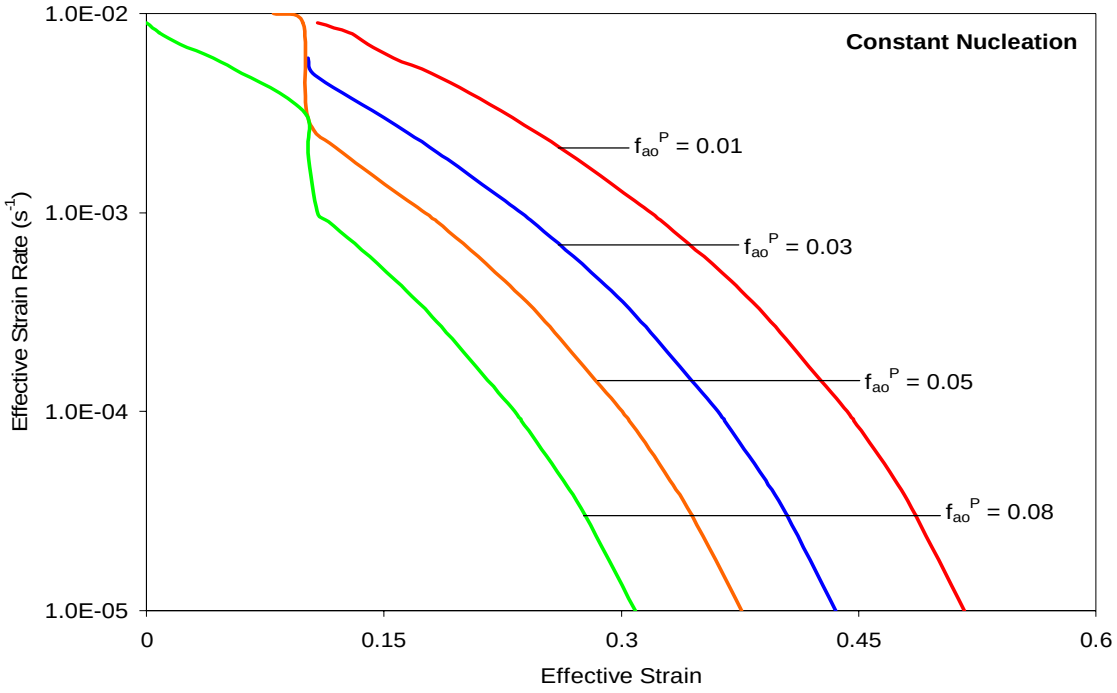

Figure 4-8 Effect of pre-existing cavities on the Optimum Forming paths of SP CDA 638 @ d_o =1.3 microns, p=2.4, ε_n =0.1, (constant nucleation) f_{ao}^N = 0.05 and ρ = 0.5

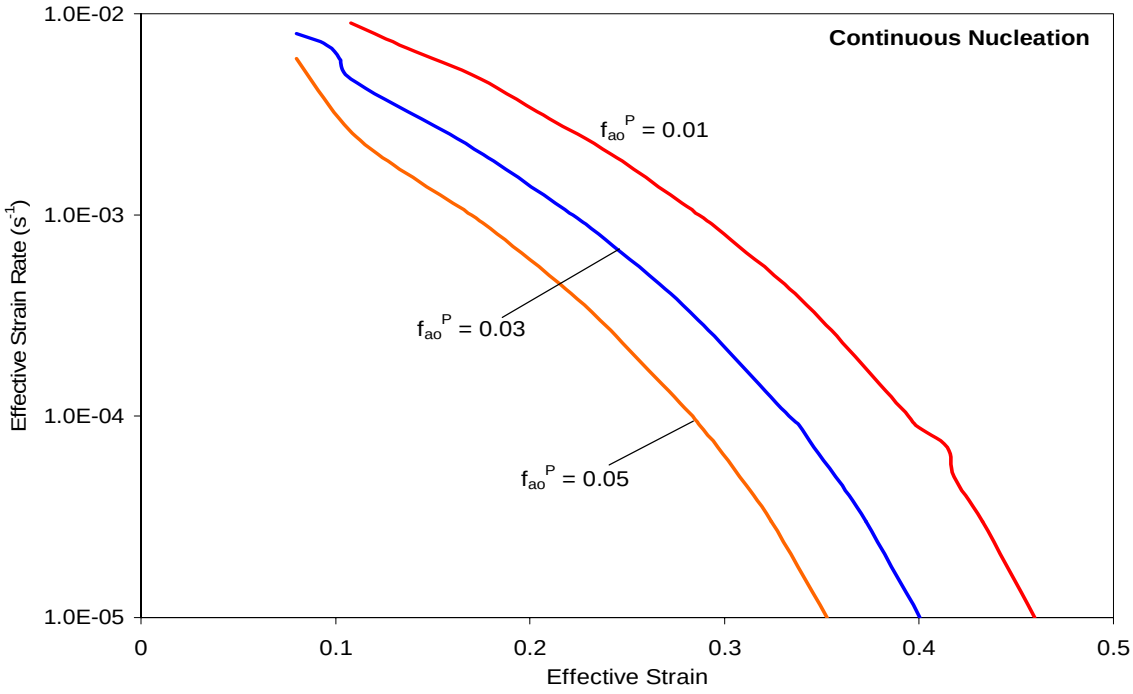

Figure 4-9 Effect of pre-existing cavities on the Optimum Forming paths of SP CDA 638 @ d_o =1.3 microns, p=2.4, ε_n =0.1, (continuous nucleation) f_{ao}^N = 0.05 and ρ = 0.5

The effect of varying initial area fraction of pre-existing cavities considering a certain initial area fraction of nucleating cavities in constant and continuous nucleation cases on the optimum forming paths of CDA 638 alloy are shown in Figure 4-8 and Figure 4-9 respectively. As one would expect, the maximum strains attainable are less in case of continuous nucleation when compared to the constant nucleation case. Also, the maximum strains attained significantly reduce with an increase in the initial area fraction of cavities in both cases.

4.2.4 Effect of Nucleating cavities on the Optimum Forming paths:

Effect of nucleating cavities on the optimum forming paths of SP CDA 638 alloy without accounting for pre-existing cavities, for constant and continuous nucleation cases is shown in Figure 4-10 and Figure 4-11 respectively. The combined effect of pre-existing and nucleating cavities on the optimum paths for constant and continuously nucleating cavities is shown in Figure 4-12 and Figure 4-13 respectively.

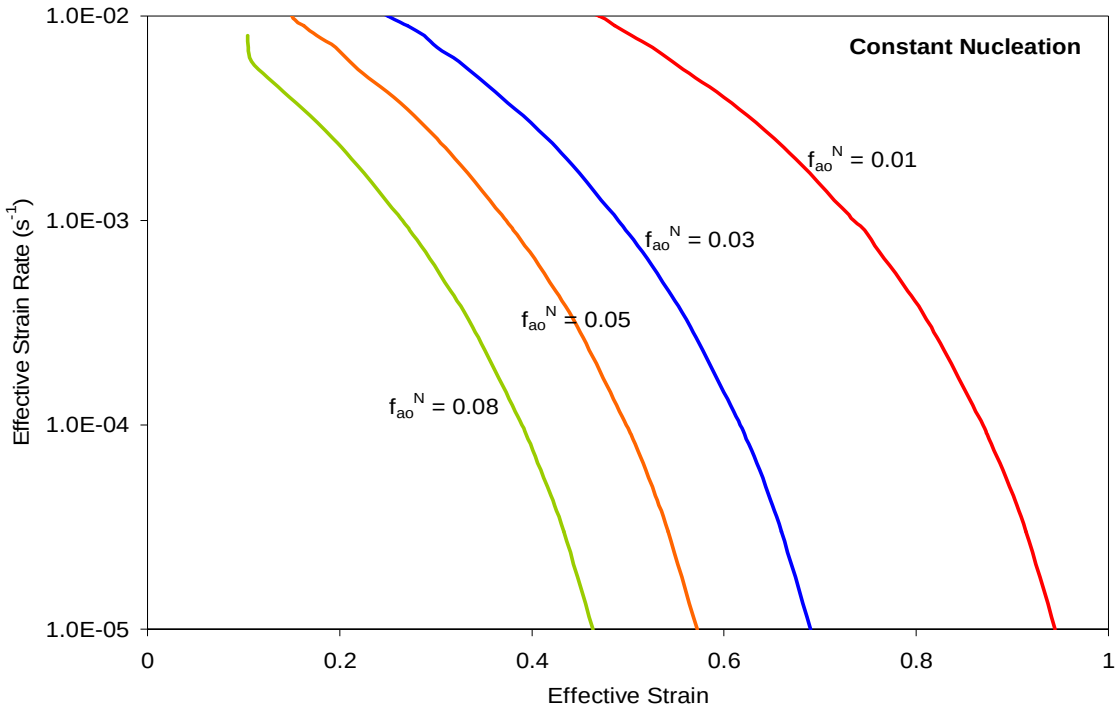

Figure 4-10 Effect of nucleating (constant) cavities on the Optimum Forming paths of SP CDA 638 @ d_o =1.3 microns, p=2.4, ε_n =0.1, f_{ao}^P = 0.0 and ρ = 0.5

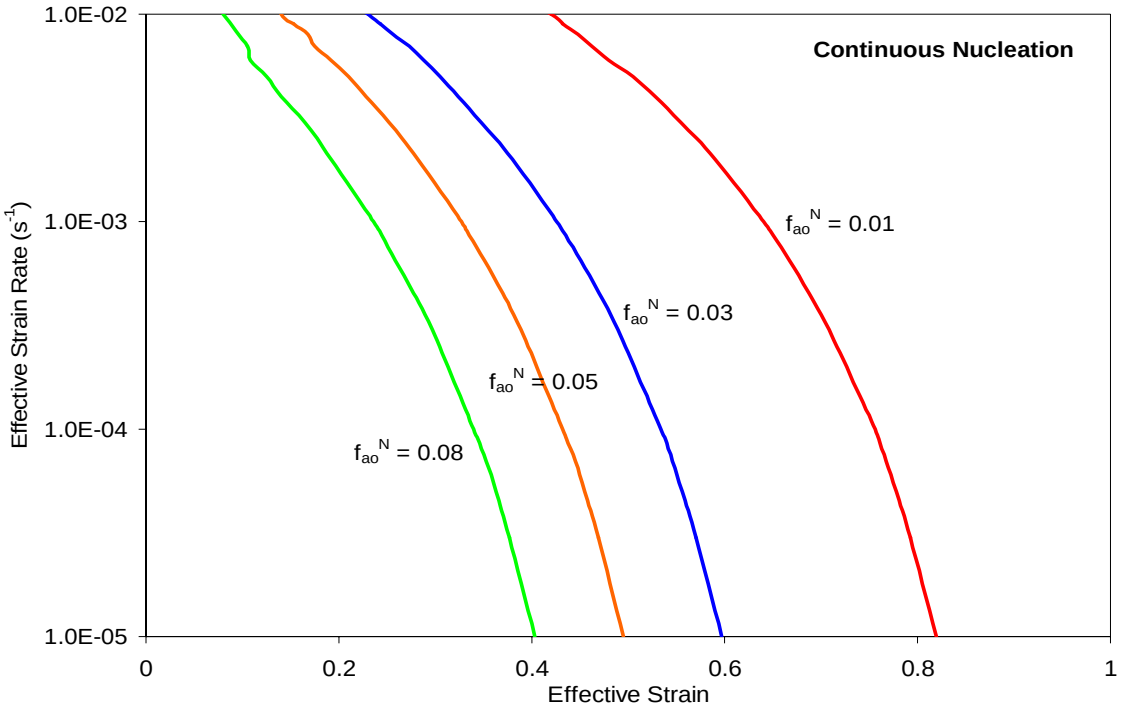

Figure 4-11 Effect of nucleating (continuous) cavities on the Optimum Forming paths of SP CDA 638 @ d_o =1.3 microns, p=2.4, ε_n =0.1, f_{ao}^P = 0.0 and ρ = 0.5

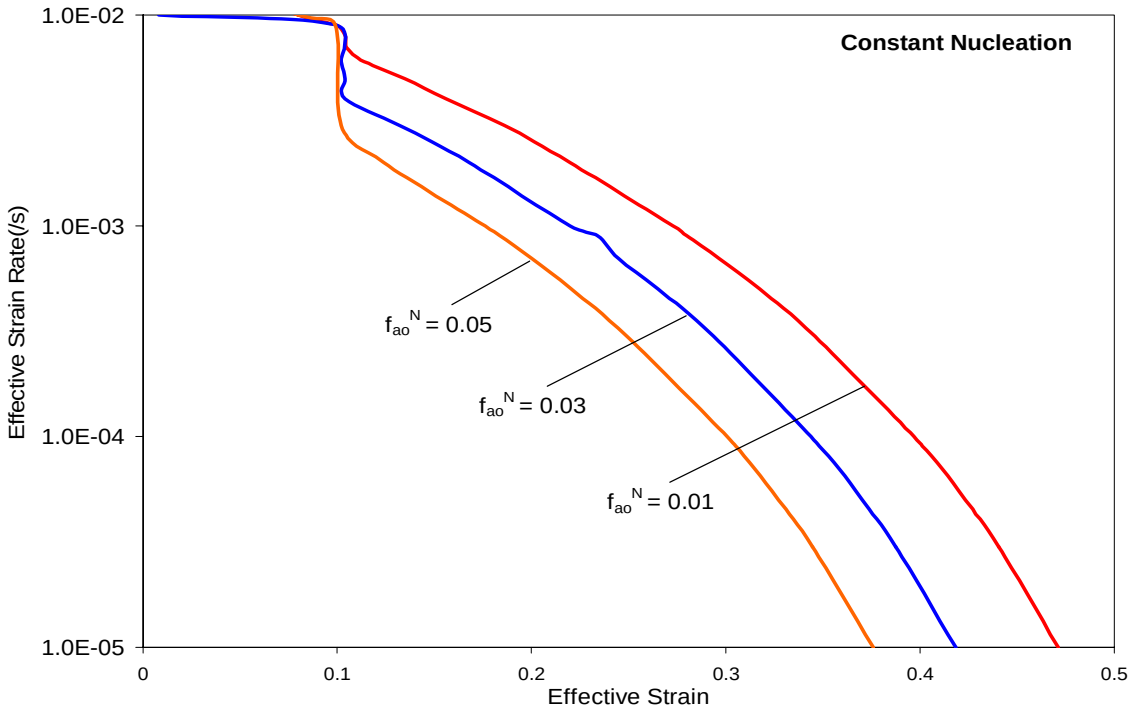

Figure 4-12 Effect of nucleating (constant) and pre-existing cavities on the Optimum Forming paths of SP CDA 638 @ d_o =1.3 microns, p=2.4, ε_n =0.1, f_{ao}^P = 0.05 and ρ = 0.5

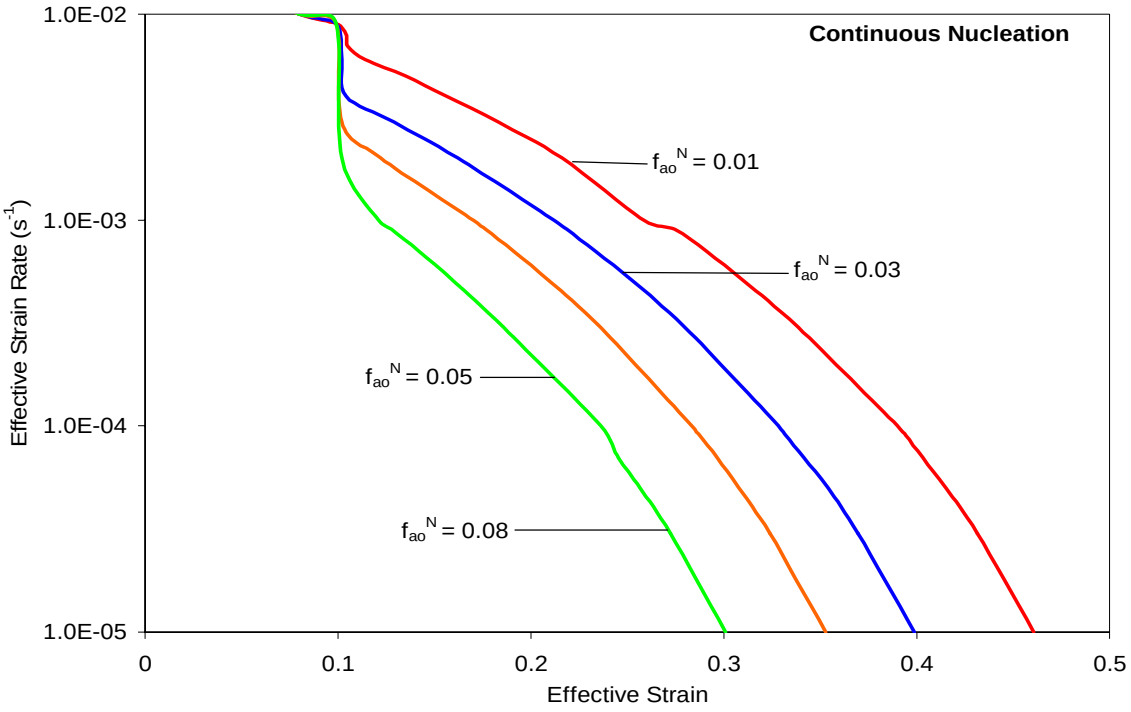

Figure 4-13 Effect of nucleating (continuous) and pre-existing cavities on the Optimum Forming paths of SP CDA 638 @ d_o =1.3 microns, p=2.4, ε_n =0.1, f_{ao}^P = 0.05 and ρ = 0.5

Critical strains (corresponding to no instability condition) attained decrease with an increase in the initial area fraction of nucleating cavities. The reduction is more when the nucleating cavities are assumed to be continuously increasing in number with strain, than when they (nucleating cavities) are assumed to be constant. Similar effect, but further reduction in maximum strains attained is observed when both pre-existing and nucleating cavities are taken into account.

4.2.5 Effect of Biaxiality / Stress ratio (ρ):

The effect of biaxiality ratio on the optimum forming paths of SP Coronze CDA 638 is investigated in order to understand the effect of various loading conditions/stress states on the ductility of SP materials. To explain the sharp reduction in ductility under biaxial loading, the optimum strain rate path is generated for different biaxiality ratios for the case of no cavitation,

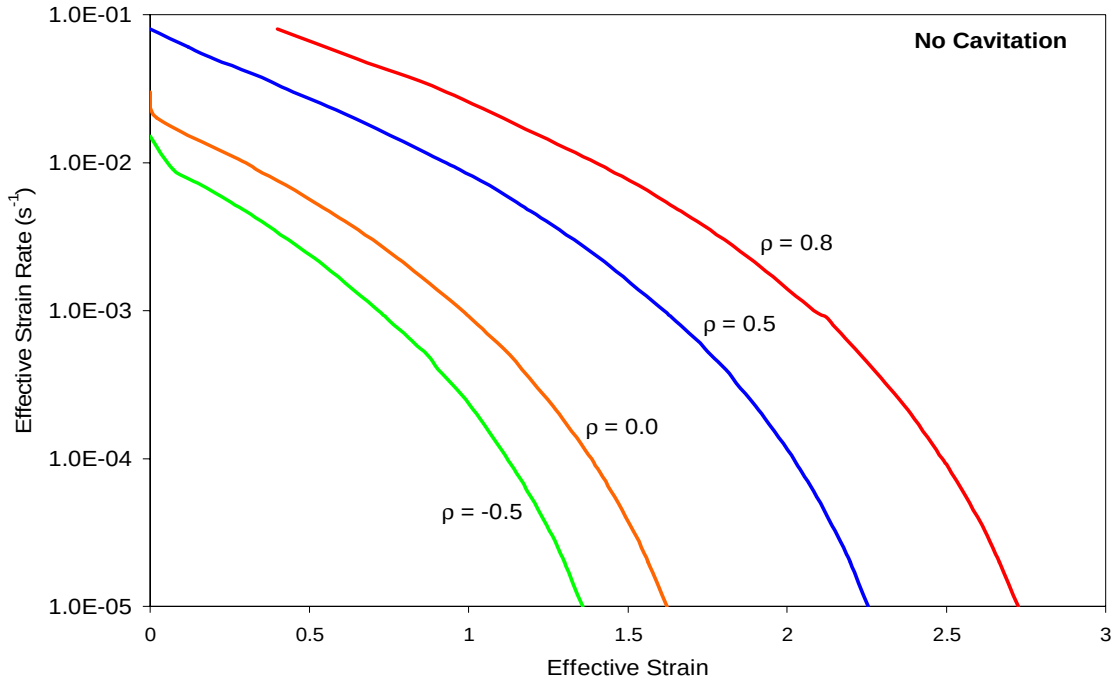

Figure 4-14 Effect of biaxiality ratio (ρ) on the optimum forming paths for SP CDA 638 alloy @ d_o = 1.3 microns, m = 0.45, p=2.4 and no cavitation

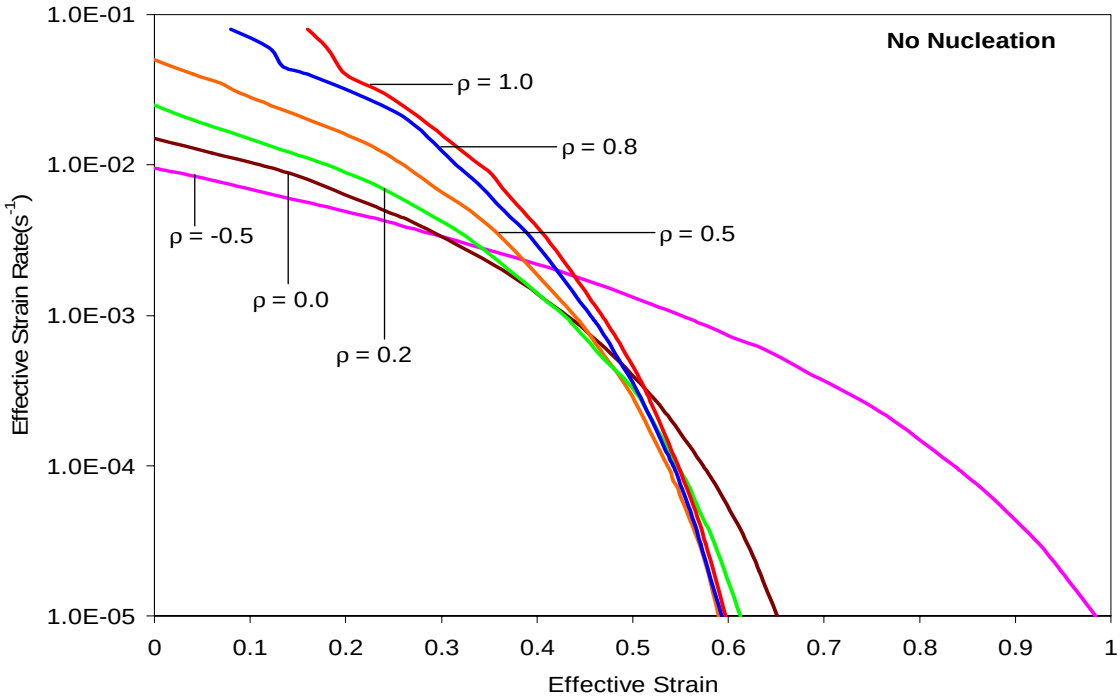

Figure 4-15 Effect of biaxiality ratio (ρ) on the optimum forming paths for SP CDA 638 alloy @ d_o = 1.3 microns, m = 0.45, p=2.4, f_{ao}^{P} = 0.01 and no nucleation

as shown in Figure 4-14 and for an initial area fraction of pre-existing cavities of 1% without accounting for nucleation , as shown in Figure 4-15. For the case of no cavitation (i.e. considering only geometrical instabilities) increasing the biaxiality ratio increases the maximum strain that can be achieved prior to necking. This can be explained due to the fact that additional biaxial tensile load tends to delay the onset of necking perpendicular to the major stress axis. The behavior is significantly different when cavitation is accounted for. In Figure 4-15, the same trend that was observed in Figure 4-14 is only valid at low strain values (up to a strain value of about 0.4). For higher strain values, the ductility for uniaxial loading case (ρ=-0.5) is much higher than the ductility for biaxial loading case. These observations can be explained as follows: at low strain values (i.e. at early stages in the forming process) the dominant failure mode is geometrical (necking) since microstructural features need time to evolve and contribute to the deformation and failure. At higher strains (i.e. at later stages in the forming process), the dominant failure mode is due to microstructural aspects (mainly cavitation). By incorporating the effect of constant nucleation and also accounting for pre-existing cavities, it is observed that the maximum attainable strain decreases significantly from ~ 0.74 in case of uniaxial (ρ = -0.5)

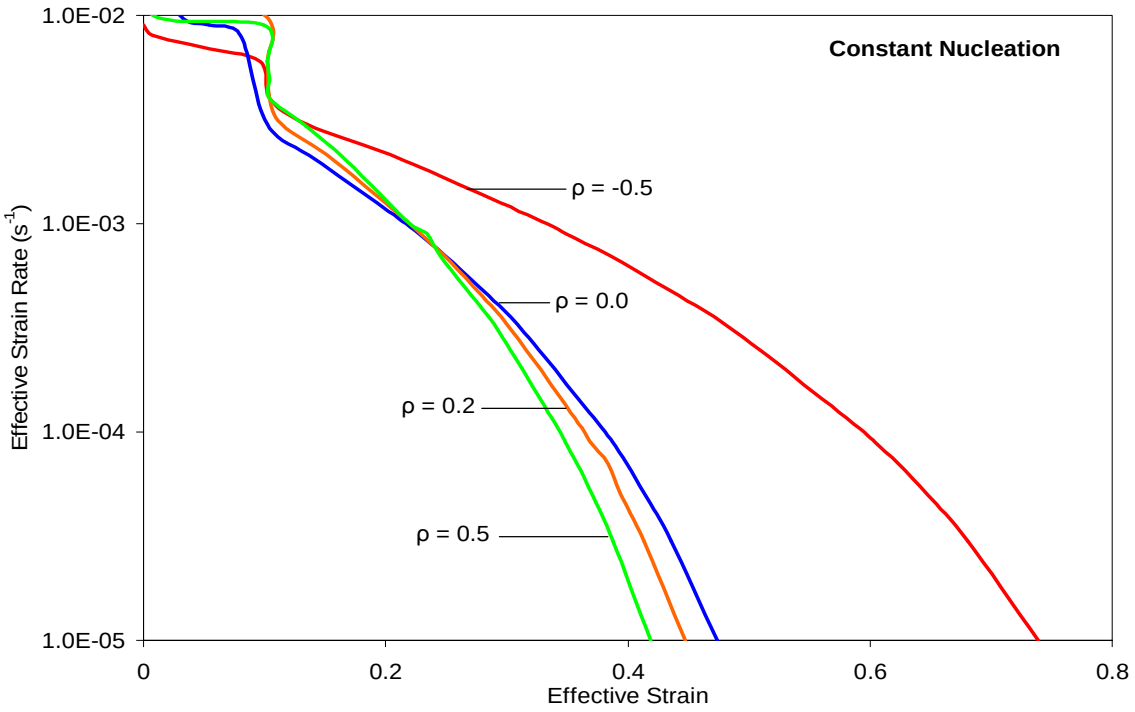

Figure 4-16 Effect of biaxiality ratio (ρ) on the optimum forming paths for SP CDA 638 alloy @ d_o = 1.3 microns, m = 0.45, p=2.4, f_{ao}^{P} = 0.03 and ε_n =0.1, f_{ao}^{N} = 0.05 (constant nucleation)

deformation to ~ 0.42 in case of equi-biaxial (ρ = 0.5) tensile deformation. The change in the optimum forming paths when continuous nucleation of cavities along with pre-existing cavities is taken into account for SP CDA 638 alloy is shown in Figure 4-17. Reduction in the maximum strains attained caused when accounting for continuous nucleation and pre-existing cavities is more in comparison to the case accounting for constant nucleation and pre-existing cavities. It can observed that with an increase in the biaxiality ratio value, there is not much of a change in the maximum strains attained at lower strain rates and faster is the rate of deformation at lower strains for higher values of biaxiality ratios.

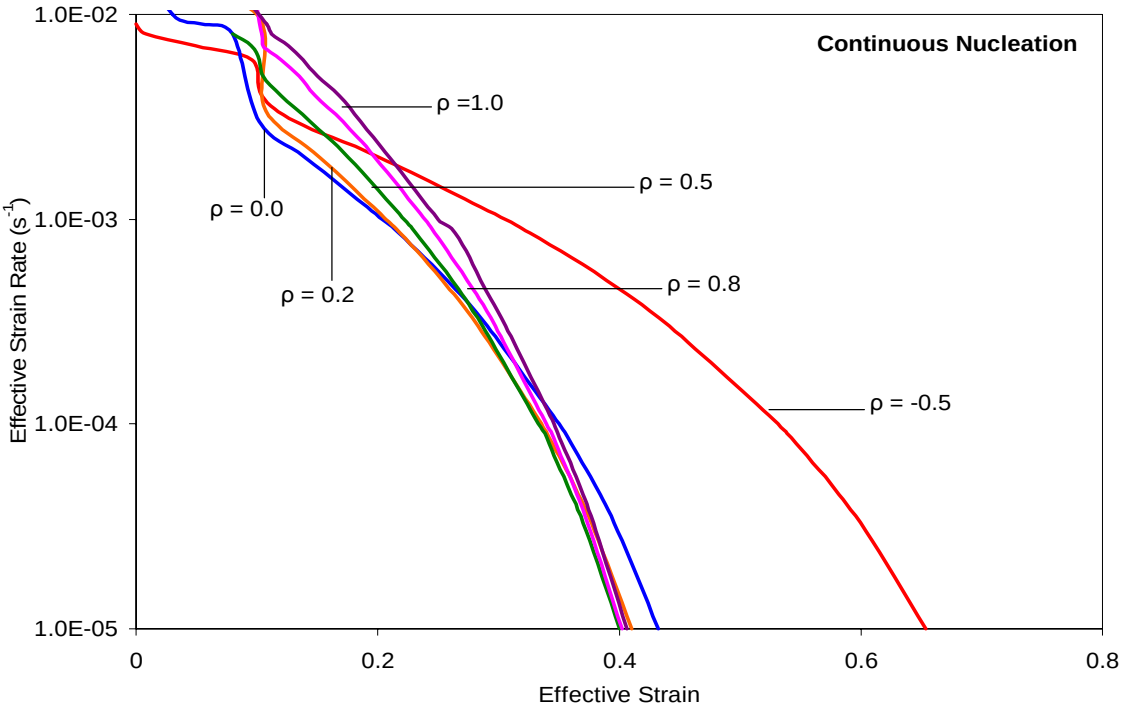

Figure 4-17 Effect of biaxiality ratio (ρ) on the optimum forming paths for SP CDA 638 alloy @ d_o = 1.3 microns, m = 0.45, p=2.4, f_{ao}^{P} = 0.03 and ε_n =0.1, f_{ao}^{N} = 0.05 (continuous nucleation)

4.2.6 Effect of Nucleation strain on the Optimum Forming paths:

The strain at which the nucleating cavities come into existence or in fact affect the deformation is crucial in designing optimum deformation paths for SP alloys. The effect of nucleation strain in case of constant nucleation and continuous nucleation is shown in Figure 4-18 and Figure 4-19 respectively. It can observed that the influence of nucleation strain on the

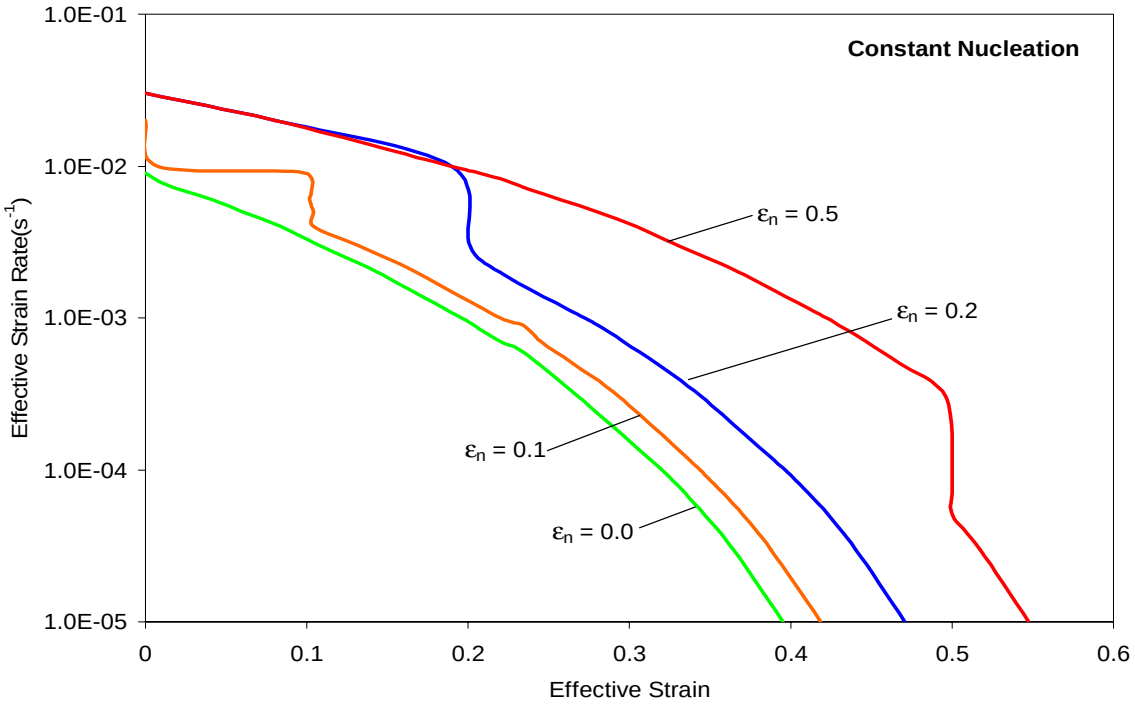

Figure 4-18 Effect of nucleation strain (ε_n) on the optimum forming paths for SP CDA 638 alloy @ d_o = 1.3 mic, ρ=0.5, m = 0.45, p=2.4, f_{ao}^{P} = 0.03, f_{ao}^{N} = 0.05 (constant nucleation)

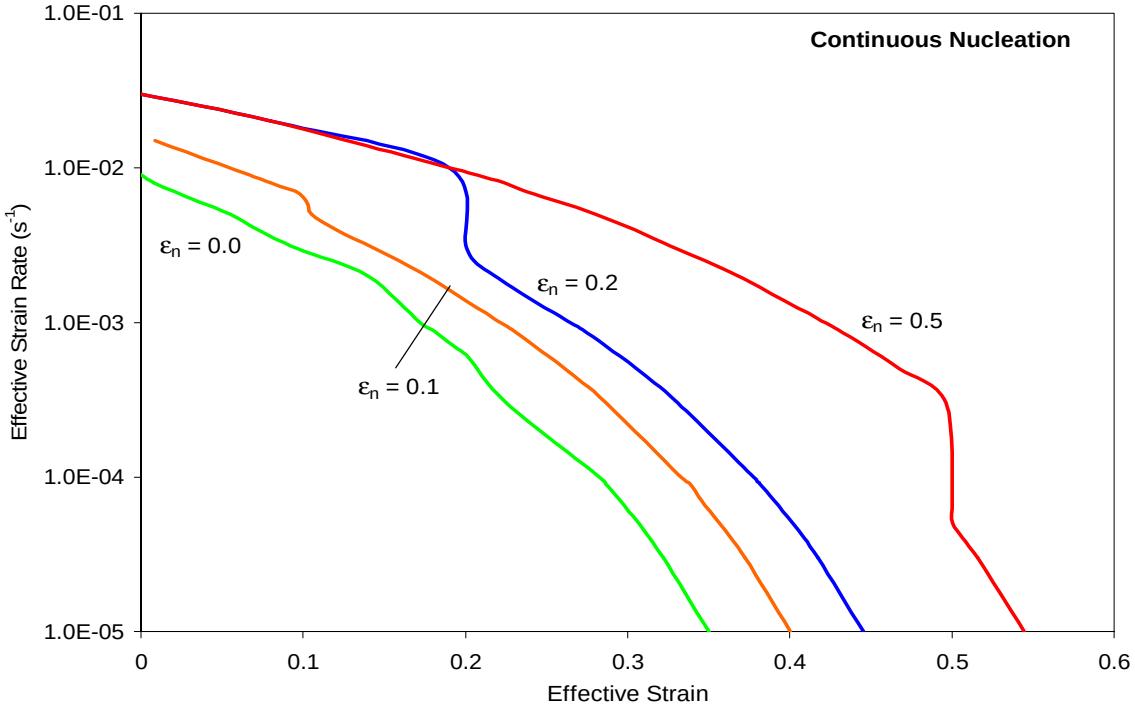

Figure 4-19 Effect of nucleation strain (ε_n) on the optimum forming paths for SP CDA 638 alloy @ d_o = 1.3 mic, ρ=0.5, m = 0.45, p=2.4, f_{ao}^{P} = 0.03, f_{ao}^{N} = 0.05 (continuous nucleation)

optimum deformation paths of SP CDA 638 alloy is almost insignificant when the nucleation strain is high, as the role of nucleating cavities is delayed in the event of large nucleation strains. Hence there is not much of a difference between constant or continuous nucleation. However for lower nucleation strains, the maximum critical strains attained are less in case of continuous nucleation when compared to the case of constant nucleation of cavities, as the influence of nucleating cavities begins earlier in the deformation.

4.2.7 Effect of Grain Growth Exponent (p):

The effect of grain size exponent on the optimum variable strain rate path of SP CDA 638 alloy accounting for constant nucleation + pre-existing cavities and continuous nucleation + pre-existing cavities, for a equi-biaxial loading case is shown in Figure 4-20 and Figure 4-21 respectively. As was seen in uniaxial loading case, material with larger 'p' value yields more stable deformation. Also, constant nucleation consideration yielded higher values of maximum strain when compared to the case considering continuous nucleation of cavities.

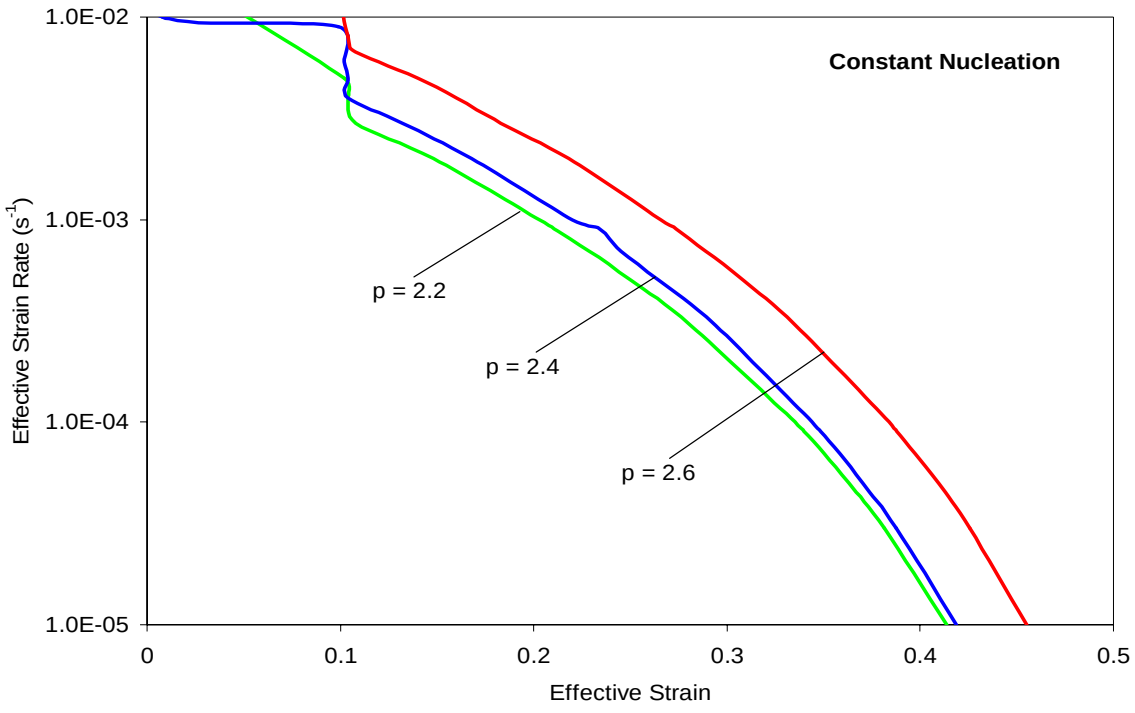

Figure 4-20 Effect of 'p' on the optimum forming paths for SP CDA 638 alloy @ d_o = 1.3 microns, ρ=0.5, m = 0.45, f_{ao}^{P} = 0.03, f_{ao}^{N} = 0.05 (constant nucleation)

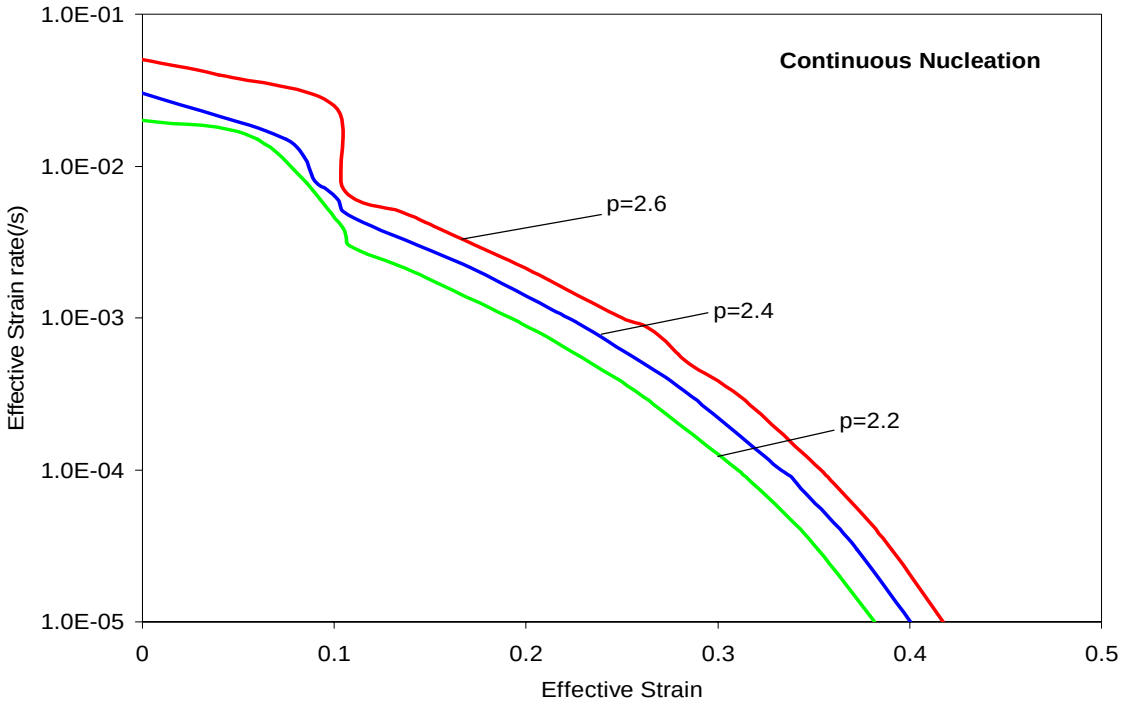

Figure 4-21 Effect of 'p' on the optimum forming paths for SP CDA 638 alloy @ d_o = 1.3 microns, ρ=0.5, m = 0.45, f_{ao}^{P} = 0.03, f_{ao}^{N} = 0.05 (continuous nucleation)

4.3 Conclusion

The stability of superplastic deformation under biaxial plane stress condition is investigated. Biaxial plane stress condition was considered for this analysis because it is the dominant stress state in blow forming of superplastic sheets. A new multiscale stability criterion is developed that accounts for both geometrical instabilities and microstructural features including grain growth and cavitation. Effect of nucleation (constant and continuous) of cavities was also incorporated into the model. A two dimensional linear stability analysis of biaxial stretching of a thin sheet under plane stress condition is carried out. The proposed stability criterion was then used to design optimum variable strain rate forming paths, for SP alloys under different stress states. Effect of initial grain size, grain size exponent, strain rate sensitivity, initial area fraction of pre-existing and nucleating cavities, nucleation strain and biaxiality ratio on the stable deformation of SP CDA 638 alloy was investigated. Material with fine grain size

and high strain rate sensitivity with low levels of cavitation and high nucleation strain with high grain growth exponent seem to yield maximum stable deformation.

Chapter 5 Multiscale Stability Analysis and Optimization of SPF accounting for Anisotropy

Modeling superplastic deformation is generally based on assumptions of isotropic behavior which leads to use of von Mises flow rules [53, 86]. However, it has been observed that superplastic materials exhibit a strong degree of anisotropy [49] during large deformations. Swift [86] found that samples of aluminum, copper, stainless steel and brass which were initially isotropic in nature, exhibited an extension of 5-10% for a shear strain of 3, during torsion tests. This length change was attributed to anisotropy which could have resulted from preferred orientation or internal stresses or a combination of both, by Hill [65], who then proposed a yield criterion for an anisotropic material by extending the basic theory of anisotropy to account for length change during torsion tests. Relation between the length changes and texture development in copper brass with temperature, subjected to free-end torsion tests was investigated by Toth et al [87]. They suggested that the length of the sample increases at room temperature and the textures are entirely attributed to dislocation glide. They also observed that the length increases and then decreases at higher temperatures and the corresponding textures displayed evidence of dynamic recrystallization.

Thus, it is important to account for anisotropy during modeling of superplastic deformation [49]. However, there seems to be very limited work being done on this area and almost no work has been reported (to our knowledge) that would refer to accounting anisotropy and develop a multiscale stability criterion. Thus, an attempt has been made to study the effect of anisotropy on the optimum variable strain rate forming paths during superplastic deformation (besides the effect of geometrical and microstructural aspects) under uniaxial loading condition.

5.1 Model Development:

The functional form of constitutive equation accounting for anisotropic parameters and hardening (isotropic hardening and anisotropic hardening) can be expressed as follows:

$$\dot{\varepsilon} = \dot{\varepsilon}(\sigma, d, f_{a,} R, \alpha) \qquad \text{Eq. 5.1}$$

where R represents isotropic hardening and α is the internal stress tensor representing kinematic hardening. The differential form of the above equation can be expressed as follows:

$$d\dot{\varepsilon} = \frac{\partial \dot{\varepsilon}}{\partial \sigma} d\sigma + \frac{\partial \dot{\varepsilon}}{\partial d} dd + \frac{\partial \dot{\varepsilon}}{\partial f_a} df_a + \frac{\partial \dot{\varepsilon}}{\partial R} dR + \frac{\partial \dot{\varepsilon}}{\partial \alpha} d\alpha \qquad \text{Eq. 5.2}$$

A general associated flow rule for of the above expression is given as [49,88]:

$$D^p = f \frac{\partial J}{\partial \sigma} \qquad \text{Eq. 5.3}$$

where D^p is the plastic component of the strain tensor, f is the overstress function, J is the generalized anisotropic yield function and J (σ-α) is a positive scalar valued isotropic function of the state variables having dimensions of Cauchy stress tensor (σ) and back stress (α). There are many different forms for the function that have been presented in the literature. Here we use a form which describes the characteristics of superplastic materials motivated by the work of Hamilton et al [32]:

$$f = \frac{C_i \left(J - (k_o + R)\right)^{\frac{1}{m}}}{d^P} + C_{ii} J^n \qquad \text{Eq. 5.4}$$

where (ko + R) is a reference stress whose variable part, R, represents isotropic hardening, m is the strain rate sensitivity index, d is the grain size, p is the grain size exponent, C_i, C_{ii}, and n are material constants. Kinematic hardening is represented by the internal (back) stress (α), in J. The generalized anisotropic yield function for uniaxial stress state is expressed as [53]:

$$J^2 = K_I \sigma^2 + K_{II} \sigma\alpha + K_{III} \alpha^2 \qquad \text{Eq. 5.5}$$

where K_I, K_{II}, and K_{III} are material constants, which are functions of anisotropic parameters, as expressed below:

$$K_I = \left[1 + c_1 \left(\cos^2\phi \sin^2\phi \right) + c_2 \left(\frac{2}{3}\cos^2\phi - \frac{1}{3}\sin^2\phi \right)^2 + c_3 \left(\frac{2}{3}\sin^2\phi - \frac{1}{3}\cos^2\phi \right)^2 \right]$$

$$K_{II} = \left[\begin{array}{l} -3 - 3c_1\left(\cos^2\phi \sin^2\phi\right) + c_2\left(-\frac{4}{3}\cos^4\phi + \frac{4}{3}\cos^2\phi\sin^2\phi - \frac{1}{3}\sin^4\phi\right) + \\ c_3\left(-\frac{4}{3}\sin^4\phi + \frac{4}{3}\cos^2\phi\sin^2\phi - \frac{1}{3}\cos^4\phi\right) \end{array} \right]$$

$$K_{III} = \left[\frac{9}{4} + \frac{9}{4}c_1\left(\cos^2\phi\sin^2\phi\right) + c_2\left(\cos^2\phi - \frac{1}{2}\sin^2\phi\right)^2 + c_3\left(\sin^2\phi - \frac{1}{2}\cos^2\phi\right)^2 \right]$$

where c_1, c_2 and c_3 are anisotropic parameters and ϕ is the anisotropic angle describing the direction of anisotropy.

Applying Eq's (5.3-5.5), the constitutive equation for SP materials accounting for grain growth, cavitation, isotropic hardening, kinematic hardening and anisotropic parameters can be expressed as follows:

$$\dot{\varepsilon} = \left(\left\{ \frac{C_i}{d^p} \left[\frac{\sqrt{\left(K_I\sigma^2 + K_{II}\sigma\alpha + K_{III}\alpha^2\right)}}{\left(1 - f_a\right)} \right] - \left(k_o + R\right) \right\}^{1/m} + C_{ii} \left[\frac{\sqrt{\left(K_I\sigma^2 + K_{II}\sigma\alpha + K_{III}\alpha^2\right)}}{\left(1 - f_a\right)} \right]^n \right) * \left(\frac{2K_I\sigma + K_{II\alpha}}{2\sqrt{\left(K_I\sigma^2 + K_{II}\sigma\alpha + K_{III}\alpha^2\right)}} \right) \quad \text{Eq. 5.6}$$

To simplify the above expression, let:

$$X = \left(\left[\frac{J}{1 - f_a} \right] - \left(k_o + R\right) \right);\ Y = \left[\frac{J}{1 - f_a} \right];\ Z = \left(\frac{2K_I\sigma + K_{II}\alpha}{2J} \right) \quad \text{and} \quad \text{Eq. 5.7}$$

$$W = \left(\frac{C_i}{d^p} X^{1/m} + C_{ii} Y^n \right)$$

The grain growth evolution equation accounting for the total grain growth kinetics and the differential form of its representation are given by Eq. 3.11 and Eq. 3.12, respectively. The evolution equation for cavitation accounting for constant nucleation and growth of cavities and its differential form are given by Eq.3.14 and Eq. 3.15, respectively.

The evolution equations for the internal variables (isotropic hardening, R, and kinematic hardening, α) used here are similar to the ones used for viscoplastic materials [88]. They include hardening and dynamic recovery terms and are expressed as follows:
Evolution equation of isotropic hardening can be expressed as:

$$\dot{R} = H\dot{\varepsilon} - C_D \dot{\varepsilon} R \qquad \text{Eq. 5.8}$$

where H is the hardening coefficient and C_D is the dynamic recovery coefficient. The differential form of the above expression can then be expressed as:

$$dR = (H - C_D R)d\varepsilon \qquad \text{Eq. 5.9}$$

Evolution equation for kinematic hardening can be expressed as:

$$\dot{\alpha} = H\dot{\varepsilon} - C_D \dot{\varepsilon}\alpha \qquad \text{Eq. 5.10}$$

The differential form of the above equation can be expressed as:

$$d\alpha = (H - C_D \alpha)d\varepsilon \qquad \text{Eq. 5.11}$$

By substituting the parameters into Eq.5.2, we get the following expression:

$$\frac{d\dot{A}}{dA} = \frac{\sigma}{\dot{\varepsilon}}\frac{\partial\dot{\varepsilon}}{\partial\sigma} + \frac{k_4}{\dot{\varepsilon} d^q}\frac{\partial\dot{\varepsilon}}{\partial d} + \frac{f_a \eta}{\dot{\varepsilon}}\frac{\partial\dot{\varepsilon}}{\partial f_a} + \frac{\partial\dot{\varepsilon}}{\partial R}\frac{[H - C_D R]}{\dot{\varepsilon}} + \frac{\partial\dot{\varepsilon}}{\partial\alpha}\frac{[H - C_D\alpha]}{\dot{\varepsilon}} - 1 \qquad \text{Eq. 5.12}$$

Applying Hart's stability criterion [60], the condition for stability crieterion at the onset of instability becomes:

$$0 = \frac{\sigma}{\dot{\varepsilon}}\frac{\partial\dot{\varepsilon}}{\partial\sigma} + \frac{k_4}{\dot{\varepsilon} d^q}\frac{\partial\dot{\varepsilon}}{\partial d} + \frac{f_a \eta}{\dot{\varepsilon}}\frac{\partial\dot{\varepsilon}}{\partial f_a} + \frac{\partial\dot{\varepsilon}}{\partial R}\frac{[H - C_D R]}{\dot{\varepsilon}} + \frac{\partial\dot{\varepsilon}}{\partial\alpha}\frac{[H - C_D\alpha]}{\dot{\varepsilon}} - 1 \qquad \text{Eq. 5.13}$$

Thus, the new multiscale stability criterion describing the condition for onset of instability during deformation of SP materials, accounting for anisotropy and hardening besides grain growth and cavitation can be expressed as:

$$\gamma^* + m^* + \zeta^* + \lambda^* + \xi^* = 1 \qquad \text{Eq. 5.14}$$

where:

$$\gamma^* = \frac{\dot{d}}{\dot{\varepsilon}^2}\frac{\partial\dot{\varepsilon}}{\partial d}$$

$$m^* = \frac{\sigma}{\dot{\varepsilon}}\frac{\partial \dot{\varepsilon}}{\partial \sigma}$$

$$\zeta^* = \frac{f_a \eta}{\dot{\varepsilon}}\frac{\partial \dot{\varepsilon}}{\partial f_a}$$

$$\lambda^* = \frac{(H - C_D R)}{\dot{\varepsilon}}\frac{\partial \dot{\varepsilon}}{\partial R} \qquad \text{and}$$

$$\xi^* = \frac{(H - C_D \alpha)}{\dot{\varepsilon}}\frac{\partial \dot{\varepsilon}}{\partial \varepsilon}$$

The first term in the above expression accounts for strain hardening due to grain coarsening, second term accounts for the effects of strain rate sensitivity, third term accounts for the effects of cavitation, fourth term represents isotropic hardening and the fifth term accounts for kinematic hardening. The effect of anisotropy is accounted through the definition of yield function.

By simultaneously solving the stability criterion along with the constitutive equation and evolution equations of grain growth, cavitation, isotropic hardening and kinematic hardening for a particular strain rate would yield the value of critical strain (maximum strain without any instability). Thus, repeating the procedure for different constant strain rates, the corresponding critical strain values are determined, which could then be used to construct the optimum variable strain rate forming path, which would describe a path for faster rate of production yet retaining the stability of the material. However, due to lack of sufficient and required experimental data in literature, we could not apply the model to any material.

5.2 Conclusion:

A multiscale microstructure based stability criterion accounting for grain growth, cavitation, isotropic hardening, kinematic hardening and anisotropic parameters is developed, for SP materials. An optimum forming path for SP materials is constructed using the stability criterion along with constitutive equation and evolution equations of the variables. The model could not be applied to any SP alloy due to lack of experimental data on the effect of anisotropy during large deformation under various loading conditions. However, the generalized model developed can be applied to any alloy, provided the required parameters could be obtained from experimental data.

Chapter 6 Conclusion and Future Recommendations

This project mainly aims at developing a multiscale stability criterion for Superplastic deformation and thereby construct optimum variable strain rate forming paths for SP materials. Optimum variable strain rate forming paths suggest that the deformation can be carried out at much faster/higher strain rates at lower strains but with increase in strain the deformation rate must be reduced – in order to prevent any instability to occur. This meets the challenge of forming components at a faster rate yet retaining the ductility of the material (i.e., ensuring stable deformation). This was achieved by using a microstructure based constitutive equation - representing the stress-strain rate variations of SP materials along with evolution equations of grain growth, cavitation, isotropic hardening, kinematic hardening and anisotropy parameters.

6.1 Conclusions:

The stability model was first developed for a uniaxial deformation case accounting for grain growth and pre-existing cavities. Since, most SP alloys cavitate and is a major cause for pre-mature failure of SP alloys besides having adverse effects on formed final products, accounting for cavitation while modeling SPD is very essential. Also, as literature suggests that most of the cavities nucleate during SPD, the evolution equations for cavitation were developed to account for nucleating (constant and continuous) cavities besides the pre-existing cavities. Growth of cavities by diffusion was also incorporated into the model, but since plasticity controlled growth was suggested to be a dominant growth mechanism during large deformations, diffusional growth aspect of cavitation was ignored. Effects of initial grain size, strain rate

sensitivity, nucleation strain, pre-existing cavities, nucleating (constant and continuous) cavities and grain growth exponent on the optimum forming paths of different SP alloys like: Ti-6Al-4V, AA 5083 and CDA 638 were examined.

The results obtained clearly indicate the importance of accounting for geometrical instabilities (like necking) and microstructural features including grain growth and cavitation on the optimum forming paths. It was observed that more stable deformation occurred when (a) the initial grain size was lower (b) strain rate sensitivity was higher and (c) lower levels of cavitation were present. Higher the value of nucleation strain, higher was the slope of the optimum forming paths as more time was required for the nucleating cavities to come into existence. Results also indicate the difference in effect of nucleating cavities on the optimum forming paths, when treated as constant and continuous nucleation. The effect of the said parameters on the optimum forming paths of three different SP alloys: Ti6Al4V, AA 5083 and CDA 638 were examined and it was found that though the plots had a slightly different patterns and slopes for different alloys, the net deduction remained the same in case of all the alloys. This clearly indicates the ability of the model to predict stable deformation for any SP alloy.

The model was then extended to develop a multiscale stability criterion for SP materials under various loading conditions. Biaxial plane stress condition was considered for this analysis because it is the dominant stress state in blow forming of superplastic sheets. The model was then fitted to the experimental data of SP CDA 638 (obtained from literature) and the effects of strain rate sensitivity, initial grain size, initial levels of cavitation (pre-existing, constant/continuous nucleation), different stress states, nucleation strain and grain growth exponent were examined. Material with fine grain size and high strain rate sensitivity with low levels of cavitation and high nucleation strain with high grain growth exponent seem to yield maximum stable deformation.

With an increase in the initial grain size, the maximum attainable strains without any instability is reduced. Accounting for only pre-existing cavities suggest that more stable deformation is possible for any given condition, when compared to the cases accounting for nucleation and pre-existing cavities. Maximum stable deformation attained is less in case of continuous nucleation when compared to the case considering constant nucleation. It was observed that there is a sudden drop in the effective strain rate values corresponding to the nucleation strain when the strain rate sensitivity is less. The drop decreases as strain rate sensitivity increases. For the case of no cavitation (i.e. considering only geometrical instabilities) increasing the biaxiality ratio increases the maximum strain that can be achieved prior to necking. This can be explained due to the fact that additional biaxial tensile load tends to delay the onset of necking perpendicular to the major stress axis. The behavior is significantly different when cavitation is accounted for. At higher strain values, the ductility for uniaxial loading case (ρ=-0.5) is much higher than the ductility for biaxial loading case. These observations can be explained as follows: at low strain values (i.e. at early stages in the forming process) the dominant failure mode is geometrical (necking) since microstructural features need time to evolve and contribute to the deformation and failure. At higher strains (i.e. at later stages in the forming process), the dominant failure mode is due to microstructural aspects (mainly cavitation).

Finally the model was extended to account for isotropic hardening, kinematic hardening and anisotropy besides necking, grain growth and cavitation during SPD. Incorporating microstructure based constitutive equation along with the evolution equations of grain growth, cavitation, isotropic hardening and kinematic hardening into the framework of Hart's stability analysis; the multiscale stability crieterion for SP materials accounting for anisotropy besides other parameters was developed. Due to lack of required experimental data, the model could not be fitted to experimental data of any SP alloy. However, the model is capable of investigating the effect of anisotropy parameters, isotropic hardening and kinematic hardening on the optimum variable strain rate forming paths besides other parameters as examined in previous sections.

6.2 Future Recommendations:

The project addressed modeling of several geometrical and microstructural issues relating to the stable deformation of SP alloys. A multiscale stability criterion was developed to construct optimum variable strain rate forming paths. Significance of accounting for cavitation during modeling SPD was established by incorporating the effect of nucleation and growth aspects of cavitation. Effect of isotropic hardening and kinematic hardening was also included and a modified stability criterion was presented, which also accounted for anisotropy. However, during the course of this work some important issues, which could become next phase of this project, were realized. These include:

1) One of the major recommendations for future would be to validate the proposed model and its results by performing experimental investigations. Suitable test set up needs to be built to perform high temperature testing for various loading conditions followed by a thorough microstructural analysis for grain growth and cavitation levels. The experimental results obtained can then be compared with the model results which indicate the accuracy of the model predictions. Based on these observations, the model can be further refined in order to predict results more closely to those obtained experimentally. The model finally emerging would then become a powerful tool to predict failure and thereby enable attainment of maximum stable deformation at much faster rates.

2) Further growth of this project lies in incorporating the model into finite element analysis and investigate the effects of various parameters on the forming of different complex and complicated geometries. This would be of prime interest for many industries as it would indicate the reduction in the time of manufacturing. It would also enable to develop pressure time profiles for different control schemes. These results should also be compared with the experimental results to confirm the validity of the finite element model. Discrepancy between the two would mean further refinement to the FE model.

3) The anisotropy stability criterion was not applied to any SP alloy due to lack of required experimental data. Required experiments and their set up must be designed, built and tested in

order to fit the model and achieve values for different material parameters in the evolution equations. Studying the evolving microstructure during deformation would also enable to better understand the mechanisms responsible for deformation-induced anisotropy. Achieving this, would enable predicting the effect of anisotropy parameters, isotropic hardening and kinematic hardening on the optimum variable strain rate paths. Also, the evolution equations for isotropic and kinematic hardening considered ignore the static recovery term, which is very important due to viscous nature of SP alloys. Hence this also needs attention, while refining the model and the stability criterion, to predict deformation and failure of SP alloys – more accurately.

4) The present model considered two of the three stages of cavitation - nucleation and growth of cavities. To complete the analysis, the third stage of cavitation which is coalescence should also be incorporated into the model. It would be interesting to investigate the effect of coalescence of cavities on the optimum variable strain rate forming paths of different SP alloys.

5) Since friction between the die and the work-piece is crucial in determining the pressures required to deform SP alloys during high temperature deformation, experiments need to be conducted to determine the values of friction and its influence on forming for different strain rates and high temperatures. This aspect also needs to be incorporated into the model to predict the effect of friction.

6) The grain growth – cavitation interaction is an interesting phenomenon. There has been a limited amount of work done on this issue, but this needs to be studied in detail to quantify the interactive effect on forming components. The effect of one on the other would also be a prominent result.

References

[1]. Pilling, J. and N. Ridley, “Superplasticity in Crystalline Solids”, Institute of Metals, 1989.

[2]. Higashi, K., T. Ohnishi and Y. Nakatami, Scripta Metallurgica, Vol.-19, pp.821-824,1985.

[3].Sherby O.D. and J. Wadsworth, “Development and Characterization of Fine Grain Superplastic Material”, Deformation, Processing and Structure, ASM, pp. 355-389, 1984.

[4]. Bochvar, A. A. and Z.A. Sviderskaya, Izvest.Akad.Nauk, Vol.-9, pp.821, 1945.

[5]. Backofen W.A., I.R.Turner and D.H. Avery, Transactions of ASM, Vol.- 57, pp. 980-990, 1964.

[6]. Nieh, T.G., J. Wadsworth and O.D. Sherby; “Superplasticity in metals and ceramics”, Cambridge University Press.

[7]. Thuramalla, N.V. and M.K. Khraisheh, “Effects of microstructural evolution on the stability of Superplastic Deformation” Proceedings: Second MIT Conference on Computational Fluid and Solid Mechanics, Elsevier-Vol: 1, pp-683-686, 2003.

[8]. Alden, T.H., “The origin of superplasticity in the Sn-5% Bi alloy”, Acta Metall., Vol.-15, pp. 469, 1967.

[9]. Falk, L.K., P.R.Howell, G.L. Dunlop and T.G. Langdon, “The role of matrix dislocations in the superplastic deformation of a copper alloy”, Acta Metall., 34(7), 1203, 1986.

[10].Edington, J.W., K.N. Melton and C.P. Cutler, “Superplasticity”, Progress in Materials Science, Vol.-21, pp.63-170, 1976.

[11].Wilkinson, D.S. and C.H. Caceres, “On the mechanism of strain-enhanced grain growth during superplastic deformation”, Acta Metallurgica – Vol.-32 (9), pp.1335-1345, 1984.

[12].Atul Chokshi, “The role of cavitation in superplastic materials”, Ph.D. dissertation, University of Southern California, 1984.

[13].Riley, N. and Z.C.Wang, “The effect of microstructure and deformation conditions on cavitation in superplastic materials”, Materials Science Forum, Vol.- 233-234, pp. 63-80, 1997.

[14].Ding, X., “Modeling and optimization of superplastic forming processes”, Ph.D. dissertation, Washington State University, 1996.

[15]. Bampton, C.C., A.K. Ghosh and M.W.Mahoney, in “Superplasticity in Aerospace Aluminum”, edited by R.Pearce and L.Kelly, Vol.-1, 1985.

[16]. Ding, X.D., H.M. Zbib, C.H. Hamilton and A.E. Bayoumi, “On the stability of biaxial stretching with application to the optimization of superplastic blow-forming”, Journal of Engineering Materials and Technology, Transactions of ASME, Vol.-119, pp. 26-31, 1997.

[17]. Ghosh, A.K. and C.H. Hamilton, “Influences of Material Parameters and Microstructure on Superplastic Forming”, Metallurgical Transactions A, Vol.- 13A, pp. 733-743, 1982.

[18]. Cottrell, A.H., “The Mechanical Properties of Matter”, John Wiley and Sons, Inc., 1964.

[19]. Lee, D., “The nature of superplastic deformation in Mg-Al eutectic”, Acta Metall., Vol.-17, pp.1057, 1969.

[20]. Bae, D., “Superplasticity and cavitation in an Al-Mg alloy”, Ph.D. dissertation, The University of Michigan, 2000.

[21]. Padmanabhan, K.A. and G.J. Davies, “Superplasticity”, Springer-Verlang, Berlin, 1980.

[22]. Hamilton, C.H., A.K. Ghosh and J.A. Wert, “Superplasticity in engineering- A review”, Metals Forum, Vol.- 8, pp.172-190, 1985.

[23].Ghosh, A.K. and C.H. Hamilton, “Mechanical behavior and hardening characteristics of a Superplastic Ti6Al4V alloy”, Metallurgical Transactions, Vol.-10A, pp. 699-706, 1979.

[24].Langdon, T.G., “Cavitation in High Strain Rate Sensitivity: Implications for the Flow Process”, Materials Science Forum, Vol.- 233-234, pp. 47-62, 1997.

[25]. Johnson, C.H., “Microstructural and constitutive behavior of superplastic titanium alloy Ti-6Al-4V”, Ph.D. dissertation, Washington State University, 1994.

[26] Mukherjee, A.K., “Mechanical behavior and hardening characteristics of a Superplastic Ti6Al4V alloy”, Materials Science and Engineering, Vol.-8, pp. 83, 1971.

[27]. Ashby, M.F. and R.A. Verall, “Diffusion accommodated Flow and Superplasticity”, Acta Metallurgica, Vol.-21, pp. 149-163 ,1973.

[28]. Clark, M and T. Alden, “Deformation Enhanced Grain Growth in a Superplastic Sn-1%Bi Alloy”, Acta Metallurgica, Vol.- 21, pp. 1195-1206, 1973.

[29].Wilkinson, D.S., and C.H. Caceres, “Mechanism of Plastic Void Growth During Superplastic Flow”, Materials Science and Technology, Vol.- 2, pp. 1086-1092, 1986.

[30]. Li, F., D.H. Bae and A.K. Ghosh, “Grain Elongation and Anisotropic Grain Growth Suring Superplastic Deformation in an Al-Mg-Mn-Cu alloy” Acta Materialia, Vol. 45, pp. 3887-3895, 1997.

[31]. Caceres, C.H. and D.S. Wilkinson, “Large Strain Behavior of a Superplastic Copper Alloy-I. Deformation”, Acta Metallurgica, Vol.-32, pp. 415-422 , 1984.

[32]. Hamilton C.H., H. M. Zbib, C.H. Johnson and S.K. Richter, “Microstructural Coarsening and its Effect on Localization of Flow in Superplastic Deformation”, Superplasticity in Advanced Materials. Ed’s: S.Hori, M. Tokizane and N. Furushiro, The Japan Society for Research on Superplasticity, pp. 127-132, 1991.

[33]. Nicolaou, P.D., S.L. Semiatin and A.K. Ghosh, “ An Analysis of the Effect of cavity Nucleation rate and cavity Coalescence on the Tensile Behavior of Superplastic Materials”, Metallurgical and Materials Transactions A, Vol.-31A, pp. 1425-1434, 2000.

[34].Harris, J.E., M.O. Tucker and G.W. Greenwood, “The Diffusional Creep Strain Due to the Growth of Intergranular Voids”, Metal Science, Vol.8, pp. 311-314, 1974.

[35]. Miller, D.A., F.A. Mohammed and T.G. Langdon, “An Analysis of cavitation failure Incorporating Cavity nucleation with Strain”, Materials Science and Engineering, Vol.- 40, pp. 159-166, 1979.

[36]. Ghosh, A.K., D.H. Bae and S.L. Semiatin, “Initiation and Early Stages of Cavity Growth during Superplastic and Hot deformation”, Materials Science Forum, Vol.-304-306, pp.609-616, 1999.

[37]. Hiranga, K. and K. Nakano, “Cavitation Damage Mechanisms in a Superplastic Zirconia (3Y-TZP)”, Materials Science forum, Vol.-243-245, pp. 387-392, 1997.

[38]. Chokshi, A.H., A.K. Mukherjee and T.G. Langdon, Materials. Science Engineering, Vol.-10, pp.237, 1993.

[39]. Speight, M.V. and W. Beere, “Vacancy potential and void growth on grain boundaries”, Metal Science, Vol.-9, pp. 190, 1975.

[40]. Hancock, J.W., “Creep cavitation without a vacancy flux”, Metal Science, Vol.-10, pp. 319, 1976.

[41].Iwasaki, H., K.Higashi, S.Tanimura, T. Komatubara and S. Hayami, “Superplastic Deformation Charactristics of 5083 Aluminum Alloy”, Superplasticity in Advanced Materials, Ed’s: S.Hori, M.Tokizane and N. Furushiro, The Japan Society for Research on Superplasticity, pp. 447-452, 1991.

[42].Imamura, H and N. Ridley, “Superplastic and Recrystallisation Behavior of a Commercial Al-Mg Alloy 5083” Superplasticity in Advanced materials, Ed’s: S.Hori, M.Tokizane and N. Furushiro, The Japan Society for Research on Superplasticity, pp. 453-458,1991.

[43]. Stowell, M.J., “Cavity growth and failure in Superplastic alloys”, Metal Science, Vol.-17, pp. 92-98, 1983.

[44]. Cocks, A.C.F. and M.F. Ashby, “Creep fracture by coupled power-law creep and diffusion under multiaxial stress”, Metals Science, Vol.-16, pp. 465,1982.

[45]. Maboa, L and W.Shichun, “A Model for Cavity growth in a Superplastic Material During Uniaxial Tension”, Journal of Materials Processing Technology, Vol.-41, pp. 115-124, 1994.

[46]. Stowell, M.J., D.W. Livesey and N. Ridley, “Cavity Coalescence in Superplastic Deformation”Acta Metallurgica, Vol.-32, pp. 35-42, 1984.

[47]. Nicolaou, P.D. and S.L. Semiatin, “Modeling of Cavity Coalescence During Tensile Deformation”, Acta Materialia, Vol.- 47 (13), pp. 3679-3686, 1999.

[48].Martin, C.F., C. Josserond, L.Salvo, J.J. Blandin, P.Cloetens and E.Boller, “Characterization by X-ray Micro-tomography of Cavity Coalescence during Superplastic Deformation”, Scripta Materialia, Vol.-42, pp. 375-381, 2000.

[49]. Khraisheh, M.K., H.M. Zbib, C.H. Hamilton, A.E. Bayoumi, “Constitutive Modeling of Superplastic deformation. Part I : Theory and Experiments”, International Journal of Plasticity, Vol.-13, pp. 143-164, 1997.

[50]. Chandra, N., “Constitutive Behavior of Superplastic Materials”, International Journal of Non-Linear mechanics, Vol.- 37, pp.461-484, 2002.

[51]. Padmanabhan, K.A., R.A. Vasin and F.U. Enikeev, “ Superplastic Flow: Phenomenology and Mechanics”, Springer.

[52]. Ghosh, A.K., “A New Physical Model for Superplastic Flow”, Materials Science Forum, Vol.- 170-172, pp.39-46, 1994.

[53]. Khraisheh, M.K., “The mechanism of multiaxial deformation of superplastic materials:application to manufacturing concepts”, Ph.D. dissertation, Washington State University, 1996.

[54]. Hart, E.W., “A Theory for Flow of Polycrystals”, Acta Metallurgica, Vol.-15, pp. 1545-1549,1967.

[55]. Avery, D.H. and W.A. Backofen, “A Structural Basis for Superplastcity”, Transactions of ASM, Vol.-58, pp.551, 1965.

[56]. Mukherjee, A., “The Rate Controlling Mechanism in Superplasticity”, Materials Science and Engineering, Vol.-8, pp. 83-89, 1971.

[57].Suery, M. and B. Baudelet, “Hydrodynamical Behavior of a Two Phase Superplastic Alloy: α/β Brass”, Philosophical Magazine A, Vol.-41 (1), pp.41-64, 1980.

[58]. Caceres C.H. and D.S. Wilkinson, “Large Strain Behavior of a Superplastic Copper Alloy – I. Deformation”, Acta Metallurgica, Vol.-32, pp.415-422, 1984.

[59]. Khaleel, M.A., H.M. Zbib and E.A. Nyberg, “Constitutive Modeling of Superplastic Deformation and Damage in Superplastic Materials”, International Journal of Plasticity, Vol.-17, pp.277-296, 2001.

[60]. Hart, E.W., “Theory of the Tensile Test”, Acta Metallurgica, Vol.-15, pp.351-355, 1967.

[61]. Duncombe, E., “Plastic Instability and Growth of Groves and Patches in Plates or Tubes”, International Journal of Mechanical Science, Vol.-14, pp.325-337, 1972.

[62]. Ghosh, A.K., “Tensile Instability and Necking in Material with Strain Hardening and Strain Rate Hardening”, Acta Metallurgica, Vol.-25, pp.1413-1424,1977.

[63]. Nichols, F.A., “Plastic Instabilities and Uniaxial Tensile ductilities”, Acta metallurgica, Vol.-28, pp.663-673, 1980.

[64].Swift, H.W., “Plastic Instability under Plane Stress”, Journal of the Mechanics and Physics of Solids, Vol.-1, pp.1, 1952.

[65]. Hill, R., “On Discontinuous plastic States with spcial reference to Localized necking in thin sheets”, Journal of the Mechanics and Physics of Solids, Vol.- 1, pp.19, 1952.

[66]. Marciniak,Z and K.Kuczynski, “Limit Strains in the Processes of Stretch-Forming Sheet Metal”, International Journal of Mechanical Science, Vol.-9, pp.609-620, 1967.

[67]. Storen, S and J.R. Rice, “Localized Necking in Thin Sheets”, Journal of the Mechanics and Physics of Solids, Vol.-23. pp. 421-441, 1975.

[68]. Tipper, C.F., “The Fracture of Metals”, Metallurgica, Vol.-39, pp.133-137, 1949.

[69]. Puttick, K.E., “Ductile Fracture in Metals”, Philosophical Magazine, Vol.- 4(8), pp.964-969, 1959.

[70].Bluhm, J.I. and R.J. Morrissey, “Fracture in a Tensile Specimen”, Proceedings of First International Conference on Fracture”, Japanese Society for Strength and Fracture of materials, vol.-3, pp. 1739-1780, 1966.

[71]. McClintock, F.A., “A Criterion for Ductile Failure by the Growth of Holes”, Journal of Applied mechanics, Transactions of ASME, pp.363-371, 1968.

[72]. Gurland, J. and J. Plateau, “The Mechanism of Ductile rupture of Metals Containing Inclusions”, Transactions of A.S.M., Vol.56, pp. 443, 1963.

[73]. Gurson, A.L., “Continuum Theory of Ductile Rupture by Void Nucleation and Growth: part I – Yield Criteria and Flow Rules for Porous Ductile Media”, Journal of Engineering Materials and Technology, Transactions of the ASME, pp. 2-14, 1977.

[74]. Perzyna, P., “Constitutive Modeling of Dissipative Solids for Postcritical Behavior and Fracture”, Journal of Engineering Materials and Technology, Transactions of ASME, Vol.-106, pp. 410-419, 1984.

[75]. Jonas, J.J. and B. Baudelet, “Effect of Crack and Cavity generation on tensile Stability”, Acta Metallurgica, Vol.-25, pp.43-50, 1977.

[76]. Thuramalla, N.V., P.V.Deshmukh and M.K.Khraisheh, “Multiscale Analysis of Failure during Suprplastic Deformation”, Materials Science Forum, Vol.- 447-448, pp.105-110, (2004).

[77]. Ren, B., C.H. Hamilton and B.A. Ash, “An Appraoch to rapid SPF of an al-Li-Cu-Zr Alloy”, fifth international Aluminum-Lithium Conference, Ed’s: Jr. E.A. Starke and Jr. T.H. Sanders, The Metallurgical Society, 1989.

[78].Ardell, A.J., “On the Coarsening of Grain Boundary Precipitates”, Acta Metall. Vol.-20, pp.601-609, 1972.

[79].http://www.superform-aluminium.com/index.html

[80]. Shei, S.A. and T.G. Langdon, “The Activation Energies for Plastic Flow in a Superplastic Copper alloy”, Acta Metall., Vol. - 26, pp.1153-1158, 1978.

[81] Wu, X.Y., K.T. Ramesh, and T.W. Wright, “The Dynamic Growth of a Single Void in a viscoplastic Material under Transient Hydrostatic Loading”, J. of the Mech. and Phy. of Solids, Vol.- 51, pp.1-26, 2003.

[82]. Chow, K.K. and K.C. Chan, “Effect of Stress State on Cavitation and Hot forming of a Coarse Grained Al5052 alloy”, Mtls. Letters, Vol.- 52, pp. 62-68, 2002.

[83]. Zbib, H.M and E.C. Aifantis, “On the localization and postlocalization behavior of plastic deformation. Part I: On the initiation of shear bands. Part II: On the evolution and thickness of shear bands. Part III: On the structure and velocity of the Portevin-Le-Chatelier bands”, Res. Mechanica, Vol-23, pp. 261-305, 1988.

[84]. Zhu, H., H.M. Zbib and E.C. Aifantis, “On the effect of anisotropy and inertia on shear banding: Instability of biaxial stretching”, Appl. Mech. Rev., Vol.- 45 (3), part 2, pp. 110-117, 1992.

[85]. Marciniak, Z, K.Kuczynski and T. Pokara, Intl. J. Mech. Sci., Vol.- 15, pp. 789, 1973.

[86]. Swift, H.W., Engineering, Vol.-163, pp. 253-257,1947.

[87]. Toth, L.S., J.J. Jonas, D.Daniel and J.A. Baily, Textures and Microstructures, Vol.- 19, pp.245-262, 1992.

[88]. Dafalias, Y.F., “The plastic spin in viscoplasticity”, Intl. J. of Solid Structures, Vol.- 26 (2), pp. 149, 1990.

VITA

I was born in the state of Andhra Pradesh in India on the twenty second day of the seventh month of the year nineteen hundred and seventy nine (07/22/1979). I completed my secondary school education at St. Patrick's High School, Hyderabad and finished my pre-college from Ratna Junior College, Hyderabad. I then pursued my Bachelors in Mechanical Engineering at M.J. College of Engineering and Technology, affiliated to Osmania University, Hyderabad. I was awarded merit certificates for my outstanding performance during my schooling and also during my Bachelors. My paper on "Air Ambiator" won the Best Undergraduate Student Award at a National Technical Symposium. I was also awarded second prize for my performance in a Declamation contest organized by Govt. of India.

I then joined University of Kentucky, to pursue my Masters in Mechanical Engineering in August 2001. I served as a Teaching and Research assistant during the course of my MS. Awards won and list of publications, during my MS are listed below:

Publication and Presentations:

Journals:

1) N.V.Thuramalla, P.V.Deshmukh and M.K.Khraisheh, "Multiscale analysis on the stability of Superplastic deformation"- **Materials Science Forum**, pp. 105-110, 2003.
2) N.V. Thuramalla and M.K. Khraisheh, "Multiscale – Based Optimization of Superplastic Forming", **Transactions of NAMRI/SME,** Vol.32, pp.637-643, 2004**.**
3) N.V. Thuramalla and M.K. Khraisheh, "Analysis on the effect of constant/continuous nucleation, and growth of cavities on the stable deformation of Superplastic alloys", submitted to **Materials Science and Engineering A**.

Conference Publications and Presentations:

1) N.V. Thuramalla and M.K. Khraisheh, "Effects of microstructural evolution on the stability of Superplastic Deformation" Proceedings: Second MIT Conference on Computational Fluid and Solid Mechanics, Elsevier-Vol: 1, pp-683-686, 2003.
2) N.V. Thuramalla, F.K. AbuFarha and M.K.Khraisheh, "Multiscale-Stability analysis on Superplastic deformation", was presented in the poster session at the 2003-TMS annual meeting.

3) N.V.Thuramalla, F.K. AbuFarha and M.K.Khraisheh, "A new failure criterion for Superplastic deformation" was presented at Plasticity-03, Quebec, Canada.

4) F.K.AbuFarha, P.V.Deshmukh, N.V.Thuramalla and M.K.Khraisheh, "Superplastic Forming: Stretching the Limits of Fabricating Biomedical Devices and Implants", pp.368-373, Proceedings from the Materials and Processes for Medical Devices Conference, 2003.

5) N.V. Thuramalla and M.K. Khraisheh, "Instability Analysis on the Biaxial Stretching of Superplastic Materials" was presented at the 40th. SES conference, 2003.

6) M.K.Khraisheh, N.V. Thuramalla, F.K.AbuFarha and P.V.Deshmukh, "Multiscale analysis of deformation and failure of Superplastic materials" has been presented at IMECE 2003, Washington.

7) P.V.Deshmukh, N.V.Thuramalla, F.K.AbuFarha and M.K.Khraisheh, "Integrated approach for optimization of SPF", pp. 361-369, Proceedings of TMS Annual Meeting, 2004.

8) N.V. Thuramalla and M.K. Khraisheh, "Effect of Cavitation on the Stability of Superplastic Deformation under Various Loading Conditions" presented in the poster session at TMS Annual Meeting-2004.

9) N.V. Thuramalla, "Designing Optimum Forming Paths for Superplastic Materials based on a Multiscale Stablity Criterion" presented at ASME regional conference, 2004.

Honors and Distinctions:

1) Awarded ***Young researcher award*** at the Second **MIT** conference, 2003.

2) Awarded ***Commonwealth research award*** by **University of Kentucky** - 2003

3) Awarded ***Best student poster award*** at **TMS** annual meeting – 2003.

4) Awarded ***Student travel assistance scholarship*** to present at the **TMS** Annual meeting-2003 by the Metals, Minerals and Materials Society.

5) Awarded ***Student travel assistance*** to present at the 40th. Annual meeting-2003 by the Society of Engineering Sciences.

6) Awarded ***Kentucky Graduate Scholarship*** by **University of Kentucky**

7) Secured ***First position*** in fifth semester during under-graduation (Bachelor of Engineering) in the university.

8) Awarded prize for paper titled Air Ambiator at a National level technical symposium, INDIA.

9) Awarded prize in Declamation contest organized by Government of INDIA.

Naveen Thuramalla.